University of Stuttgart
Institute of Geodesy

Copula–based Analysis of Correlation Structures in Case of GRACE Coefficients

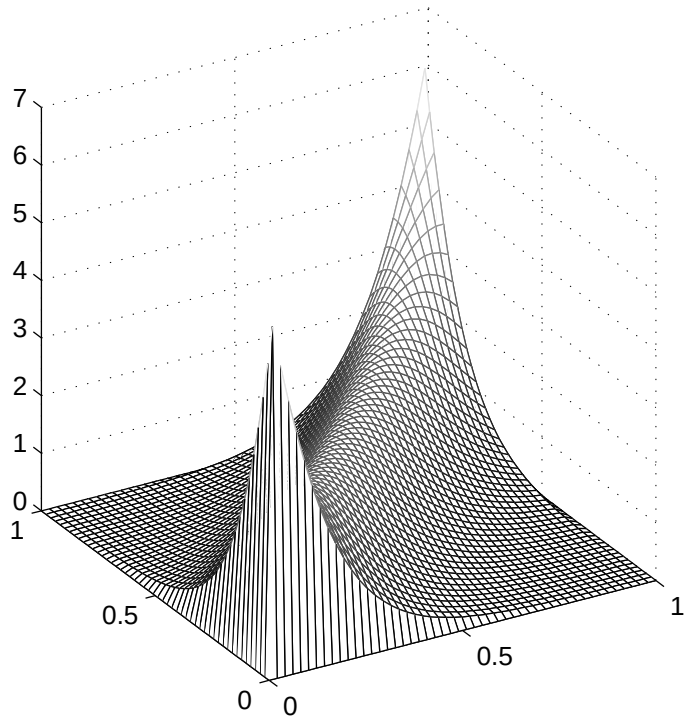

Master thesis in study program

GEOENGINE

University of Stuttgart

Sadegh Modiri

Stuttgart, May 2015

Supervisor: Prof. Dr.-Ing. Nico Sneeuw
University of Stuttgart

Prof. Dr. Harald Kunstmann
University of Augsburg

Dipl.-Ing. Christof Lorenz
Karlsruhe Institute of Technology

Declaration

Hereby, the following is confirmed – according to the Geomatics Engineering (GEOENGINE) examination regulations §22(7):

- I, the author, have prepared the thesis fully independently.
- I have not used any other than the specified sources. All statements that are literally taken from other sources are clearly marked. All these sources are explicitly listed in the thesis.
- The submitted thesis in whole or in substantial parts is not been involved in any other examination.
- This thesis has not been published previously in whole or in parts.
- The electronic version submitted fully complies with this thesis.

....

Place, Date Signature of thesis author

Acknowledgment

First of all, I want to thank Prof. Dr.-Ing. Sneeuw for his friendly encouragements. I am also grateful to Prof. Dr. Kunstmann for giving me the opportunity of working with his group at Karlsruhe Institute of Technology in Garmisch-Partenkirchen.

I will forever be thankful to Christof Lorenz. He has been helpful in providing advice many times during my thesis. I also appreciate that he has been always available for discussions and answering questions. He helped me a lot and supported me all the time during my stay in Garmisch. For all of this I owe him more than I can describe.

I would like to thank all the members of the groups of Prof. Dr. Harald Kunstmann in IMK-IFU, KIT, for the friendly environment they have created. Among them are Joel Arnault, Patrick Laux, Salack Seyni, Ganquan Mao, Noah Kerandi, Christian Chwala, Verena Wedler, and my great brother Moussa Waongo.

I would like to express my deep gratitude to Mohammad Javad Tourian and Omid Elmi in Institute of Geodesy for their helpful comments and very useful assistance.

Words cannot express how grateful I am to my parents and siblings, Elham and Ehsan.

Abstract

Data from the Gravity Recovery and Climate Experiment (GRACE) has significantly improved our knowledge of the terrestrial water cycle. With the availability of GRACE data from 2002, we are now able to perform even climate change studies with respect to water storage variations. However, as GRACE is already after its expected lifetime, we have to find methods for filling the missing months in the past data and to possibly bridge the gap until GRACE Follow On.

In this study, we, therefore, analyze the potential of Copula-based methods for simulating GRACE coefficients data from other hydrological data sources. The method exploits linear and non-linear relationships between two or more variables by fitting a theoretical Copula function into an empirical bivariate or multivariate distribution function. Finally, new data, which is then consistent with the previously derived dependence structure, can be simulated by evaluating the conditional distribution function given by the theoretical Copula.

First, we want to analyze the applicability of the proposed method to spherical harmonic coefficients data from GRACE. As the approach involves several drawings of random data, we are interested if this random nature has any impact on the results. We therefore generate filtered out of unfiltered GRACE coefficients, based on the previously derived dependence structure. The comparison between the simulated and filtered data shows a very good agreement with negligible differences in both of the spatial and spectral domain.

We also want to evaluate if Copula-based methods are able to estimate reliable water storage changes from the independent hydrological data. Therefore, we derive the dependence structure between filtered water storage changes from GRACE and global gridded precipitation data from the Global Precipitation Climatology Center GPCC. Based on the fitted theoretical Copula, we then simulate water storage changes from precipitation data. The Copula-based estimates are compared with filtered GRACE coefficients data in both of the spectral and spatial domain. We also perform a catchment-based analysis between area-aggregated time-series of simulated and GRACE-derived water storage change. The analysis shows that our estimates and the original filtered GRACE coefficients data are in very good agreement. Thus, we conclude that the proposed method is indeed able to fill the missing months in the GRACE-dataset and to extend even the time-series until the launch of GRACE Follow On.

Contents

1 Introduction **1**
1.1 Problem statement . . . 3
1.2 Literature review and research questions . . . 5

2 Method **9**
2.1 Distribution functions of uni-, bi-, and multivariate random variables . . . 9
2.1.1 Probability Density Function (PDF) . . . 9
2.1.2 Cumulative Distribution Function (CDF) . . . 10
2.1.3 Marginal distribution . . . 11
2.2 Copula theory . . . 12
2.2.1 Sklar's theorem . . . 12
2.2.2 Characteristic of Copulas . . . 13
2.2.3 Copula density . . . 13
2.2.4 Empirical Copulas . . . 13
2.3 Theoretical Copula . . . 14
2.3.1 Elliptical Copula . . . 14
2.3.2 Archimedean Copula . . . 15
2.3.3 Copula parameter estimation . . . 18
2.3.3.1 CMLE and IFME . . . 18
2.4 Computation of conditional CDF of Archimedean Copula . . . 21
2.5 Simulating from Copula-based conditional random data . . . 22

3 Data **23**
3.1 GRACE . . . 23
3.1.1 Mission states . . . 23
3.1.2 Data source . . . 25
3.2 Data preprocessing . . . 25
3.2.1 Removing degree 0 and 1 . . . 25
3.2.2 Removing annual cycle . . . 26
3.3 Precipitation . . . 27

4 Proof of concept **29**
4.1 Applying Copula-based method to monthly data . . . 29
4.2 Applying Copula-based method to each coefficient . . . 34
4.2.1 Fitting marginal distribution . . . 34
4.2.2 Transforming data into rank space . . . 36
4.2.3 Computing Copula parameter . . . 40

4.2.4 Fitting theoretical Copula . . . 42
4.2.5 Simulating Copula-based derived random data . . . 43
4.2.6 Transferring data from rank space to data space . . . 43
4.3 Comparison . . . 44
4.3.1 Degree variance . . . 45
4.3.2 Residual . . . 48
4.3.3 Analysing time series in different area and their RMS . . . 49

5 Prediction of water storage changes from precipitation 51
5.1 Introduction . . . 51
5.2 Prediction of water storage anomalies from precipitation using Copula-based approach . . . 53
5.2.1 Transforming data into rank space . . . 54
5.2.2 Computing Copula parameter . . . 58
5.3 Fitting theoretical Copula to dependency structure . . . 59
5.3.1 Comparison . . . 60
5.3.2 Degree variance . . . 61
5.3.3 Residual . . . 63
5.3.4 Analysing time series in different areas and their RMS . . . 64
5.3.5 Prediction of precipitation from GRACE coefficients using Copula-based approach . . . 66

6 Summary, conclusion and outlook 69
6.1 Summary and conclusion . . . 69
6.2 Outlook . . . 71

A Time variable GRACE coefficients and surface density changes XXV
A.1 Computation of the time variable GRACE coefficients . . . XXV
A.2 Computation of surface density changes . . . XXVI

B Overview of different parametric distribution XXVII
B.1 Normal distribution . . . XXVII
B.2 Generalized extreme value distribution . . . XXVIII
B.3 Extreme value distribution . . . XXVIII
B.4 Generalized Pareto distribution . . . XXIX

C Rank correlation XXXI
C.1 Spearman's ρ and Kendall's τ . . . XXXI
C.2 Upper/Lower tail dependence . . . XXXI
C.3 Relation between Copulas and spearman's ρ, kendall's τ . . . XXXII

D Copula modelling of unfiltered and filtered GRACE coefficients XXXV

E Copula modelling of precipitation and filtered GRACE coefficients XLVII

F Degree variance of Copula-based data and filtered GRACE LXI

G Degree variance of Copula-based data and precipitation LXVII

List of Figures

1.1 Overview of the hydrological compartments . . . 1
1.2 Overview of CHAMP mission . . . 2
1.3 Configuration of the GRACE . . . 3
1.4 Lifetime predictions of GRACE . . . 4
1.5 Missed data in GRACE . . . 5

2.1 Probability Density Function "PDF" . . . 10
2.2 Cumulative Distribution Function "CDF" . . . 11
2.3 Bivariate distribution . . . 11
2.4 Gaussian Copula . . . 14
2.5 t-Copula . . . 15
2.6 Frank Copula . . . 16
2.7 Clayton Copula . . . 17
2.8 Gumbel Copula . . . 18
2.9 Frank, Gumbel, and Clayton Copula with parameter $\theta = 1.5$ . . . 20
2.10 Frank, Gumbel, Clayton Copula with parameter $\theta = 2$ . . . 20
2.11 Frank, Gumbel, Clayton Copula with parameter $\theta = 5$ . . . 20

3.1 GRACE mission concept . . . 24
3.2 Sorted Spherical Harmonic Coefficients . . . 25
3.3 Time series of data before and after removing annual cycle . . . 26
3.4 Precipitation data in July 2009 . . . 27

4.1 Filtered and unfiltered GRACE coefficients in 2005. . . . 30
4.2 Overview of fitting Copula to bivariate data and the Copula-based data merging algorithm . . . 31
4.3 Unfiltered and filtered GRACE data in February 2005 . . . 32
4.4 Copula-based data in February 2005 . . . 32
4.5 Fitting the marginal CDF to unfiltered and filtered GRACE coefficients . . . 33
4.6 Marginal CDF distribution of coefficients . . . 35
4.7 The unfiltered and filtered GRACE coefficients for degree 2–10 and order 0 36
4.8 The unfiltered and filtered GRACE coefficients for degree 11–25 and order 0 . . . 37
4.9 The unfiltered and filtered GRACE coefficients for degree 26–40 and order 0 . . . 38
4.10 The unfiltered and filtered GRACE coefficients for degree 41–55 and order 0 . . . 39

4.11 The unfiltered and filtered GRACE coefficients for order 0 40
4.12 The Copula parameters for each coefficient of unfiltered and filtered data 41
4.13 Copula-based modeling of the dependency structure between unfiltered and filtered GRACE 42
4.14 Simulated data using Archimedean Copula (Frank, Clayton, and Gumbel Copula) 44
4.15 Degree variance unfiltered and filtered GRACE data and Copula filtered data. 46
4.16 Residual of simulated data using Copula-based approach 48
4.17 Time series of filtered data and Copula derived random data in Amazon, Mississippi, and Ganges 49

5.1 Overview of fitting Copula to bivariate data and overview of the Copula-based data merging algorithm 52
5.2 Precipitation and filtered GRACE data in September 2009 53
5.3 Precipitation and filtered GRACE coefficients. Degree 2–16 and order 0. . 54
5.4 Precipitation and filtered GRACE coefficients. Degree 17–31 and order 0. 55
5.5 Precipitation and filtered GRACE coefficients. Degree 32–46 and order 0. 56
5.6 Precipitation and filtered GRACE coefficients. Degree 47–60 and order 0. 57
5.7 Copula parameters of the dependency structure between Precipitation and filtered GRACE data 58
5.8 Fitting the Archimedean Copula to dependency structure between filtered and precipitation data. 59
5.9 Simulated water storage anomalies data using Copula-based approach . 60
5.10 Degree variance precipitation, unfiltered and filtered GRACE data, and Copula derived random data 62
5.11 Residual of Copula-based data derived from dependency between precipitation and filtered GRACE data 63
5.12 Time series of the Copula-based data and GRACE data in Zambezi, OB, and Victoria River 64
5.13 Overview of Simulating precipitation data using Copula 66
5.14 Overview of predicting precipitation data using Copula 67
5.15 Simulating precipitation data using Copula 67

B.1 Normal distribution XXVII
B.2 Generalized extreme value distribution XXVIII
B.3 Extreme value distribution XXIX
B.4 Generalized Pareto distribution XXIX

D.1 Dependency structure between unfiltered and filtered GRACE data . . . XLVI

E.1 Dependency structure between precipitation and filtered GRACE data . . LIX

F.1 Degree variance of GRACE and Copula-based data 2005. LXII
F.2 Degree variance of GRACE and Copula-based data 2006. LXIII
F.3 Degree variance of GRACE and Copula-based data 2007. LXIV

F.4 Degree variance of GRACE and Copula-based data 2008. LXV
F.5 Degree variance of GRACE and Copula-based data 2009. LXVI

G.1 Degree variance of precipitation and GRACE, and Copula-based data 2005 LXVIII
G.2 Degree variance of precipitation and GRACE, and Copula-based data 2006 LXIX
G.3 Degree variance of precipitation and GRACE, and Copula-based data 2007 LXX
G.4 Degree variance of precipitation and GRACE, and Copula-based data 2008 LXXI
G.5 Degree variance of precipitation and GRACE, and Copula-based data 2009 LXXII

List of Tables

2.1 Archimedean Copulas, generator, parameter space, and formula 18

4.1 RMS of filtered GRACE data, Clayton, Gumbel, and Frank Copula in Amazon, Mississipi and Ganges 50
4.2 Correlation of Clayton, Gumbel, and Frank Copula with filtered GRACE data in Amazon, Mississipi and Ganges 50

5.1 RMS of filtered GRACE data, Clayton, Gumbel, and Frank Copula in Zambezi, OB, and Victoria river 65
5.2 Correlation of Clayton, Gumbel and Frank Copula with filtered GRACE data in Zambezi, OB, and Victoria river 65

C.1 Archimedean Copula and their rank correlation measure XXXIII

Chapter 1

Introduction

Terrestrial water storage is of great importance in various fields of human life. Its availability and change can affect the agricultural and industrial applications (Shiklomanov, 1998; Douglas and Lettenmaier, 2003; Fiedler and Döll, 2007). However, in the past, it was not possible to measure water storage change directly (Rodell and Famiglietti, 1999). Strassberg et al. (2007) and Yeh et al. (2006) studied water storage changes from the variations in groundwater levels and soil water saturation (1.1). However, the groundwater and soil water saturation that is observed on a single location is not adequate to be used on large spatial scales (Riegger et al., 2012; Tourian, 2013).

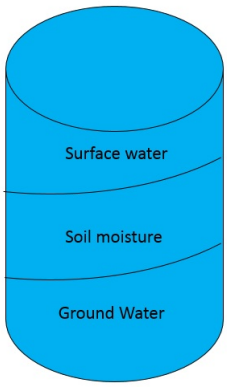

Figure 1.1: *Overview of the hydrological compartments. Surface water is the water on the surface of the planet e.g. stream, river, lake, wetland, or ocean. Soil moisture is the quantity of water contained in the soil. Ground water is the water located under the Earth's surface in soil pore spaces and the fractures of rock formations.*

Satellite observation of the time variable Earth's gravity field is an indirect way to measure water storage changes on large spatial scales. Before 2000, it was possible to measure the Earth's time variable gravity field only by Satellite Laser Ranging (SLR) at global scales. However, SLR provides observations of the seasonal variations of the long wavelengths (up to degree and order 4) (Nerem et al., 2000) and these resolutions are not enough for catchment-scale studies.

CHAllenging Minisatellite Payload (CHAMP) mission was launched with the aim of capturing the time variable gravity field based on the Satellite to Satellite Tracking (SST). The CHAMP satellite was detected by using on-board GPS receivers. However, the quality of the GPS observations and processing standards were not high enough to derive time variable gravity field estimation and to use it for hydrological studies (Qiang and Moore, 2005). Since 2002, the Gravity Recovery and Climate Experiment

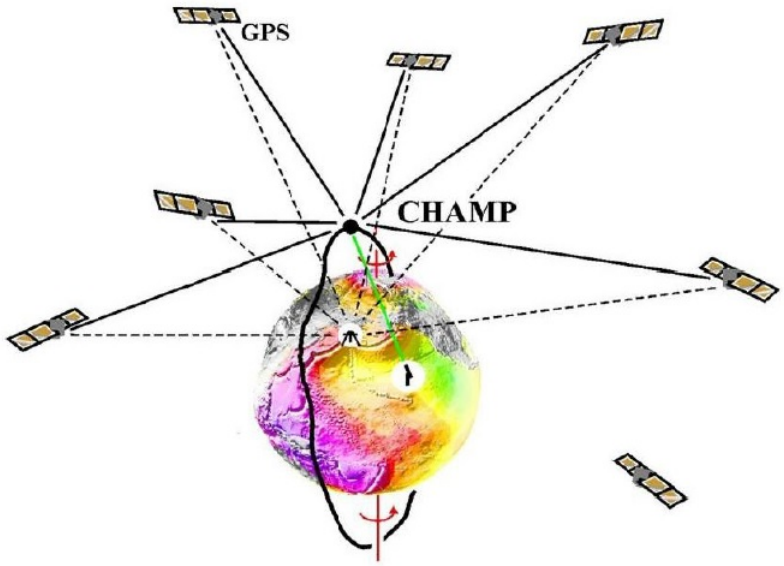

Figure 1.2: *Overview of* CHAMP *mission. For the first time, the gravity field is determined only using data from a single satellite. High-low satellite to satellite (hlSST) provides 3-D coordinates of the position of the satellite using Low Earth Orbiting* (LEO) *(Flechtner, 2014).*

(GRACE) provides an indirect measurement of the time variable part of the Earth's gravity field. GRACE is observing the relative motion of the center of mass of the two satellites by measuring the distance between the satellites with very high precision (Tapley et al., 2004).
GRACE helps hydrologists to analyse water storage changes over landmasses (Lettenmaier and Famiglietti, 2006). The total water storage change is derived from the time-variable part of the Earth's gravity field

$$\Delta TWS(t) = \Delta GW(t) + \Delta SW(t) + \Delta SWE(t) + \Delta SM(t) - \Delta R(t) \tag{1.1}$$

$\Delta TWS(t)$ is total water storage

$\Delta GW(t)$ is ground water

$\Delta SW(t)$ is surface water

$\Delta SWE(t)$ is snow water equivalent

$\Delta SM(t)$ is soil moisture

$\Delta R(t)$ is runoff

Δ is the difference of each quantity between two subsequent time steps

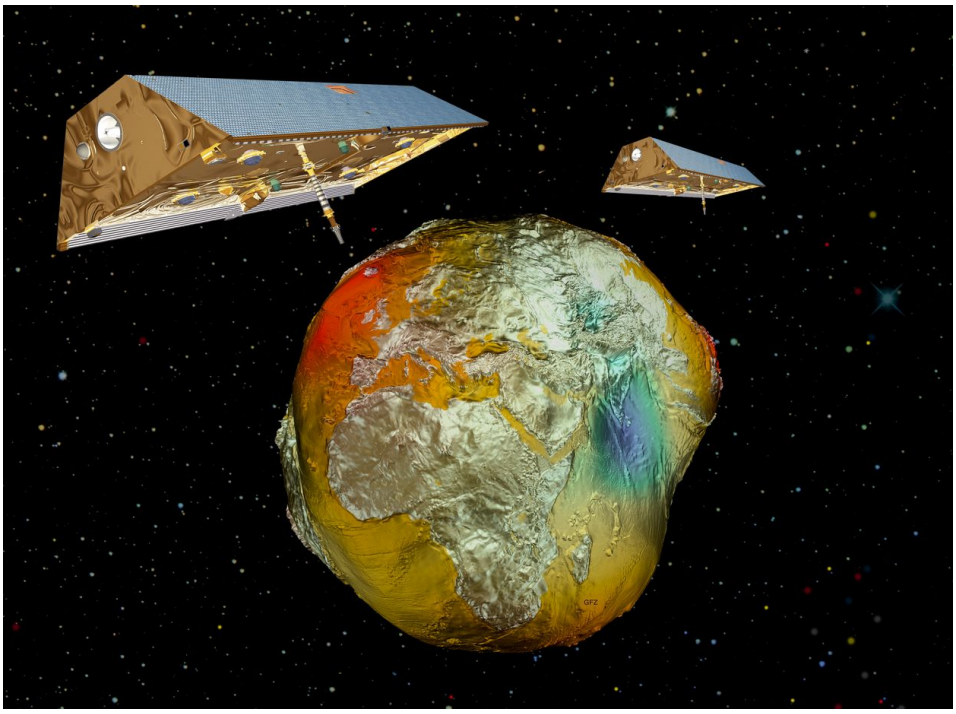

Figure 1.3: *Configuration of Gravity Recovery and Climate Experiment (*GRACE*)(www.space-airbusds.com).*

1.1 Problem statement

Besides the advantage mentioned above of GRACE, the drawbacks should also be mentioned. Wahr et al. (1998) predicted that GRACE would measure the effect of changes in large-scale continental water basin with an accuracy of approximately 2 mm of water equivalent heights. However, this accuracy could not be achieved for the time-variable gravity field because of very high noise content in the coefficients of short-wavelength observed by GRACE (Wahr et al., 2004). These errors show themselves as North-South stripes in spatial domain maps. Therefore, a certain filtering method should be applied to the GRACE data. Due to the filtering process which constrains the noisy signal to a desired output signal, the noise is reduced with the danger of losing the signal as well.

Moreover, GRACE has outlived its predicted lifetime by more than five years (Tapley et al., 2004). Consequently, there is always a high risk of data failure. Figure 1.4 shows an overview of GRACE information on July 22, 2014. The mean altitude of above 6370 km is on the left vertical axis, and solar flux in the right and the year is at

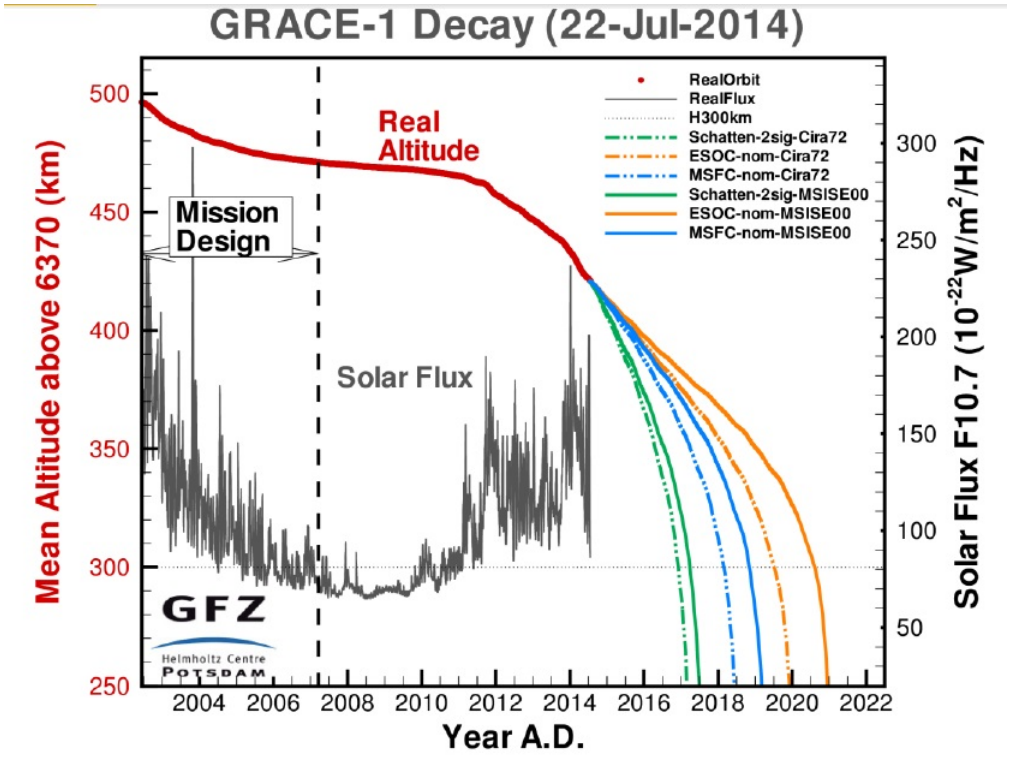

Figure 1.4: *Overview of* GRACE *lifetime predictions. Solar flux is on the right axis, and the mean altitude above 6370 km on the left axis and the year is in the bottom. It shows three different scenarios for estimating the lifetime of the* GRACE *that is based on the amount of cold gas resources and battery life. According to the different scenario, the lifetime of* GRACE *will be finished between till 2020 (*GFZ *Helmholtz Center Potsdam).*

horizontal. As shown in Figure 1.4 shows that solar flux decreased until 2009, and it has an increasing trend from 2009 until 2014. Three different scenarios are predicted to estimate the lifetime of GRACE. Figure 1.4 clearly shows the decreasing altitude of the GRACE satellites. Due to the accelerometer and K-band data problems, some months in the GRACE data set are missing as shown in Figure 1.5. Between 2004 and 2010, no data is missing in the GRACE data set. GRACE Follow On is the next satellite which will be launched late in 2017 (Flechtner et al., 2013). Like GRACE, GRACE Follow On's main objective is to obtain a high-resolution global model of the Earth's gravity field on a monthly basis for an expected length of 5 years. In case of failure of GRACE before launch of GRACE Follow On, a loss of data is expected to happen. Therefore, it would be desirable if some reliable fields of water storage changes are derived from other parameters, such as assimilation of the GRACE data with one hydrological parameter, for instance, the precipitation data.

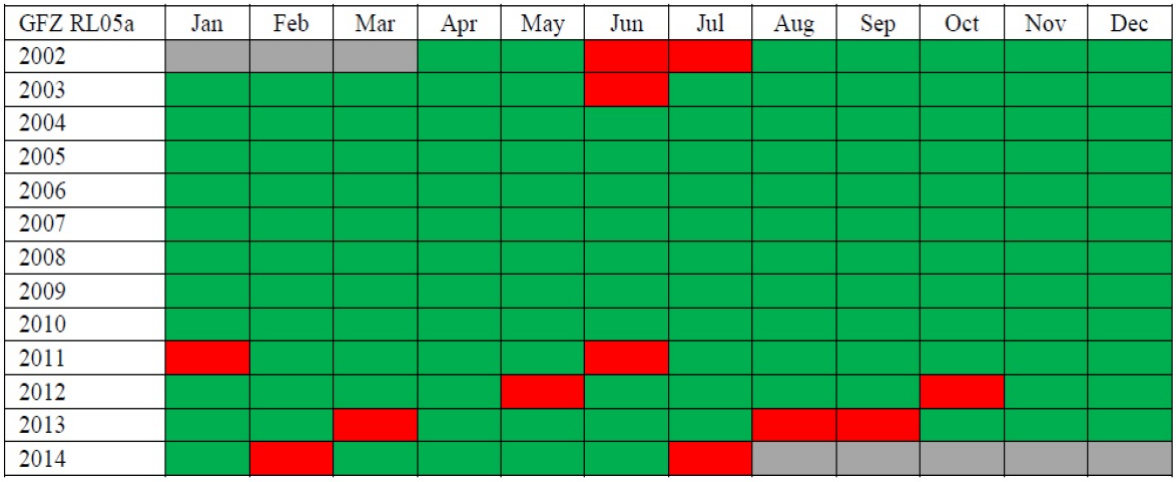

Figure 1.5: *Missed data in* GRACE. *The red boxes are the months when the data is missing, due to accelerometer or accelerometer and K-band data problems (Flechtner, 2014).*

The problems can be categorized as:

- Lack of availability of legacy data for the water storage anomalies
- GRACE data outage in observed GRACE
- GRACE always has a high risk of data gap because it already outlived its predicted lifetime
- The noise level in coefficients with high degree and order, i.e. the coefficients of short-wavelength

1.2 Literature review and research questions

Are there any alternatives for providing reasonable estimation of water storage? Could it be used to bridge the possible gap between the GRACE and GRACE Follow On mission, which will be launched in 2017?

To answer these questions, Weigelt et al. (2013) suggested that hl-SST is a viable source of information for time variable gravity field that can serve to some extent to bridge a possible gap between the end of life of GRACE and the availability of GRACE Follow On. They applied a thorough reprocessing strategy and a dedicated Kalman filter to CHAMP data to show that it is possible to derive the very long-wavelength time variable gravity field features down to spatial scales of approximately 2000 km at the annual frequency and for multi-year trends. They validated the results with GRACE data and surface height changes from long-term GPS ground stations in Greenland.

Rietbroek et al. (2014) published an article entitled "Can GPS-derived surface loading bridge a GRACE mission gap?" They investigated two "gap-filler" approaches based on GPS-derived low-degree surface loading variation (GPS-I) and (GPS-C) and (REF-S) which is a seasonal harmonic variation into the expected GRACE mission gap. Their results show in terms of noise level, the seasonal gap-filler method (REF-S) has a better performance compared to the GPS-I and GPS-C methods, which are still affected by spatial aliasing problems.

Another idea could be finding the relation between the water storage anomalies that is derived from GRACE and hydrologic parameters like precipitation to estimate and assimilate the missing data of GRACE using Copula-based analysis.

Over ten years ago, the Copula-based approach started to be used in different fields of science like economics, hydrology, and meteorology. In finance, the Copula-based method is used for various applications e.g. risk modelling in the market, asset allocation, and derivative pricing (Cherubini et al., 2004; McNeil et al., 2005). In hydrology e.g. (Bardossy and Li, 2008), they borrow the idea of the Copula method, to show the dependency structure without the influence of the marginal distribution. Both the Gaussian Copula and non-Gaussian Copula approaches are used in this paper. The results indicate the non-Gaussian Copulas give better results than the geostatistical interpolations. In meteorology science, Copula-based methods have different applications such as combining radar information and gauge measurements (Vogl et al., 2012). In this study, Copula models are applied to describe the dependency structure between gauge observations and rainfall derived from radar reflectivity at the corresponding grid cells. Also Laux et al. (2011) presented a new Copula-based method for further down-scaling regional climate simulations.

The fundamental concept of the Copula is introduced by Sklar theorem (Sklar, 1959) which is used to model the dependency structure between two or more variables. General information about Copula-based methods can be found in (Joe, 1997) and (Nelsen, 2010). The method exploits linear and non-linear dependency between two or more variables by fitting a theoretical Copula function into an empirical bivariate or multivariate distribution function. Finally, new data, which is consistent with the previously derived dependency structure, can be simulated by evaluating the conditional distribution function given by the theoretical Copula. Different types of theoretical Copula families are defined. One of the most common Copula families is Archimedean Copulas that are used in this thesis.

In this work, two approaches will be discussed, and the applicability of Copula-based methods to spherical harmonic data from GRACE are analyzed. This process involves several drawings of random data, and we are interested to know if this random nature has any impact on the results. Then, filtered data is generated out of unfiltered GRACE coefficients based on their derived dependency structure. Therefore, it is important to find out can Copula-based method find the dependency structure between filtered and unfiltered GRACE coefficients? Is simulated field equal to the

initial filtered GRACE? Does the Copula-based simulation have any impact on the resulting maps of water storage changes?

The second approach is to analyze the potential of the Copula-based approach for simulation and estimation of GRACE data from other hydrological data sources. The method exploits linear and non-linear dependency between two or more variables by fitting a theoretical Copula function into an empirical bivariate or multivariate distribution function. Finally, new data, which is consistent with the previously derived dependency structure, can be simulated by evaluating the conditional distribution function which is given by the theoretical Copula.

Then, the research question can be summarized as below:

1. Can the Copula-based approach be introduced as a tool to smooth (filter) GRACE data?
2. Can the Copula-based approach be used to assimilate hydrological data and GRACE?
3. Can Copula-based approach be used to bridge a possible gap between GRACE and GRACE Follow On?

The thesis is outlined as follows:

Chapter 2 contains brief introduction to fundamental statistical theory including definitions for PDF, CDF. Also, a brief overview of Copula theory is given. Chapter 3 describes spherical harmonic data from GRACE as well as the precipitation data from GPCC (Schneider et al., 2013), which is used in this study.

Chapter 4 discusses how the Copula-based approach can be applied to the GRACE data. The Copula-based approach will be used to capture the dependency of unfiltered and filtered data. In addition, simulated data using Copula-based approach, is compared with filtered data as reference data such as the residual map and the degree variance of the simulated data. Water storage anomalies and RMS of data are analyzed in different catchments. A leave out validation is performed to assess the Copula-based technique performance.

In chapter 5, application of the Copula-based approach is presented. Water storage anomalies estimation using precipitation is discussed. This chapter deals with the question "Can Copula-based approach capture the dependency between precipitation and GRACE data and simulate water storage?"

Chapter 6 provides the conclusion of this study and highlights of the application of the Copula-based approach. Moreover, the outlook for this study which opens rooms for future work, is discussed.

Chapter 2

Method

2.1 Distribution functions of uni-, bi-, and multivariate random variables

2.1.1 Probability Density Function (PDF)

The Probability Density Function (PDF) f_M of a continuous random variable M is a function that describes the probability for the random variable to take on a certain value. The integral of the PDF over a certain range gives the probability that the random variable take on a value within that range. The PDF is denoted by $f_M(m)$ and shown by (Walck, 2007):

$$P(a < M < b) = \int_a^b f_M(m)dm \tag{2.1}$$

Some characteristics of PDFs are as follows:

- $f_M(m)$ is always positive, that is, $f_M(m) \geqslant 0$, for all $M \in (-\infty, \infty)$ (Chan and Tong, 1985).
- The area under the curve $f_M(m) \in (-\infty, \infty)$ is equal to 1.

$$P(-\infty < M < \infty) \equiv \int_{-\infty}^{\infty} f_M(m)dm = 1 \tag{2.2}$$

The bivariate probability density function of M and N has the general form of $f_{MN}(m, n)$. It is given by (King, 2008):

$$\int_{-\infty}^{\infty}\int_{-\infty}^{\infty} f_{MN}(m, n)\, dm\, dn = 1 \tag{2.3}$$

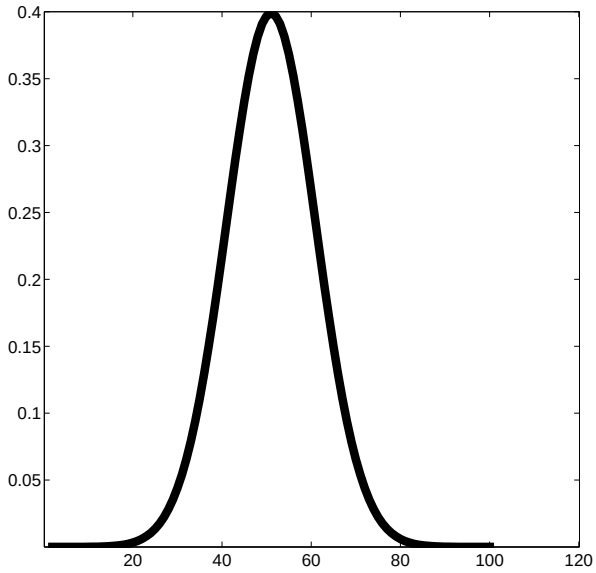

Figure 2.1: *Probability Density Function.* PDF *of a normal distribution with mean (μ)=* 50 *and standard deviation (σ)=*10 *is presented.*

2.1.2 Cumulative Distribution Function (CDF)

The Cumulative Distribution Function (CDF) of a random variable M is given by:

$$F_M(m) = Pr(M \leq m) \tag{2.4}$$

The CDF is given by equation (2.5) (Kottegoda and Rosso, 2008):

$$F_M(m) = \int_{-\infty}^{m} f_M(m)dm. \tag{2.5}$$

The CDF of random data with the mean (μ)= 50 and standard deviation (σ)=10 is shown in Figure 2.2. The properties of CDF are given by:

$0 \leqslant F(m) \leqslant 1$, when $m \in (-\infty, \infty)$,

$F(-\infty) = 0$, $F(\infty) = 1$,

if $m_1 < m_2$ then $F(m_1) < F(m_2)$,

$P(m_1 < m < m_2) = F(m_2) - F(m_1)$.

The joint probability distribution of M and N is expressed with cumulative density function (CDF):

$$F_{MN}(m,n) = Pr(M \leq m, N \leq n) = \int_{-\infty}^{n}\int_{-\infty}^{m} f_{MN}(m,n)dmdn \tag{2.6}$$

Figure 2.3 indicates the bivariate normal distribution of two random variables and their probability density functions.

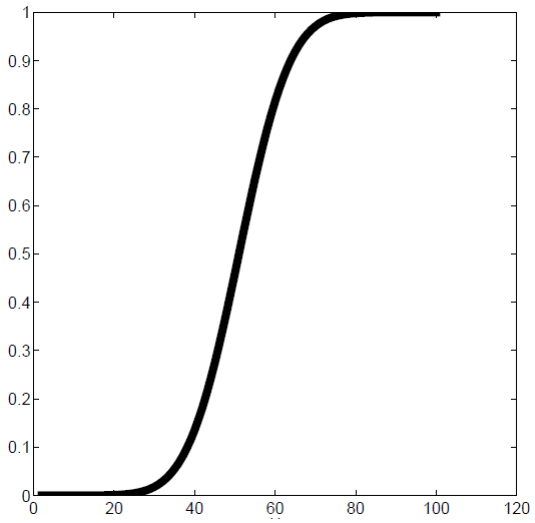

Figure 2.2: *Cumulative Distribution Function "*CDF*" of a normal distribution with mean (μ)=* 50 *and standard deviation (σ)=*10 *is presented.*

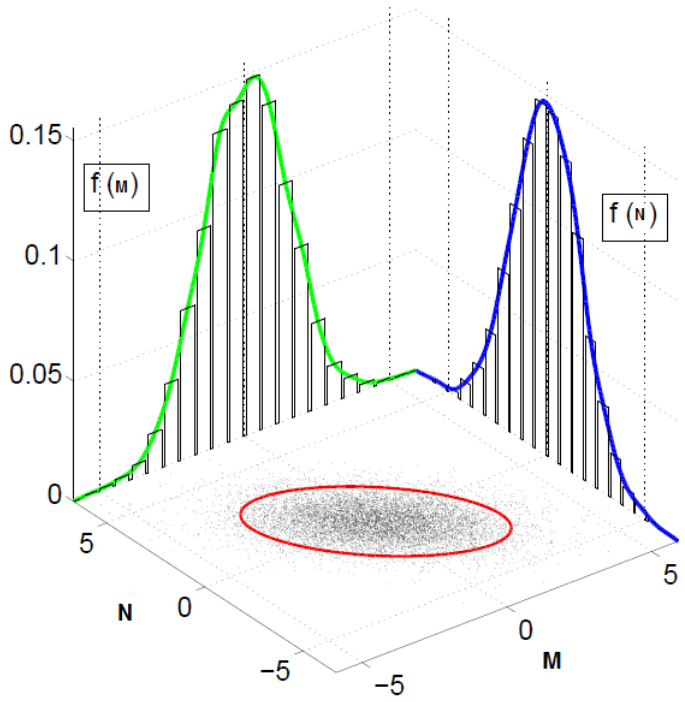

Figure 2.3: *Bivariate normal distribution of two random variables M and N with univariate marginal distributions* PDF*, $f_M(m)$ and $f_N(n)$.*

2.1.3 Marginal distribution

The stochastic behavior of the univariable data is described by its probability distribution. In Figure 2.3, the green and blue lines are the marginal distributions of random variables M and N respectively. For the bivariate case, the marginal distribution of

M is the probability of M over N. Integrating the joint probability distribution over n leads to:

$$F_M(m) = \int_n F_{MN}(m,n)\,dn = \int_n F_{M|N}(m|n)F_n(n)\,dn \tag{2.7}$$

where

$F_{MN}(m,n)$ is the joint distribution of M and N.

$F_{M|N}(m|n)$ is a conditional distribution.

The different types of marginal distributions used in this study are explained in the B.

2.2 Copula theory

Sklar (1959) introduced Copula functions as a powerful tool to model the dependency between variables. The name "Copula" is a Latin word which means a link or tie. Copula-based methods do not require any assumptions regarding the underlying probability distributions of the data. The method exploits the linear and non-linear relationships between two or more variables by fitting a theoretical Copula function into an empirical bivariate or multivariate distribution function. Finally, new data which is now consistent with the previously derived dependency structure can be simulated by evaluating the conditional distribution function which is given by the theoretical Copula. Therefore, it can model complex dependency structures.

2.2.1 Sklar's theorem

Sklar's theorem indicates that a Copula function C connects a given multivariate distribution function with its univariate marginals. For bivariate distribution, for the joint distribution $F_{MN}(m,n)$ with univariate marginal distribution functions $F_M(m)$ and $F_N(n)$, there is a Copula C (Sklar, 1959).

$$F_{MN}(m,n) = C(F_M(m), F_N(n)) = C(x,y) \tag{2.8}$$

$$C : [0,1]^2 \rightarrow [0,1] \tag{2.9}$$

If C is a Copula and F_M and F_N are distribution functions, F_{MN} can be defined as a joint distribution with F_M and F_N. The Probability Density Function (PDF) of the bivariate distribution $f_{M,N}(m,n)$, is represented through:

$$f_{M,N}(m,n) = C(F_M(m), F_N(n)) \cdot f_M(m) \cdot f_N(n) \tag{2.10}$$

where $f_M(m)$ and $f_N(n)$ are the univariate marginal PDFs of M and N. The Copula function is unique when the marginals are continuous.

2.2.2 Characteristic of Copulas

Some characteristics of Copulas are given by (Genest and Rivest, 1993) and (Jaworski et al., 2010). In the bivariate case, a Copula is represented as a function C from $[0,1]^2$ to $[0,1]$ so that $\forall x, y \in [0,1]$:

$$C(x,0) = C(0,y) = 0 \tag{2.11}$$

$$C(x,1) = x \text{ and } C(1,y) = y \tag{2.12}$$

Copula is an increasing function. It implies that $\forall x_1, x_2, y_1, y_2 \in [0,1]$ with $x_1 \leq x_2$ and $y_1 \leq y_2$ holds

$$C(x_2,y_2) - C(x_2,y_1) - C(x_1,y_2) - C(x_1,y_1) \geq 0 \tag{2.13}$$

Copula is a continuous function:

$$|C(x_2,y_2) - C(x_2,y_1)| \leq |x_2 - x_1| + |y_2 - y_1| \tag{2.14}$$

2.2.3 Copula density

The Copula density is computed by differentiating Copula cumulative distribution function.

$$c(x,y) = \frac{\partial^2 C(x,y)}{\partial x \partial y} \tag{2.15}$$

2.2.4 Empirical Copulas

The empirical Copula is an estimator for the unknown theoretical Copula distribution, and it is defined in the rank space. It is defined as (Genest and Rivest, 1993; Laux et al., 2011):

$$C_e(x,y) = \frac{1}{n}\sum_{i=1}^{n} \mathbf{1}(\frac{r_i}{n+1} \leqslant x, \frac{s_i}{n+1} \leqslant y) \tag{2.16}$$

where

$(r_1), \ldots, (r_n)$ denote the pairs of ranks of the data $(m_1, n_1), \ldots, (m_n, n_n)$

n is the length of the data vector

$\mathbf{1}(...)$ is the indicator function. If the condition is true, the indicator function is equal to 1. Otherwise, the indicator function is equal to 0.

2.3 Theoretical Copula

2.3.1 Elliptical Copula

Elliptical Copulas are derived from elliptical distributions. The multivariate normal or Student distribution leads to the Gaussian or t-Copula, respectively. The correlation between two normally distributed random variables x and y is calculated: (Schmidt, 2006) by:

$$Corr(x,y) = \frac{Cov(x,y)}{\sqrt{Var(x)Var(y)}} \tag{2.17}$$

Equation 2.17 describes the linear dependency between x and y. The Gaussian Copula for two variables x and y is defined as:

$$C(x,y) = \Phi_\Sigma(\Phi^{-1}(x), \Phi^{-1}(y)) \tag{2.18}$$

where

Σ is the correlation matrix $\begin{pmatrix} 1 & \rho \\ \rho & 1 \end{pmatrix}$,

Φ_Σ is the CDF of bivariate normal distribution with correlation matrix Σ,

and Φ is the Copula generator.

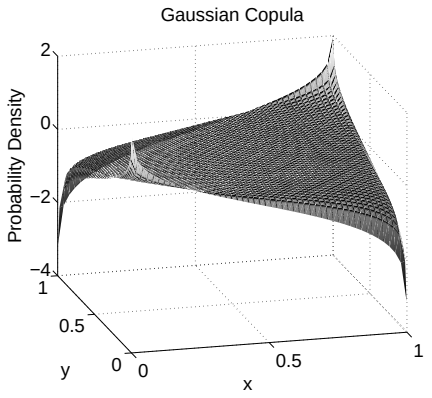

Figure 2.4: *The Gaussian Copula for two random variables x and y with* $\rho = 0.25$.

The t-Copula is derived from the multivariate t-distribution. The t-Copula is given by

$$C(x,y) = t_{\nu,\Sigma}(t_\nu^{-1}(x), t_\nu^{-1}(y)) \tag{2.19}$$

t_ν is a univariate t distribution with degrees of freedom ν

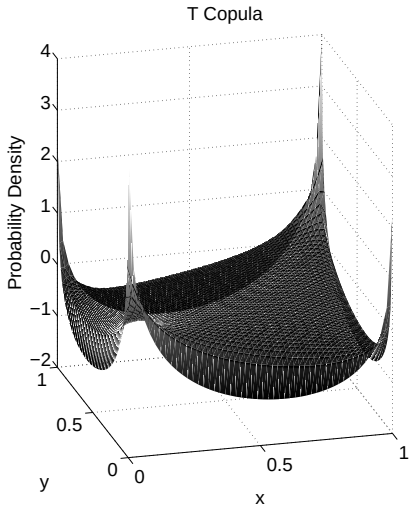

Figure 2.5: *The t-Copula for two random variables x and y with* $\rho = 0.25$.

$t_{\nu,\Sigma}$ is multivariate t distribution with a correlation matrix Σ and degrees of freedom ν

As it can be seen in Figure 2.4 and 2.5, both of Gaussian and t-Copula are defined by the same correlation coefficient $\rho = 0.25$.

The Copula families discussed so far have been derived from certain families of multivariate distribution functions.

On the other hand, a number of Copulas can be estimated directly with the simple form. They are named Archimedean Copulas.

2.3.2 Archimedean Copula

An Archimedean Copula can be presented in the following form:

$$C(x_1, \ldots, x_d; \theta) = \phi^{-1}\{\phi(x_1) + \ldots + \phi(x_d), \theta\} \tag{2.20}$$

where θ is Copula parameter and the function ϕ is the generator of the Copula with the following characteristics (Melchiori, 2003):

- for all $x \in (0,1), \phi(x) < 0$, ϕ is decreasing
- for all $x \in (0,1), \phi(x) < 0$, ϕ is convex
- $\phi(0) = \infty$
- $\phi(1) = 0$

and ϕ^{-1} is defined by

$$\phi^{-1}(t) = \begin{cases} \phi^{-1}(t;\theta), & \text{if } 0 \leq \phi \leq \phi(0) \\ 0, & \text{if} \phi(0) \leq \phi \leq \infty \end{cases}$$

also for bivariate case

$$C(x,y) = \phi^{-1}(\phi(x), \phi(y)). \tag{2.21}$$

They are three commonly used Archimedean Copula which are explained as follows.

1. **Frank Copula**
   The generator of the Frank Copula (1979) is given by

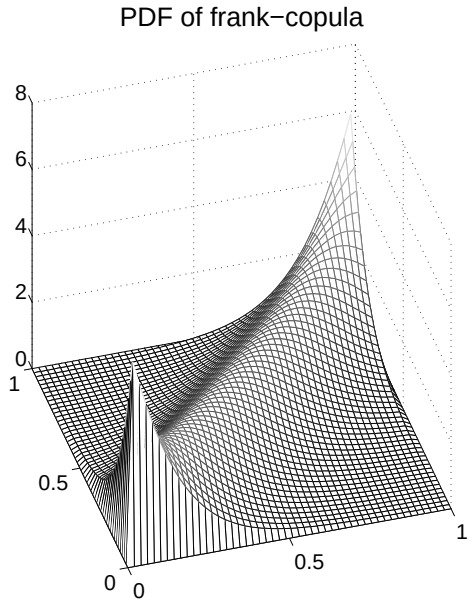

Figure 2.6: *Frank Copula with parameter $\theta = 8$. The Frank Copula is a symmetric Archimedean Copula.*

$$\phi^{Fr}(t) = -\ln\{\frac{e^{-\theta t} - 1}{e^{-\theta} - 1}\} \tag{2.22}$$

The parameter θ is defined over $\in (-\infty, \infty) - \{0\}$. The Frank Copula is given by

$$C_\theta(x,y) = \frac{1}{\theta}\ln(1 + \frac{(e^{-\theta x} - 1)(e^{-\theta y})}{e^{-\theta} - 1}) \tag{2.23}$$

Frank Copula allows to model data with positive and negative dependency. The large positive and negative θ indicate high dependency and $\theta = 1$ implies total independence. The Frank Copula is a suitable method for two data sets with the same dynamic characteristics.

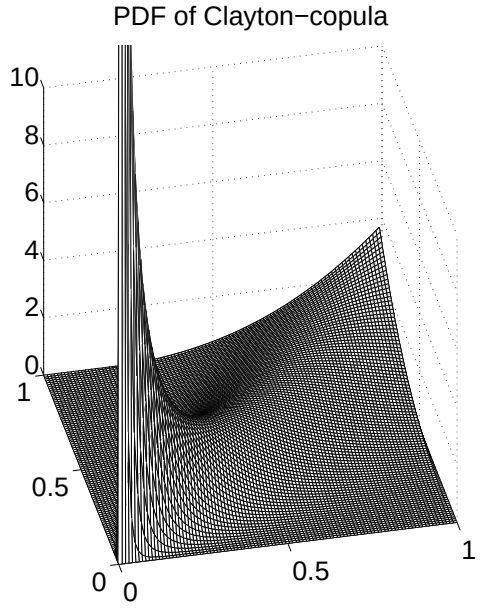

Figure 2.7: *Clayton Copula with parameter $\theta = 3$. The Clayton Copula is an asymmetric Archimedean Copula, it shows greater dependence in the lower tail than in the upper tail.*

2. **Clayton Copulas**
   The generator of the Clayton Copula (Clayton 1978) is given by:

$$\phi^{Cl}(x) = \frac{1}{\theta}(x^{-\theta} - 1) \tag{2.24}$$

   Therefore, the Clayton Copula is defined as

$$C_\theta(x, y) = (x^{-\theta} + y^{-\theta} - 1)^{-\frac{1}{\theta}} \tag{2.25}$$

   where θ is restricted on the interval $[-1, \infty)$. If $\theta = 0$, it shows the independence case and when $\theta \to \infty$, indicate high dependency in the lower rank space.

3. **Gumbel Copulas**

   This Copula is popular for its ability to capture strong upper tail dependence and weak lower tail dependence. Gumbel Copula (1960) is used to model asymmetric relationship in the data (Jaworski et al., 2010). The Gumbel Copula generator is written as:

$$\phi(t)^{Gu} = (-\ln t)^\theta \tag{2.26}$$

   The CDF of the Gumbel Copula is given as

$$C_\theta(x, y) = e^{-((-\ln(x)^\theta) + (-\ln(y)^\theta))^{\frac{1}{\theta}}} \tag{2.27}$$

   The Copula parameter θ is on the interval $[1, \infty)$. If θ is equal 1, Copula shows independence. When $\theta \to \infty$, the Gumbel Copula indicates high dependence between the random variables.

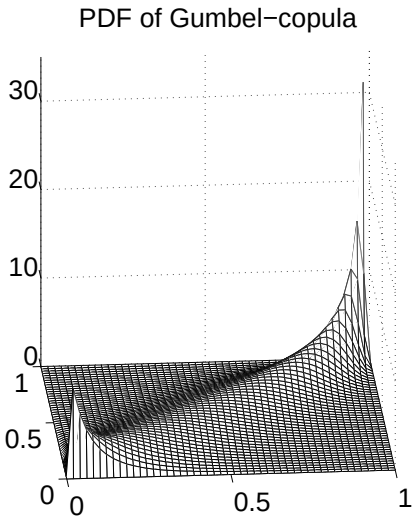

Figure 2.8: *Gumbel Copula with parameter $\theta = 3$. Gumbel Copula can capture strong upper tail dependency and weak lower tail dependency.*

Table 2.1: *Three common families of Archimedean Copulas (Clayton, Frank, and Gumbel Copula) and their generator, parameter space, and their formula. θ is the parameter of the Copula called the dependence parameter, which measures the dependence between the marginal.*

Family	Generator	Parameter	Formula
Clayton	$\phi^{Cl}(t) = \frac{1}{\theta}(t^{-\theta} - 1)$	$-1 \leq \theta$	$C_\theta(x,y) = (x^{-\theta} + y^{-\theta} - 1)^{-\frac{1}{\theta}}$
Frank	$\phi^{Fr}(t) = -\ln\{\frac{e^{-\theta t}-1}{e^{-\theta}-1}\}$	$-\infty < \theta < \infty$	$C_\theta(x,y) = -\frac{1}{\theta}\ln(1 + \frac{(e^{-\theta x}-1)(e^{-\theta y}-1)}{e^{-\theta}-1})$
Gumbel	$\phi(t) = (-\ln t)^\theta$	$1 \leq \theta$	$C_\theta(x,y) = e^{-((-\ln(x)^\theta)+(-\ln(y)^\theta))^{\frac{1}{\theta}}}$

2.3.3 Copula parameter estimation

The widely used estimation method for Copula parameter is the Maximum Likelihood ML estimation methodology. The Copula parameters in this study are derived from ML estimation.

2.3.3.1 CMLE and IFME

Canonical Maximum Likelihood Estimation CLME and Inference for Margins Estimation are two methods for estimation of the Copula parameter. For both methods, the first step is marginal distribution estimation. Then, a pseudo sample of the transformed observation is used to estimate Copula parameter. In the IFME method,

the marginal distribution's parameters are estimated and in the CMLE the univariate marginals are the empirical distribution functions (Giacomini, 2005).

It is assumed that the sample data $(m_1, m_2, m_3, \ldots, m_n)$ are n independent and identically distributed (iid) random variable. These data are transformed into uniform variates $(r_1, r_2, r_3, \ldots, r_n)$. The transformation is the non parametric estimation of the empirical CDF of the marginal distribution.

$$\hat{r_i} = \hat{F_i}(m_i) \tag{2.28}$$

where

$$\hat{F_i}(m) = \frac{1}{n+1} \sum_{i=1}^{n} \mathbf{1}(m_{i,n} \leq m) \tag{2.29}$$

and where **1** an indicator function.

The transformed data r_i have uniform marginal distributions, and they are called pseudo-samples.

$$\hat{u_i} = \frac{1}{n+1} rank(m_i) \tag{2.30}$$

where rank(m_i) is the rank among $i = 1, \ldots, n$ in increasing order.

Let $c(r_1, r_2, r_3, \ldots, r_n)$ be the density function of Copula $C(r_1, r_2, r_3, \ldots, r_n; \theta)$, and let θ be Copula parameter. The Copula parameter θ is estimated by maximizing the Maximum Likelihood equation

$$\hat{\theta} = arg \max_{\theta} \sum_{i=1}^{n} \log c(r_1, r_2, r_3, \ldots, r_n; \theta) \tag{2.31}$$

The interpretation of Copula parameter is shown in Figure 2.9. The Copula parameter $\theta = 1.5$ and 2 and 5 are used in the Copula formula and results are shown as follows:

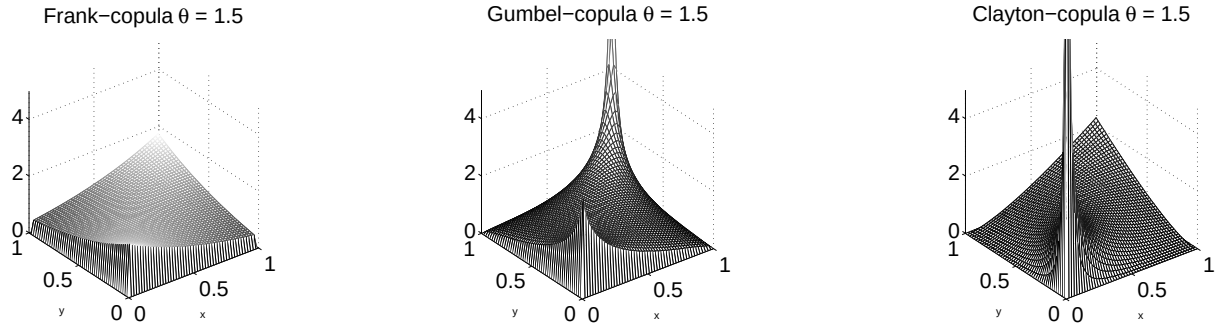

Figure 2.9: *Frank, Gumbel, and Clayton Copula with parameter $\theta = 1.5$. Frank Copula (left) shows a weak tail dependency, Gumbel Copula (center) shows an upper tail dependency and a weak linear dependency, Clayton Copula (right) shows a lower tail dependency in the data and very weak upper tail dependency with Copula parameter $\theta = 1.5$.*

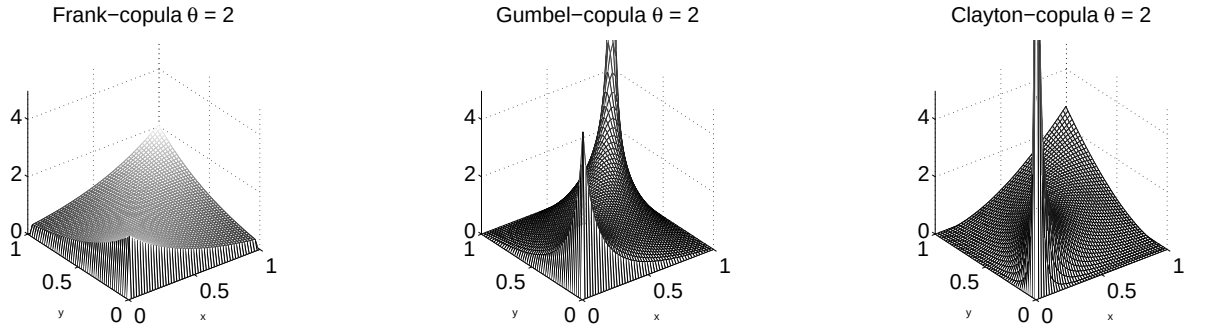

Figure 2.10: *Frank, Gumbel, Clayton Copula with parameter $\theta = 2$. Frank Copula (left) represents weak tail dependency and Gumbel Copula (center), there is upper tail dependence and weak linear dependency, Clayton Copula (right) shows a clear lower tail dependence between x and y with Copula parameter $\theta = 2$.*

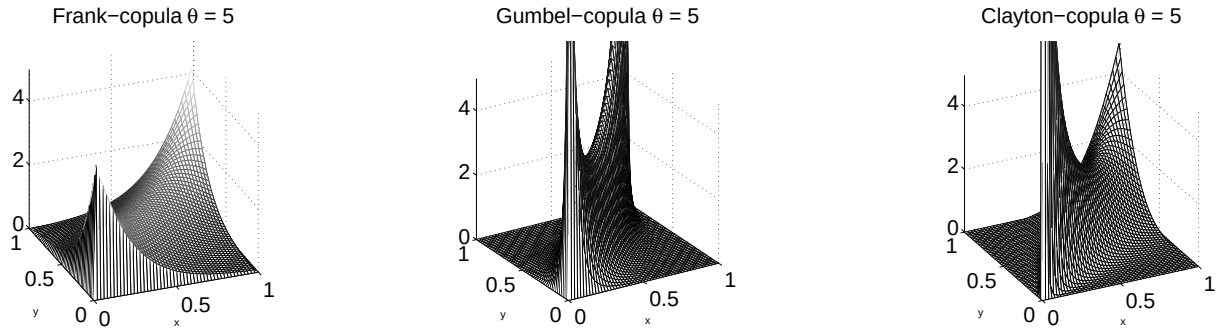

Figure 2.11: *Frank, Gumbel, Clayton Copula with parameter $\theta = 5$. Frank Copula (left) shows a weak tail dependency and Gumbel Copula (center), upper tail dependence also shows a linear dependency with dependency in lower part appears, Clayton Copula (right) indicates very high dependency on lower tail part with Copula parameter $\theta = 5$.*

2.4 Computation of conditional CDF of Archimedean Copula

In this section, the conditional CDF of Clayton, Frank, and Gumbel Copula are computed. The conditional CDF Clayton Copula is given by:

$$C_{Y=y}^{Clayton}(x,y) = x^{-\theta-1}(-1+x^{-\theta}+y^{-\theta})^{(\frac{-1}{\theta}-1)} \tag{2.32}$$

and for Frank Copula:

$$C_{Y=y}^{Frank}(x,y) = \frac{e^{-x\theta}(-1+e^{-y\theta})}{(-1+e^{-\theta})(1+\frac{(-1+e^{-x\theta})(-1+e^{-y\theta})}{-1+e-\theta})} \tag{2.33}$$

The conditional CDF Gumbel Copula is:

$$C_{Y=y}^{Gumbel}(x,y) = \frac{(-\ln x^{\theta-1})(\ln y^{(\theta-\ln y^{\theta})^{(\frac{1}{\theta}-1)}})}{xe(-\ln x^{(\theta+\ln y^{\theta})^{(\frac{1}{\theta})}})} \tag{2.34}$$

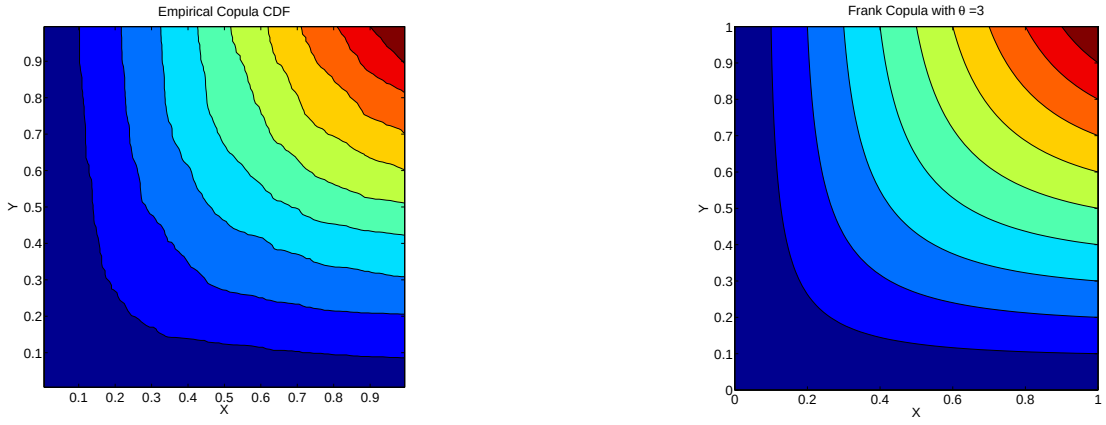

Figure 2.12: *empirical Copula (left) of two random variables and corresponding Frank Copula (right) that fitted to it.*

Figure 2.12 shows the empirical Copula of two random variables. The Frank Copula (right) is fitted to the empirical Copula. The Figure 2.13 shows the conditional CDF of Frank Copula which is simulated with Copula parameter $\theta = 3$ between two arbitrary random variables x and y. The conditional cumulative CDF is shown for different values of y. It shows the different probability for different values of y. It shows that all values for $y = 0.5$ have equal probability. However, the probability of values is not equal to other lines which are shown in this figure.

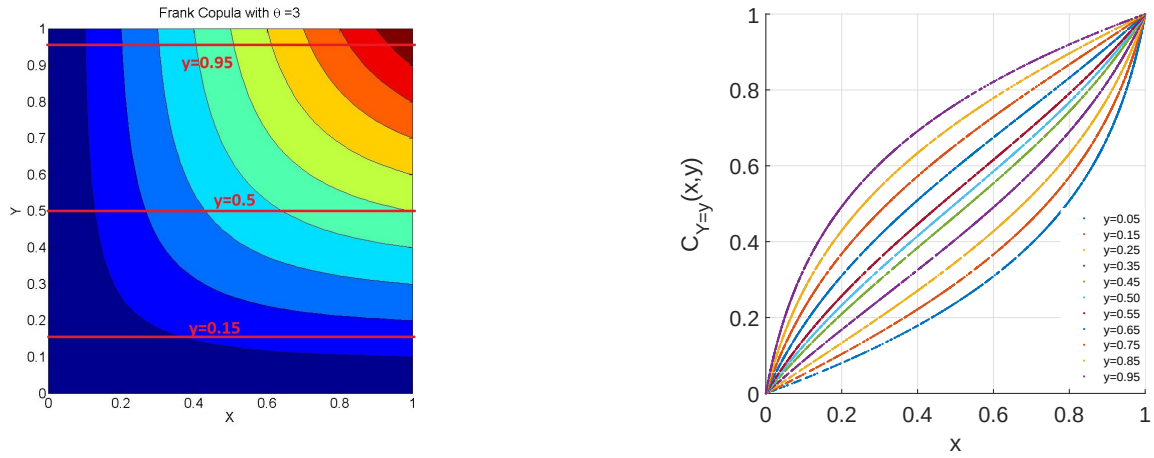

Figure 2.13: *The conditional* CDF *Frank Copula with parameter* $\theta = 3$ *and* $y = 0.05, \ldots, 0.95$.

2.5 Simulating from Copula-based conditional random data

This section provides the essential steps for simulation data using Copula-based conditional random data. The following steps are taken to fit the suitable theoretical Copula function and assimilate data (Laux et al., 2011; Vogl et al., 2012).

1. Independent identically distribution (iid)-transformation of input time-series.
2. Compute the marginal distribution $F_M(m)$ and $F_N(n)$ of the input data M and N.
3. Transform data to rank space using the estimated marginal distributions of data with r_i and s_i in rank space.
4. Compute the empirical Copula to the dependence structure of random variables using the rank transformed data.

$$C_e(x,y) = \frac{1}{n}\sum_{i=1}^{n} \mathbf{1}\left(\frac{r_i}{n+1} \leqslant x, \frac{s_i}{n+1} \leqslant y\right) \tag{2.35}$$

5. Fit a theoretical Copula function $C_\theta(x,y)$.
6. Compute the conditional Copula function,

$$P(X \leqslant x \mid Y = y) = \frac{\partial}{\partial_y} C(x,y) \tag{2.36}$$

7. Sample random data from the conditional Copula CDF.
8. Transfer the sample back to the data space using the inverse marginal.

Chapter 3

Data

3.1 GRACE

3.1.1 Mission states

The Gravity Recovery and Climate Experiment GRACE was launched on March 17, 2002 as a joint project between the US National Aeronautics and Space Administration (NASA) and German Aerospace Center (DLR). The initial goal of the project was to provide a high-resolution global model of the Earth's static and time-variable gravity field (Tapley et al., 2004).

The mission was expected to last for five years (Tapley et al., 2004), but GRACE is still in orbit. Application of GRACE in the determination of the gravity variations is useful in a variety of scientific research areas such as hydrology (Ramillien et al., 2004), oceanography (Chambers and Willis, 2009), and solid Earth sciences (Swenson et al., 2008).

The GRACE-mission satellite consists of two identical spacecrafts equipped with a GPS flight receiver very similar to CHAMP satellite. These spacecrafts move in a nearly polar orbit with the inclination of 89° and an altitude of approximately 500 km. Both satellites measure the distance to each other through K-band microwave ranging instrument. The absolute positions of the two spacecrafts are measured by GPS receiver and twin star cameras. The twin satellites are also equipped with a precise accelerometer, which can measure the non-gravitational acceleration.

GRACE satellites are tracking each other in Low Earth Orbit (LEO), so GRACE is called low-low satellite to satellite tracking (LL-SST) mission. The Earth's gravity field variation can be determined by using the observed changes in the inter-satellite distance, position, and acceleration of each satellite (Han, 2003).

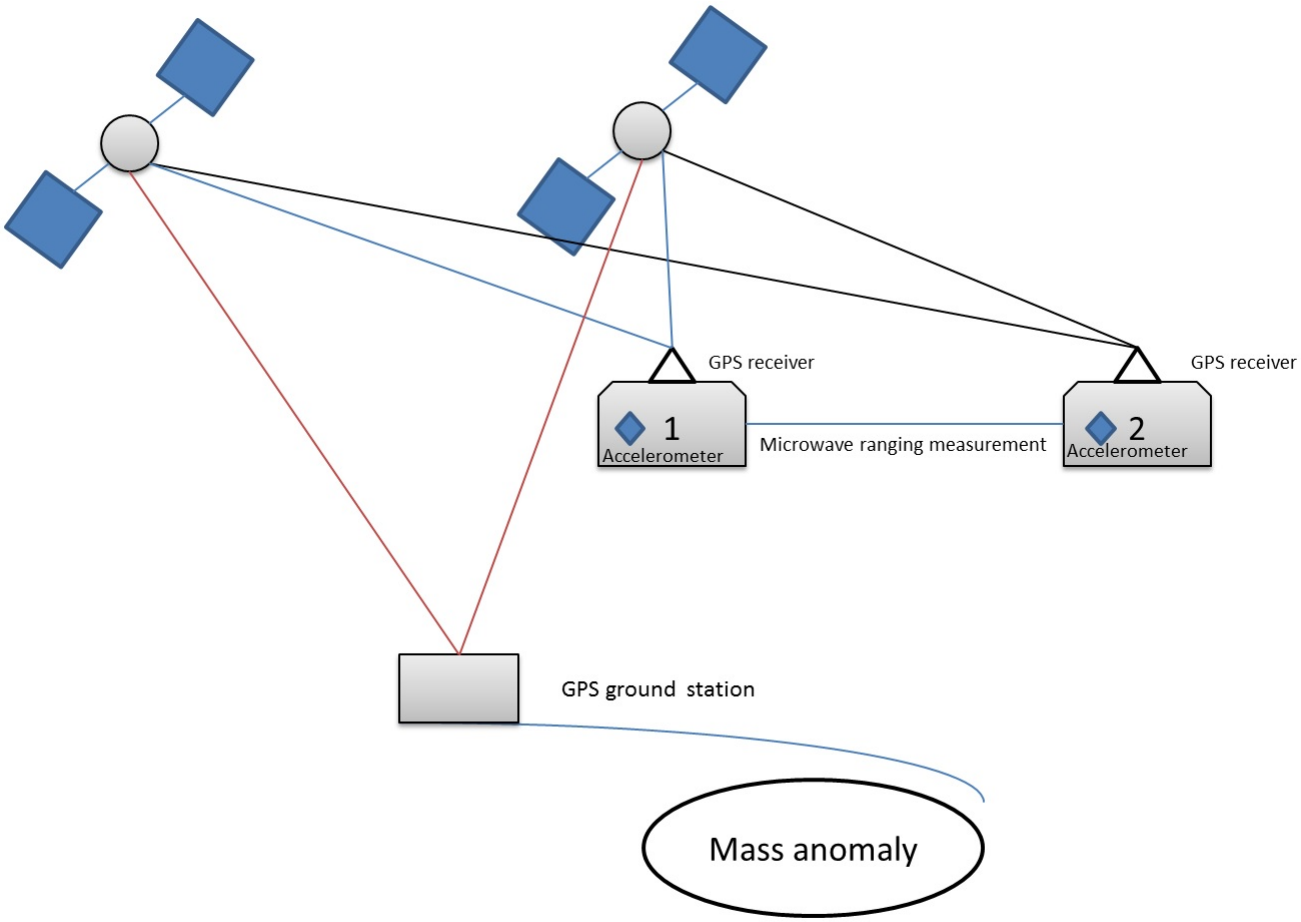

Figure 3.1: GRACE *mission concept.* GPS *satellites measure the absolute position of twin satellites and transmit the measurement to the* GPS *ground station for further processing. The distance between these two satellites is measured through the measurement of K-band distance. The non-gravitational acceleration is measured in each spacecraft precisely.*

As it is shown in Figure 3.1, these two satellites constantly maintain a two-way microwave-ranging link between them. This system detects the distance between the satellites with an accuracy of about $1\mu m$. The variation in the computed inter-satellite range can be transformed into the variation of the Earth's gravity field (Han, 2003).

3.1.2 Data source

The GRACE coefficients are provided by four different institutes: The Geo Forschungs Zentrum (GFZ) in Potsdam, Germany, the Center of Space Research (CSR) in Austin, Texas, the Centre National D'Etudes Spatiales (CNES) in Toulouse, France, the Jet Propulsion Laboratory (JPL) in Pasadena, California. In this thesis, the data are used from CSR. The CSR provides spherical harmonic coefficients up to the degree and order of 60.

In this thesis, 5 years of GRACE data (2005–2009) from CSR is used. The data is given in terms of spherical harmonics. Due to some problems in orbital configuration and de-aliasing products, high-frequency noise can be seen in the spherical harmonic. The noises present themselves as North-South stripes. Therefore, to eliminate the noise, we need to apply a filter to the data. A regularization filter, which is described in (Lorenz, 2009) and (Sneeuw et al., 2014), is applied to decrease the high noise content in the higher frequencies of the GRACE data. The degree 0 and 1 coefficients were removed throughout our computations, as GRACE is blind towards these coefficients. In this research, the monthly data is used from January 2005 until December 2009.

3.2 Data preprocessing

3.2.1 Removing degree 0 and 1

Degrees 0 and 1 are removed from the data sets. The GRACE coefficients are sorted by coefficient from of January 2005 until December 2009. As it can be seen in Figure

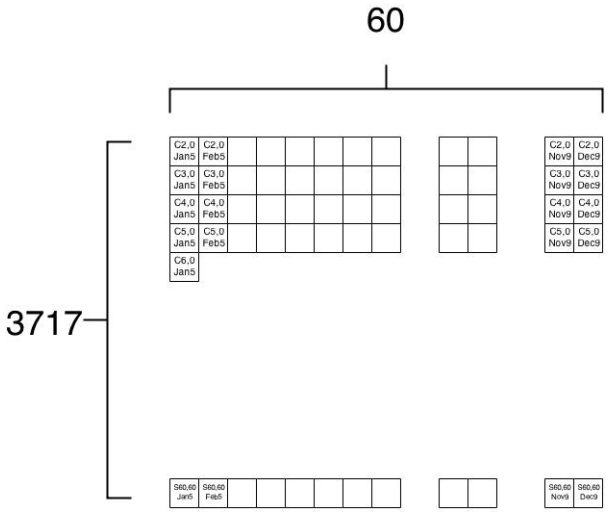

Figure 3.2: *The spherical harmonic coefficients are sorted in sixty months. There are monthly data from January 2005 till December 2009.*

3.2, the 3717 coefficients within 60 months are stored in a matrix with the size of $[3717 \times 60]$. This arrangement is applied to both filtered and unfiltered GRACE-coefficients.

3.2.2 Removing annual cycle

First, the annual cycle of the data is removed. Then, these data are assumed to be independent and identically distributed (iid, Knill, 2009). Time series data are sometimes influenced by annual effects. These effects can bring about changes in the data that normally occur at the same time, and in about the same magnitude, every year. The filtered and unfiltered GRACE coefficients show annual cycle as shown in Figure 3.3, which is caused auto-correlation in the filtered and unfiltered GRACE coefficient.

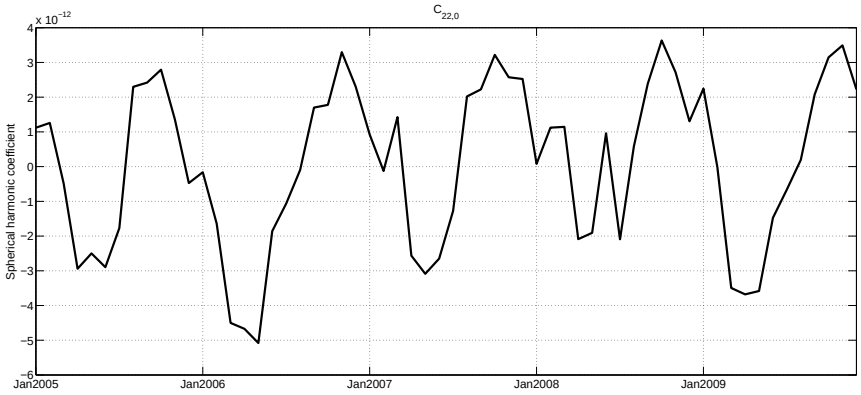

(a) $C_{22,0}$ before removing the annual cycle

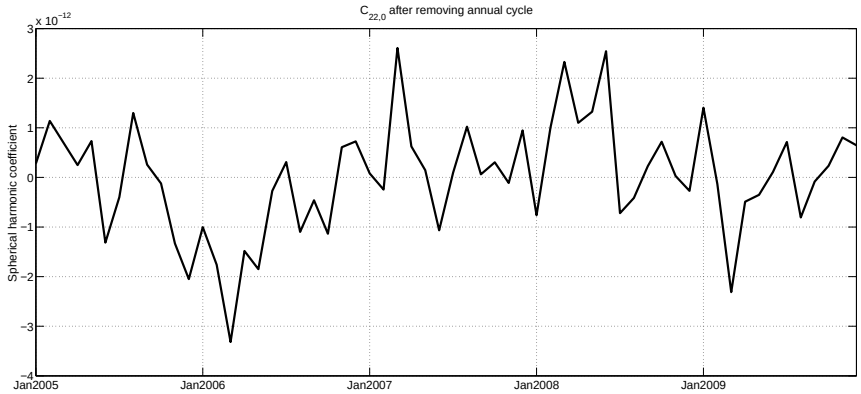

(b) $C_{22,0}$ after removing the annual cycle

Figure 3.3: *Time series of $C_{22,0}$ (degree of 22 and order of 0) in filtered* GRACE *(left). Time series of $C_{22,0}$ in filtered* GRACE *after removing the annual cycle (right).*

Figure 3.3 (a) shows $C_{22,0}$ from January 2005 until December 2009. The time-series clearly shows an annual cycle. One way to remove this effect is subtracting the mean annual cycle from the data. Therefore, the mean of January, February, ..., December is removed from the respective month in the GRACE data. The mean annual cycle is derived from 5 years of GRACE-data (2005 – 2009). The Figure 3.3 (b) shows $C_{22,0}$ after removing the annual cycle.

3.3 Precipitation

Precipitation data is provided from different data sources, e.g. the Global Precipitation Climatology Center "GPCC" (Schneider et al., 2013), Global Precipitation Climatology Project "GPCP" (Adler et al., 2003), Climate Prediction Center precipitation "CPC" (Chen et al., 2008), Climatic Research Unit "CRU" (Harris et al., 2013) and University of Delaware "DEL" (Matsuura and Willmott, 2012).

Among the available precipitation data sets, the Global Precipitation Climatology Center (GPCC) seems to deliver the most reliable data and widely used for precipitation (Lorenz and Kunstmann, 2012). Therefore, precipitation data from GPCC has been used for this study. It is developed on the basis of the most comprehensive database of monthly observed worldwide precipitation data. Between 10,000 and 40,000 stations contribute to GPCC for monthly data collection. In GPCC, some processing steps are also taken, including quality control, quality assurance, and interpolation to the desired grid size.

In this study, the precipitation data are transformed to the spherical harmonic coefficients (Sneeuw, 1994).

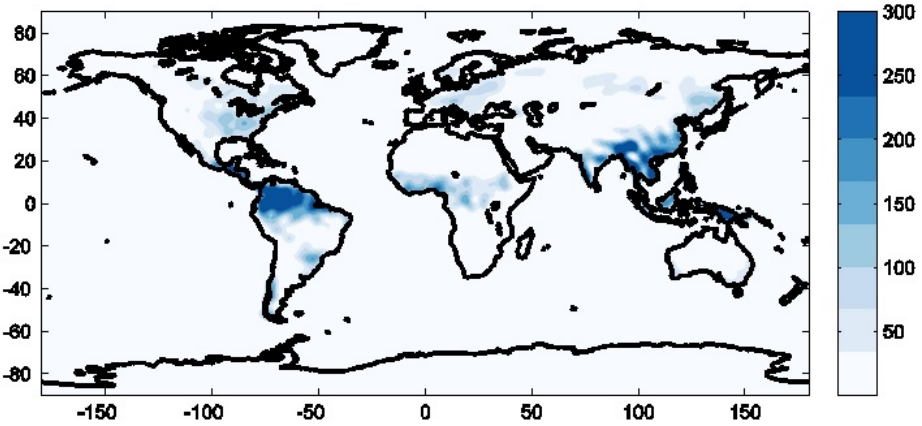

Figure 3.4: *Precipitation data in July 2009 [mm]. This data is provided from* GPCC.

Chapter 4

Proof of concept

In this chapter, the applicability of Copula-based methods in case of Spherical Harmonic Coefficients (SHC) derived from GRACE is analysed. As the approach involves several drawings of random data, the impacts of this random nature on the results are studied. The Copula method is applied to both unfiltered and filtered GRACE data. Then filtered data are generated out of the unfiltered GRACE coefficients, based on formerly derived dependency structure.

As a stochastic filtering is applied to the GRACE data, it can be assumed that a linear dependency exists between the unfiltered and filtered data. In order to capture the dependency structure between unfiltered and filtered GRACE coefficients, two approaches are studied in this thesis:

1. Applying the Copula-based approach to monthly data and finding the relation between one month in unfiltered and the corresponding month in filtered GRACE coefficients data.
2. Applying the Copula-based approach to each of the coefficients in the period from 2005 to 2009. Finding the relation between one time series of the coefficient in unfiltered and corresponding coefficient in filtered GRACE data.

In the first approach, the dependency structure between filtered and unfiltered data are derived for all SH-coefficients from a single month. In other words, all 3721 coefficients from one month for filtered data set and all 3721 coefficients from the same month for the unfiltered data are analysed. In the second approach, for each SH-coefficient the dependency structure from the time-series of the whole 60 months is derived separately.

4.1 Applying Copula-based method to monthly data

The monthly data are transformed to normalized rank space. The filtered and unfiltered GRACE coefficients show a linear dependency as it is shown in Figure 4.1.

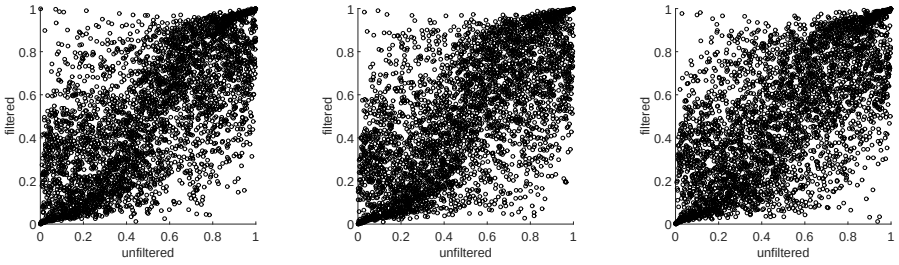

(a) January 2005 **(b)** February 2005 **(c)** March 2005

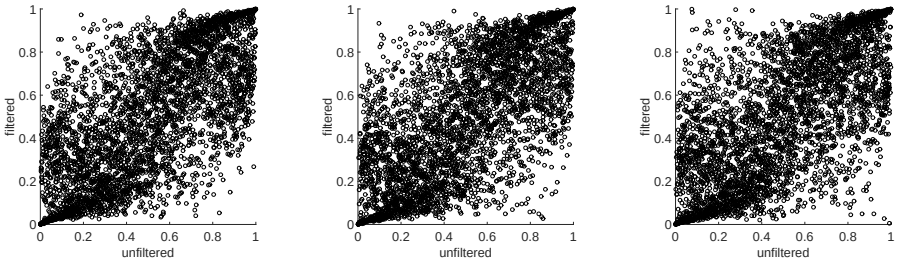

(d) April 2005 **(e)** may 2005 **(f)** June 2005

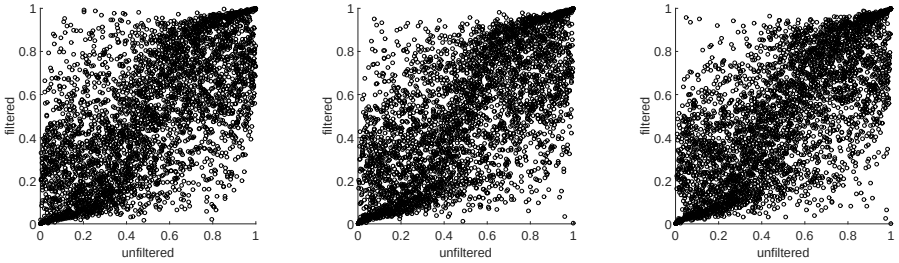

(g) July 2005 **(h)** Aguest 2005 **(i)** September 2005

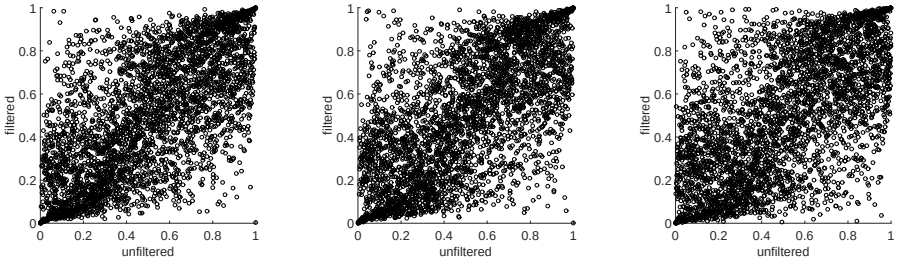

(j) October 2005 **(k)** November 2005 **(l)** December 2005

Figure 4.1: *Filtered and unfiltered* GRACE *coefficients in 2005.*

As it is shown in Figure 4.1, we can assume the Copula-based approach is able to find this dependency structure between filtered and unfiltered data. Therefore, the Copula-based method is studied for monthly filtered and unfiltered GRACE coefficients. The processes of applying Copula-based technique are explained in detail in chapter 2. All steps are also shown as an algorithm in Figure 4.2.

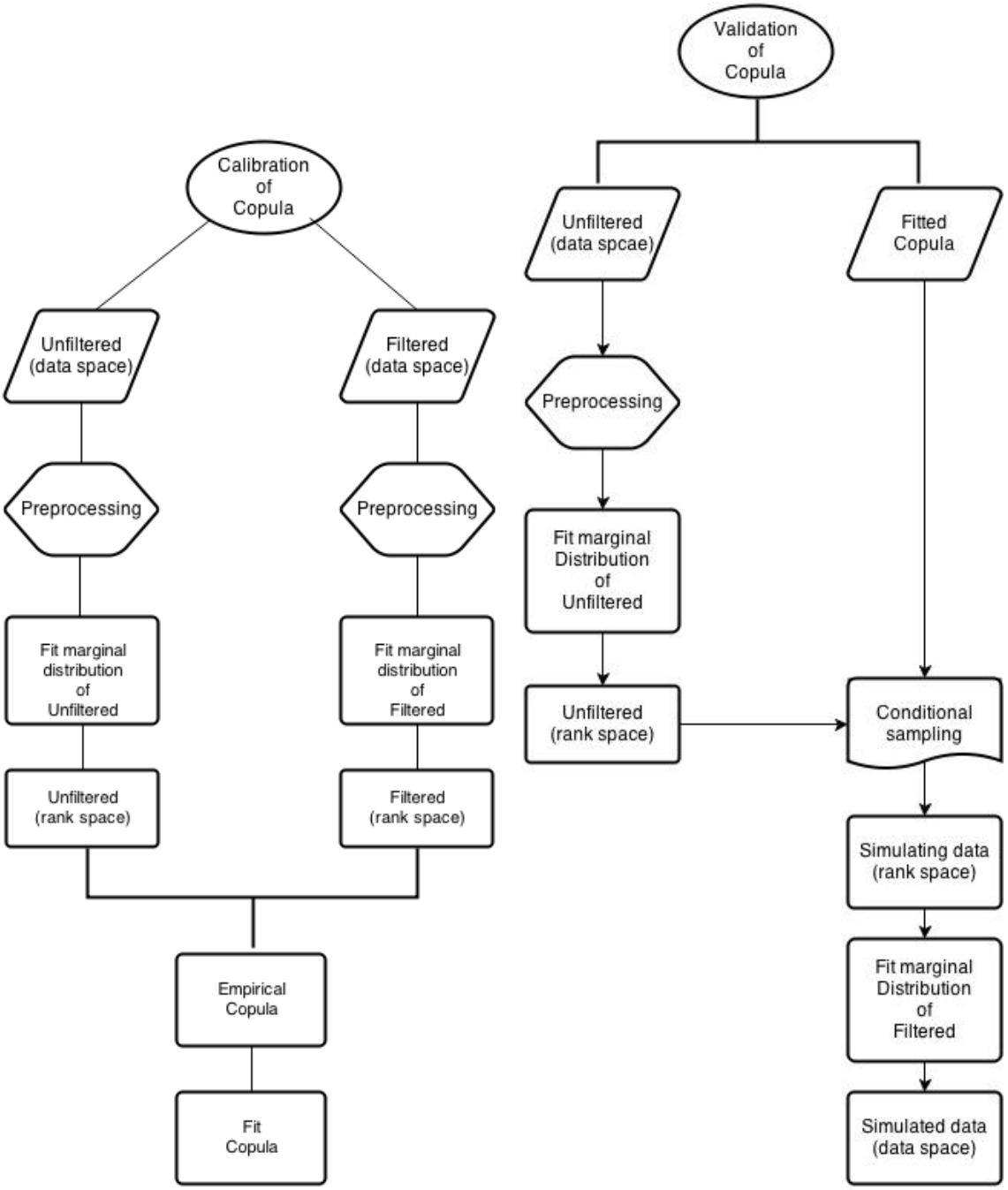

Figure 4.2: *Overview of the fitting the theoretical Copula to bivariate data and simulating data using Copula approaches. Two monthly data sets are shown for unfiltered and filtered* GRACE*-coefficients. Marginal distributions are fitted to both filtered and unfiltered* GRACE*-coefficients, respectively. These distributions can be used for transforming the data from the data to the rank space. In the next step, an empirical Copula is computed. Then, a theoretical Copula is fitted to the empirical distribution function, and data are simulated. As the data are simulated in rank space, simulated data must be transformed to data space.*

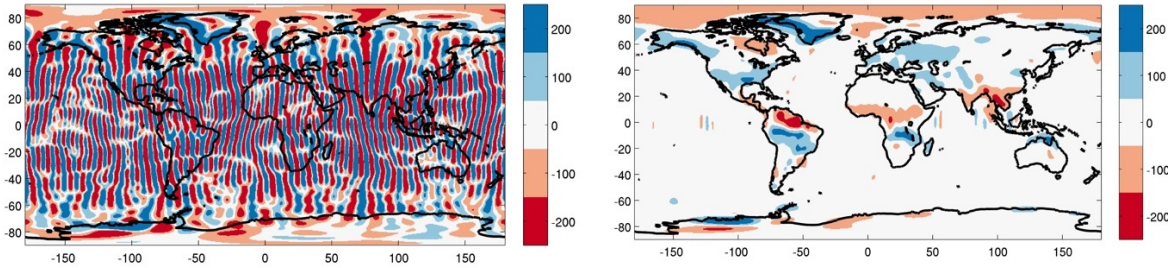

Figure 4.3: *Unfiltered (left) and filtered (right)* GRACE *data in February 2005 [mm]. As it can be seen, the noisy data in higher degrees show themselves in the map as North-South strips (Swenson and Wahr, 2006). On the right side, North-South strips are removed from the map. Some patterns are shown in South America, Himalayas and West Africa. These patterns show the water storage anomalies in February 2005.*

The monthly unfiltered and filtered GRACE data is shown for February 2005 in Figure 4.3. The Copula-based approach is expected to find the dependency structure between unfiltered (left) and filtered (right) data. The results of Copula-based random data from Clayton, Gumbel, and Frank Copula are shown as follows:

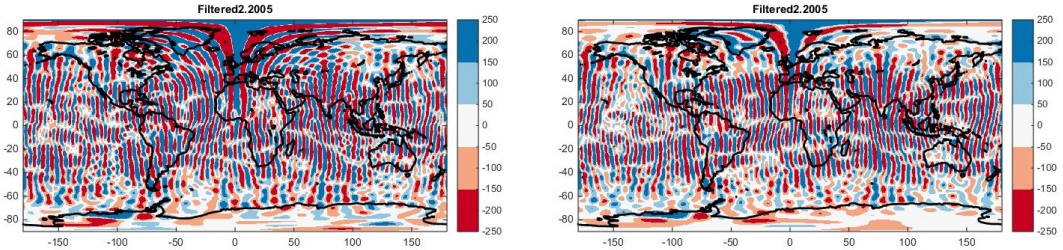

(a) Clayton **(b)** Gumbel

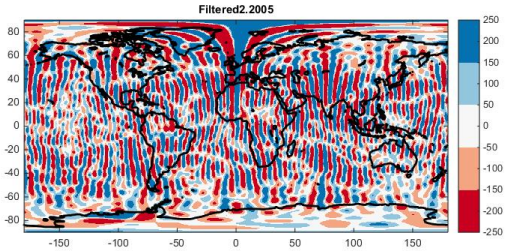

(c) Frank

Figure 4.4: *Copula-based derived random data from Clayton, Gumbel, and Frank Copula in February 2005.*

As it can be seen in Figure 4.4 the North-South stripes are still on the maps. The results show that Copula-based approach is not able to remove noisy data and simulate the filtered data in the monthly approach. One reason for failing the Copula-based approaches in monthly studies can be related to the marginal distribution of unfiltered and filtered GRACE coefficients that are shown in Figure 4.5.

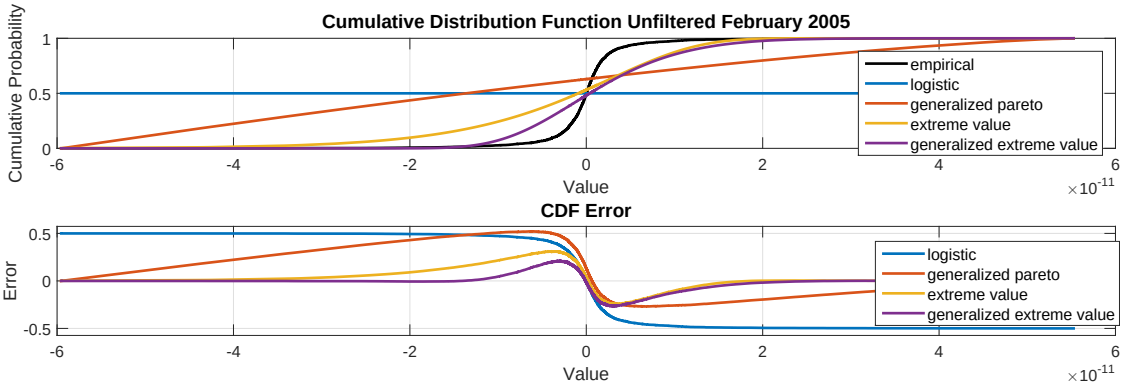

(a) Unfiltered

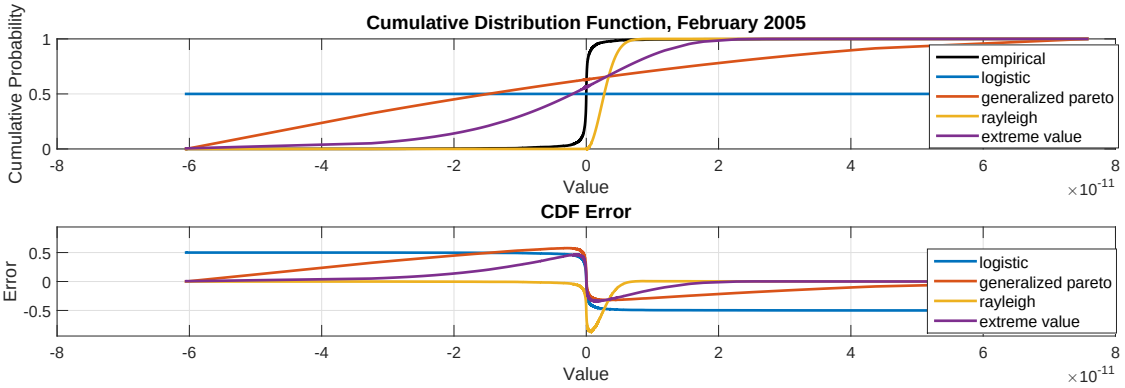

(b) Filtered

Figure 4.5: *Fitting the marginal* CDF *to unfiltered and filtered* GRACE *coefficients in February 2005.*

Figure 4.5 shows the theoretical marginal CDF distributions cannot fit to the empirical CDF distributions especially around zero. As the Figure 4.1 shows, there is still a possibility to capture the dependency of the monthly coefficients. Therefore, finding a suitable marginal distribution for monthly GRACE coefficients can be suggested for future studies. In the second approach, the Copula-based method is applied to each coefficient separately for the period from January 2005 until December 2009.

4.2 Applying Copula-based method to each coefficient

4.2.1 Fitting marginal distribution

The CDF marginal distribution of three different coefficients and their errors are presented in Figure 4.6. In this subsection, $C_{3,02}$ in lower degrees, $C_{21,00}$ in middle degrees, and $C_{59,01}$ in higher degrees are studied. The empirical (black), logistic (blue), generalized extreme value (green), t-location-scale (light green), extreme value (red), generalized Pareto (orange) and normal (light blue) are indicated in this figure.

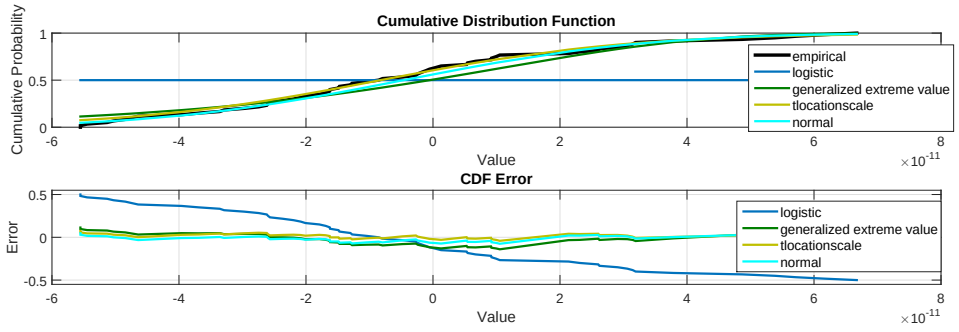

(a) $C_{3,02}$ unfiltered

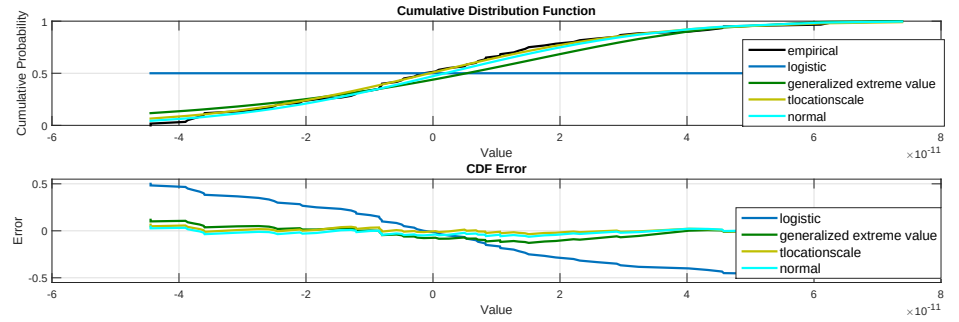

(b) $C_{3,02}$ filtered

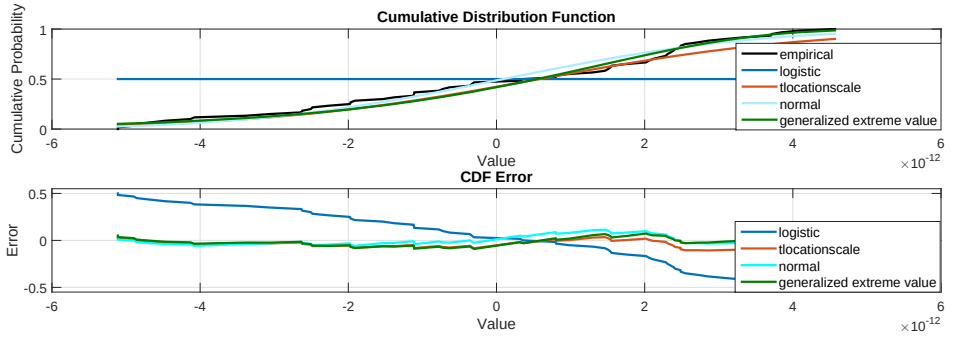

(c) $C_{21,00}$ unfiltered

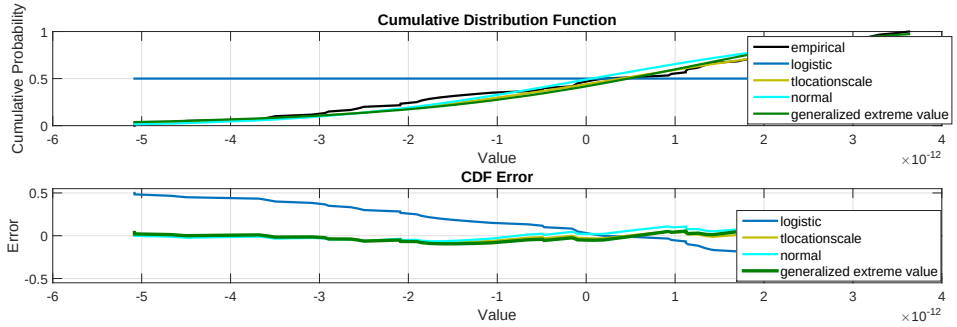

(d) $C_{21,00}$ filtered

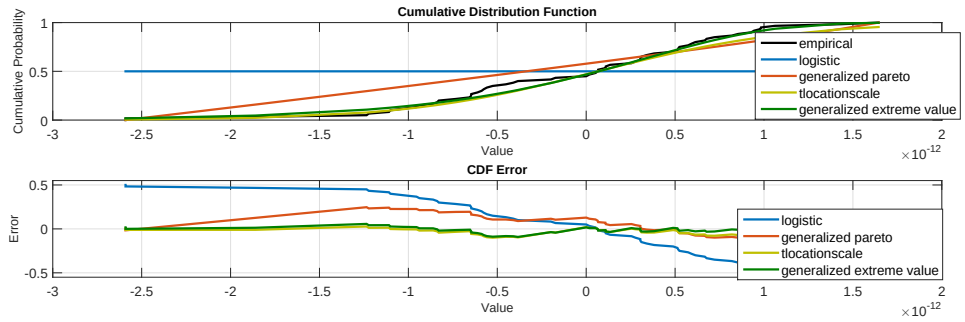

(e) $C_{59,01}$ unfiltered

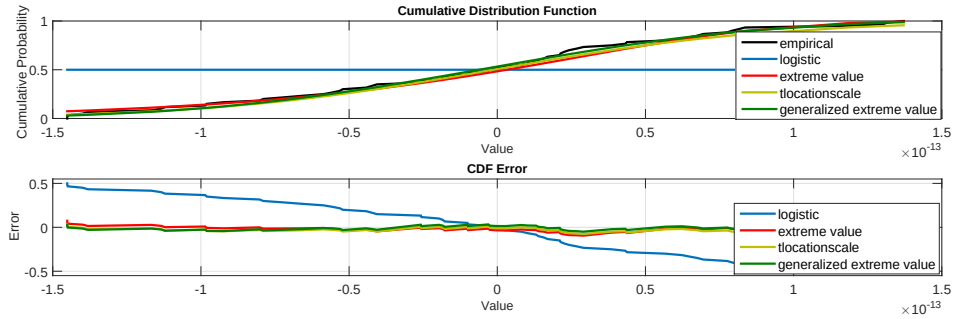

(f) $C_{59,01}$ filtered

Figure 4.6: *Marginal* CDF *distribution and their error for three different coefficients.*

In case of $C_{3,02}$, the generalized extreme value, t-location-scale, and normal distribution dedicate very small error in both the filtered and unfiltered GRACE coefficients. Also for $C_{21,00}$ degree 21 and order 0, as it can be seen in the Figures 4.6 c and d, t-location-scale, normal and generalized extreme value show better performance. They fit to empirical CDF distribution with very small error.

As it is shown in Figure 4.6 (e), for $C_{59,01}$ unfiltered GRACE coefficient, generalized extreme value and t-location-scale show less error compared to generalized Pareto. In case of $C_{59,01}$ filtered GRACE coefficient, extreme value (red), t-location-scale (light green) and generalized extreme value (green) are fitted to the empirical (black) distribution with very small error. For all the three coefficients shown, logistic

distribution function does not fit to the empirical CDF distribution.

As in all three coefficients, generalized extreme value CDF distribution gives better results with less error, in this study generalized extreme value distribution is used. However, selecting a suitable marginal CDF distribution still open to be investigated. Therefore, for future research, another marginal CDF distribution can be studied. For more information about theoretical distributions, which are performed to find the best-fitted distribution, see Appendix B.

4.2.2 Transforming data into rank space

The filtered, and unfiltered GRACE coefficients are transformed from data space to the normalized rank space of $[0, 1]$. The unfiltered and filtered GRACE coefficients show a linear dependency. Also the higher degrees show some linear dependency, even if there is more scattering than in the lower degrees. It is also the same for the other coefficients which are presented in Appendix D.

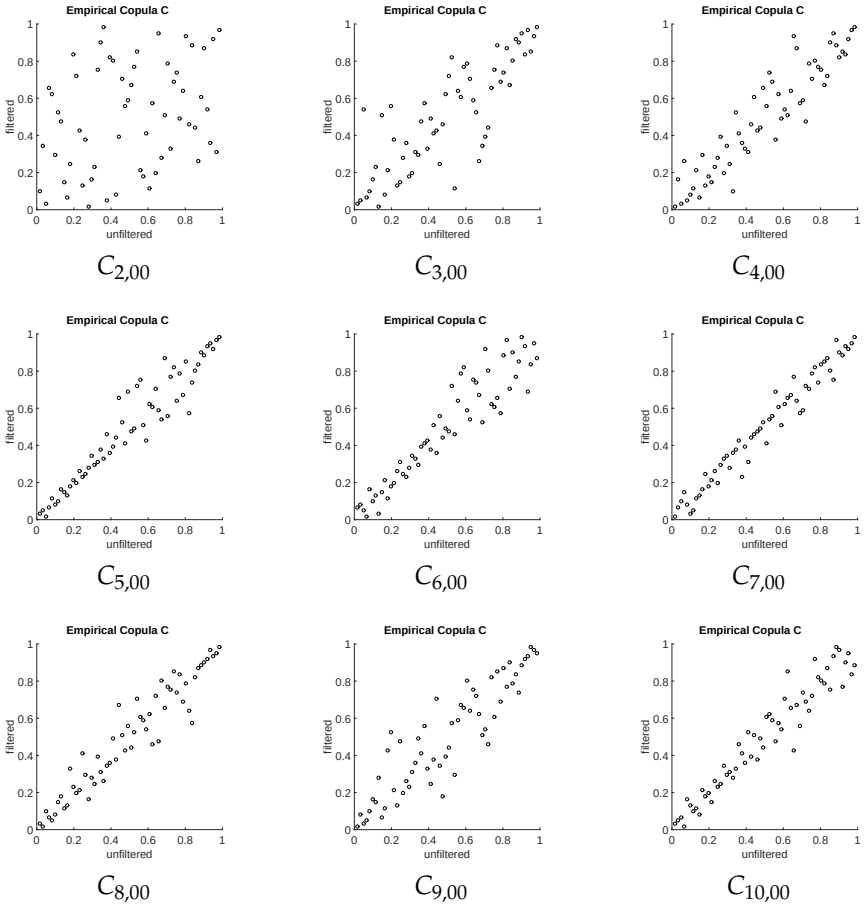

Figure 4.7: *The unfiltered and filtered* GRACE *coefficients for order 0 and degree 2 to 10.*

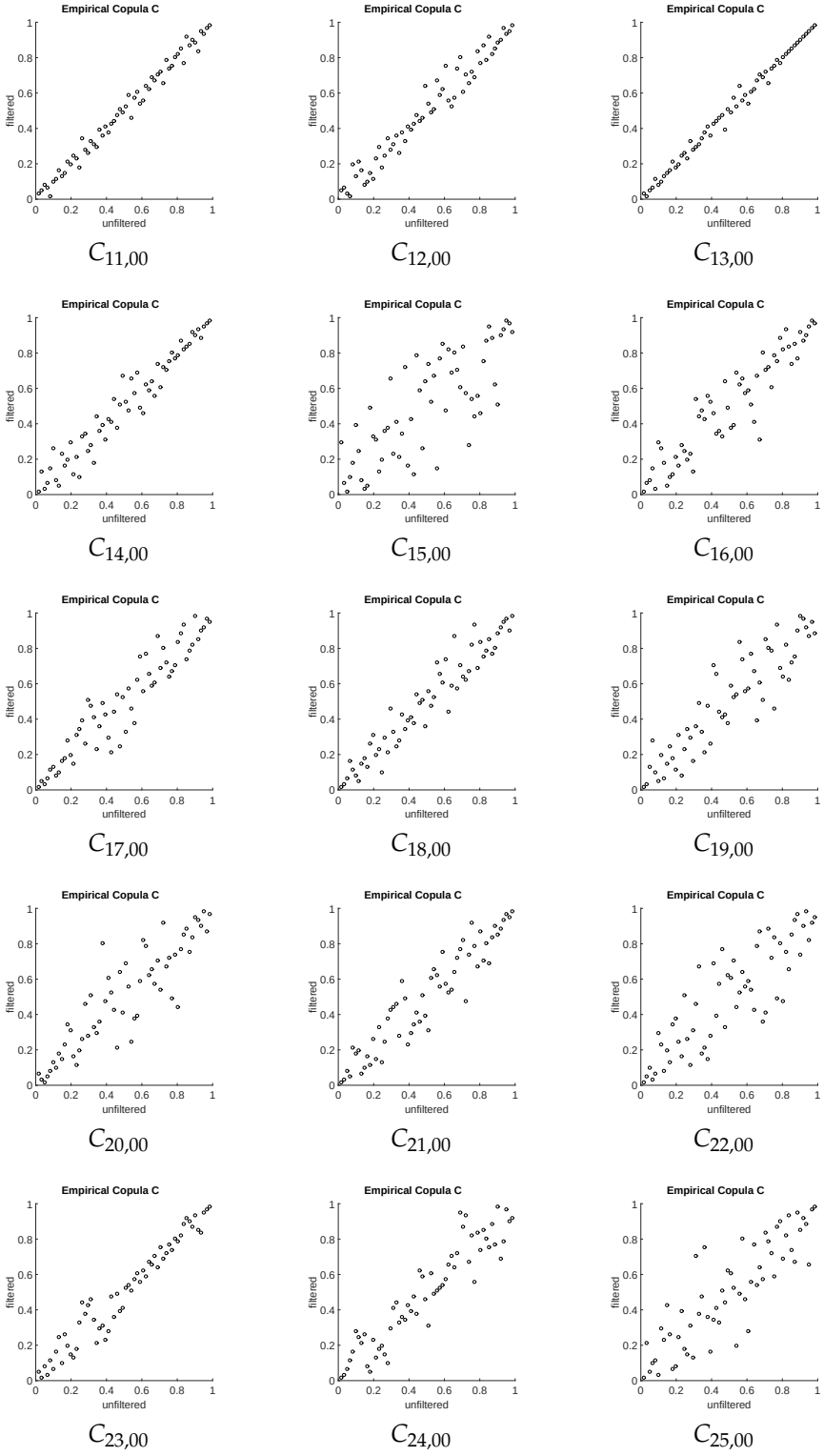

Figure 4.8: *The unfiltered and filtered* GRACE *coefficients for order 0 and degree 11 to 25.*

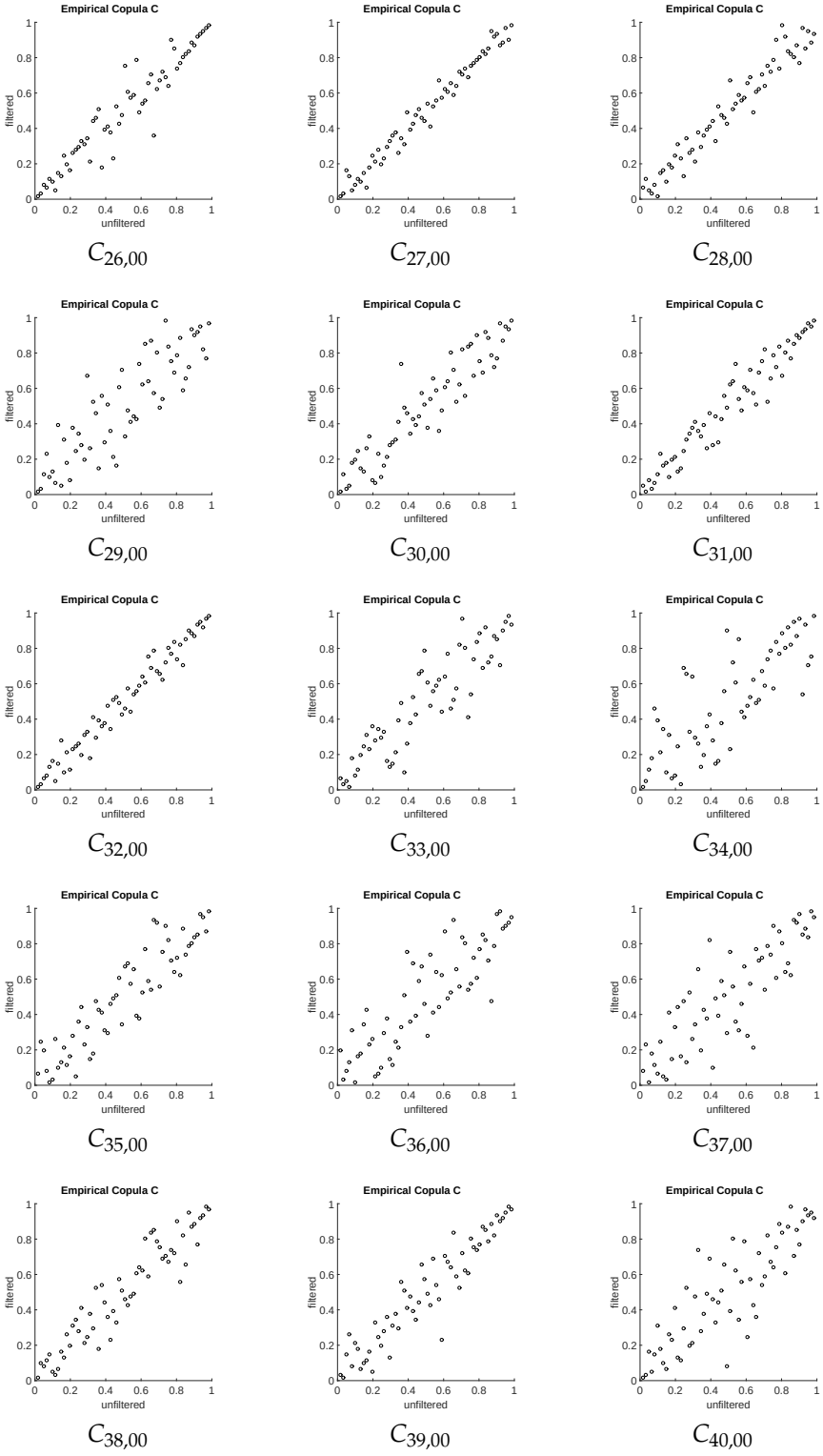

Figure 4.9: *The unfiltered and filtered* GRACE *coefficients for order 0 and degree 26 to 40.*

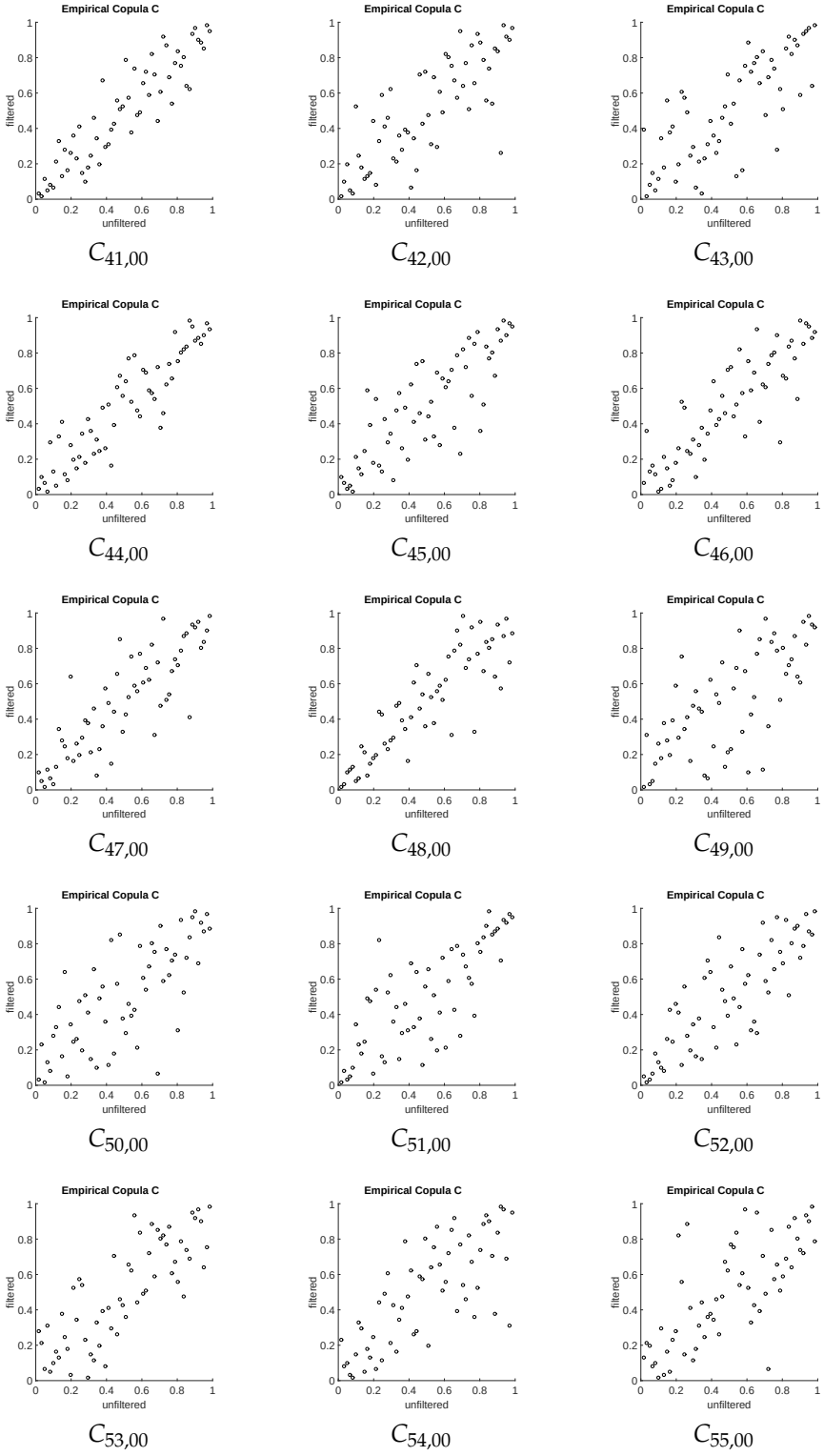

Figure 4.10: *The unfiltered and filtered* GRACE *coefficients for order 0 and degree 41 to 55.*

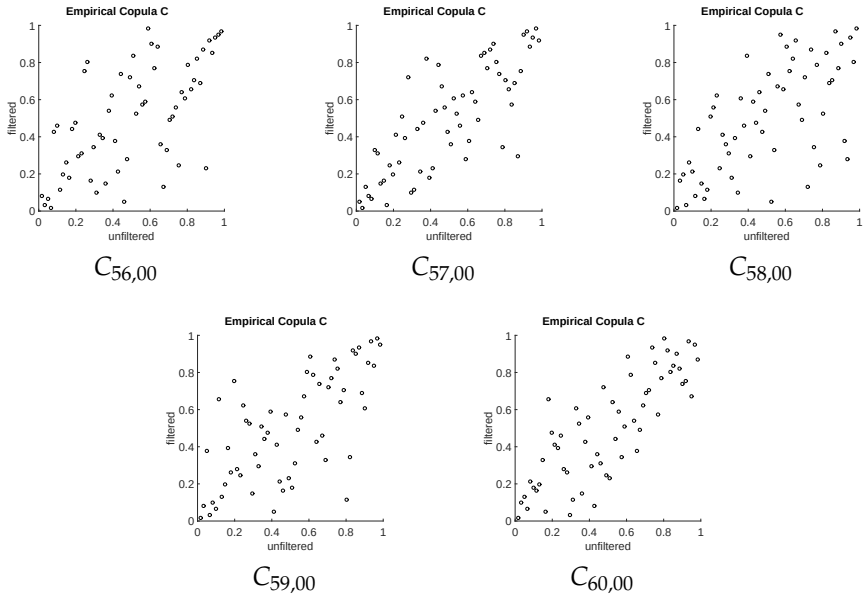

Figure 4.11: *The unfiltered and filtered* GRACE *coefficients for order 0 and degree 56 to 60. The data transformed to the rank space using the* CDF *which are shown in the Figure 4.6*

Figure 4.11 shows the scatter plots of order 0, for other order the relation between the unfiltered and filtered coefficients shows identical behavior.

4.2.3 Computing Copula parameter

The Copula parameters are computed as explained in subsection 2.3.3. Figure 4.12 shows Archimedean Copula parameters for each coefficient.

Clayton parameter for filtered and unfiltered GRACE coefficients are shown in Figure 4.12 (a), the lower degrees and orders indicate high dependency between the two data sets. However, a weak dependency between filtered and unfiltered GRACE coefficients is shown for the higher degrees and orders. As it can be seen in Figure 4.12 (b) Frank Copula parameters indicated that Frank Copula can capture the dependency between unfiltered and filtered GRACE coefficients. However, for some coefficients in higher degree and order, the Clayton is not able to capture the dependency structure between these two data sets.

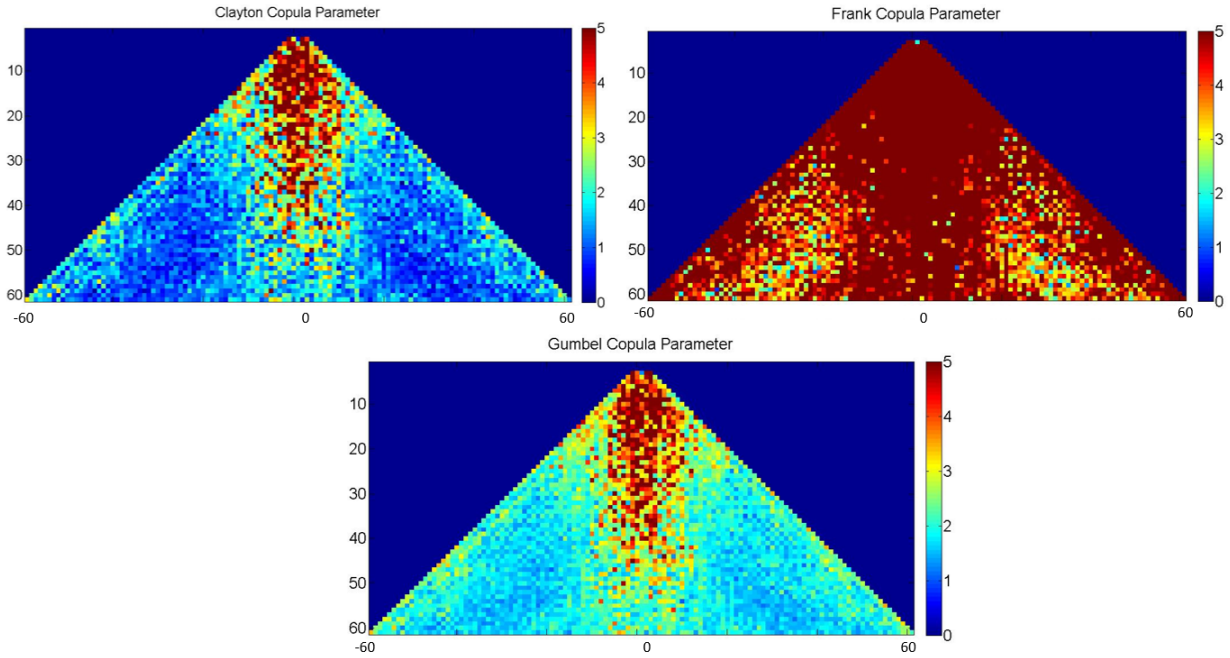

Figure 4.12: *The computed Copula parameters for each coefficient of unfiltered and filtered* GRACE *data. The vertical axis shows the degree, and horizontal shows the order of coefficients. Note the Copula parameters of these three Archimedean Copulas should not be compared to each other, because different Copula has a different range of possibility of Copula parameter. Higher parameters indicate higher dependency which can be concluded from the Copula parameter and the rank correlation Kendall's* τ*, see Appendix C.*

The Gumbel Copula parameters illustrate the high dependency between data in lower degrees and orders. Gumbel can capture the dependency of filtered and unfiltered GRACE coefficients better than Clayton.

As the dependency between the unfiltered and filtered coefficients are linear, it was predictable that Frank and Gumbel Copula can model the dependency structure between the coefficients.

4.2.4 Fitting theoretical Copula

The Figure 4.13 shows the fitted theoretical Copula for the coefficients of lower degree ($C_{2,00}$, $C_{5,01}$, and $C_{6,01}$) and higher degrees ($C_{56,00}$ and $C_{60,00}$).

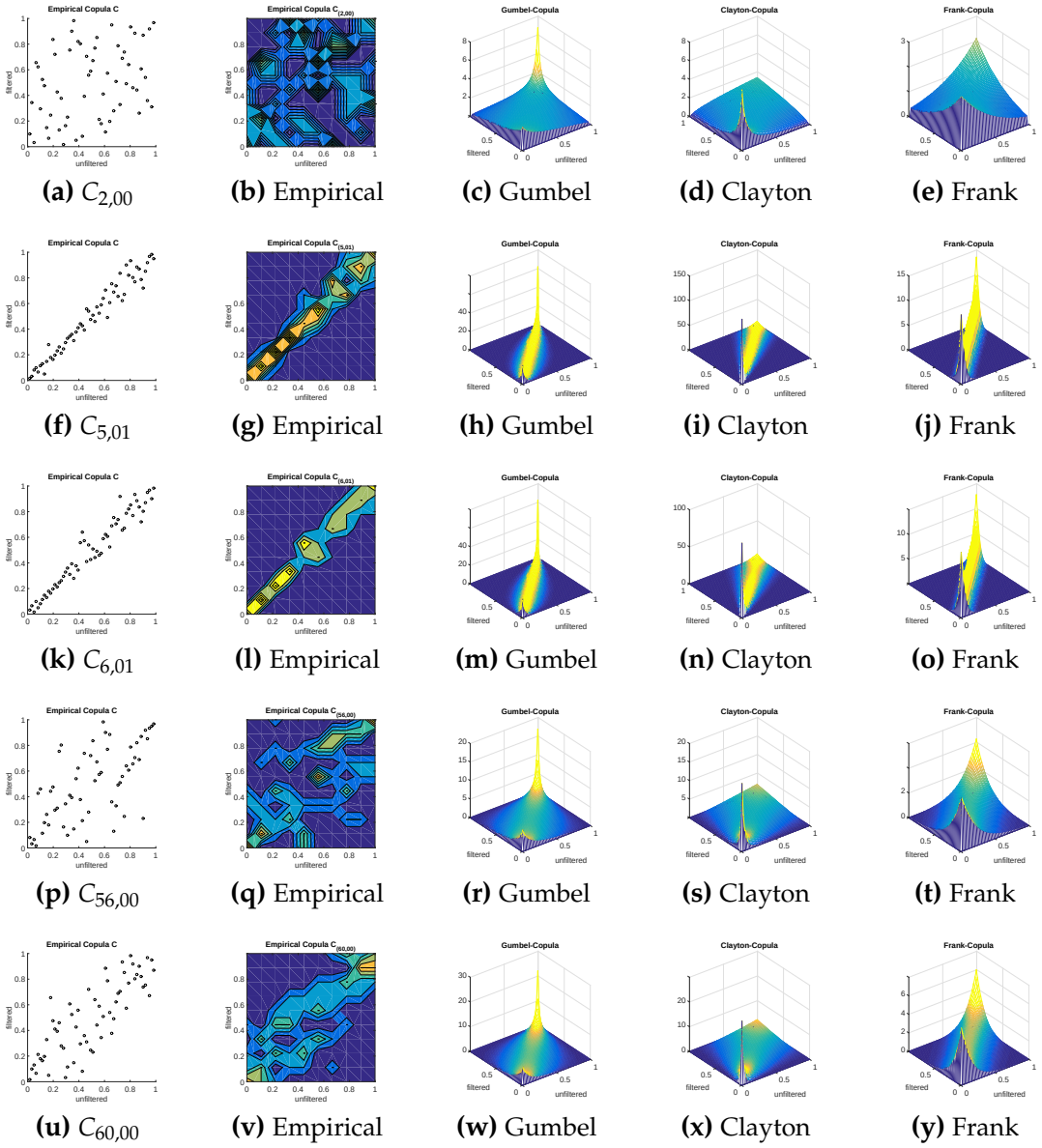

(a) $C_{2,00}$ **(b)** Empirical **(c)** Gumbel **(d)** Clayton **(e)** Frank

(f) $C_{5,01}$ **(g)** Empirical **(h)** Gumbel **(i)** Clayton **(j)** Frank

(k) $C_{6,01}$ **(l)** Empirical **(m)** Gumbel **(n)** Clayton **(o)** Frank

(p) $C_{56,00}$ **(q)** Empirical **(r)** Gumbel **(s)** Clayton **(t)** Frank

(u) $C_{60,00}$ **(v)** Empirical **(w)** Gumbel **(x)** Clayton **(y)** Frank

Figure 4.13: *Fitting the theoretical Copula to dependency structure between unfiltered and filtered data.*

$C_{5,01}$ and $C_{6,01}$ show a very high linear dependency and all the three theoretical Copulas capture this dependency. $C_{60,00}$ shows upper tail dependence and Gumbel Copula fits better to this dependency structure. For other coefficients, results are the identical which can be found in D.

4.2.5 Simulating Copula-based derived random data

After fitting the theoretical Copula to the empirical Copula, the random data are generated in the rank space using input data as it is shown in 2.5. In this research, 1000 random time series data are simulated for each coefficient. It was assumed that 1000 samples could give a reliable result. However, for future studies this process can be done using a fewer or more number of sampling data.

4.2.6 Transferring data from rank space to data space

These simulated data are transformed from the normalized rank space to the spectral space. As all of the random data have equal probability, the mean value of the 1000 random data are computed. In order to compare the data with the filtered GRACE coefficients, first, the data are transformed to the spatial domain.

4.3 Comparison

The main aim of this chapter is to see whether the Copula-based approach can capture the dependency structure between GRACE unfiltered and filtered data. Figure 4.14 presents unfiltered GRACE data (up-left) and filtered GRACE data (up-right) in February 2006. After filtering the raw data, some patterns became visible in South America and northern Australia and the Himalayas.

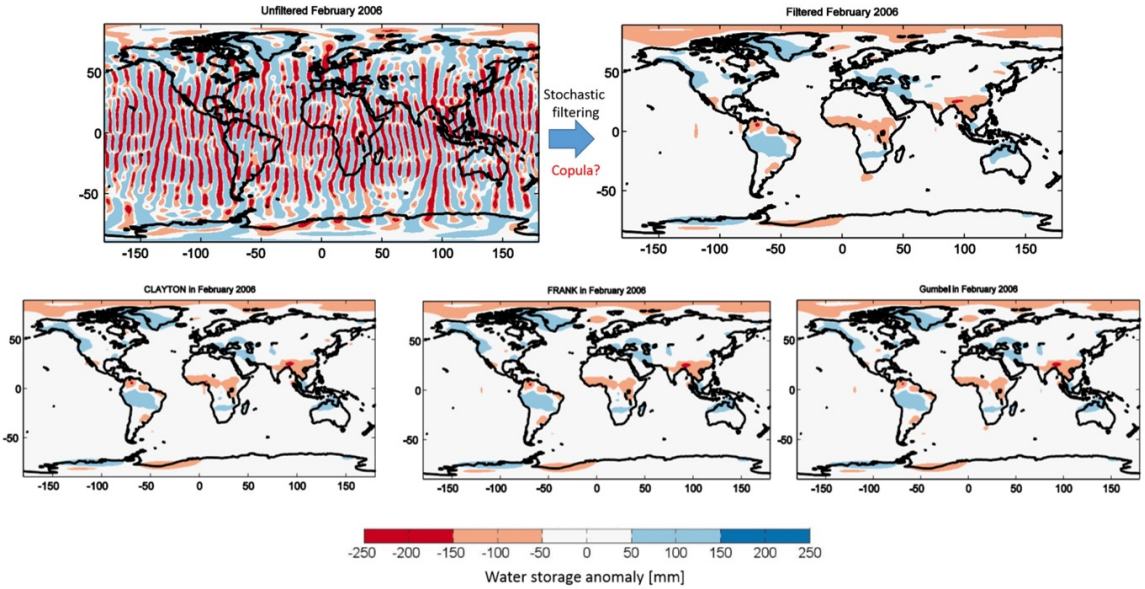

Figure 4.14: *Unfiltered and filtered* GRACE *data in February 2006 [mm]. The unfiltered data show on the left side. As it can be seen, the noisy data in higher degrees show themselves in the map as North-South strips (Swenson and Wahr, 2006). The data provided by* CSR *requires filtering to be studied. In this study, data have been filtered by stochastic filtering. On the right side, North-South strips have been removed from the map. Some patterns appear in South America, northern Australia, Himalayas and West Africa. These patterns show water storage anomalies in February 2006. The simulated data using Frank Copula, Clayton Copula, and Gumbel Copula are shown in this figure. The unfiltered data in February is considered as the source data for the Copula-based approach. The results are compared with the filtered data (top right) for validation the results. Moreover, it can be seen in the figure that the simulated data show nearly the same patterns, as the filtered data in South America, North Australia, West Africa and Himalayas.*

Figure 4.14 shows the result of simulated data using Copula-based approach. The result of Clayton Copula(left), Frank Copula (center), and Gumbel Copula (right) are shown in this figure. The Copula-based simulated data have similar patterns compared to filtered GRACE data. However, for validation of the results, some tests are needed to be ensure the results e.g. comparing of degree variance, the residual, and analysing the time series of filtered GRACE data and random data consistency with the derived dependency structure on the map.

4.3.1 Degree variance

In this step, degree variance (i.e. the total spectral power of the signal per degree) of unfiltered and filtered GRACE data, and the simulated data by the Copula-based approach are observed. The degree variance is expressed by the following equation:

$$\sigma_l^2 = \sum_{m=-l}^{l} \sigma_{lm}^2 \tag{4.1}$$

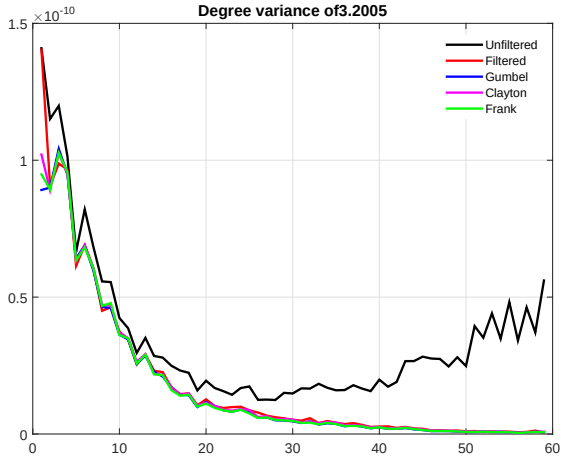

(a) March 2005

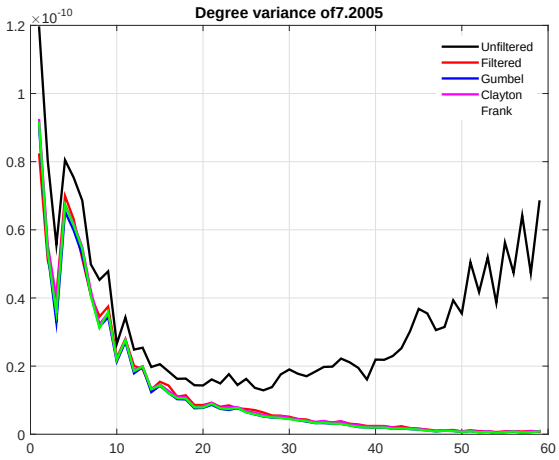

(b) July 2005

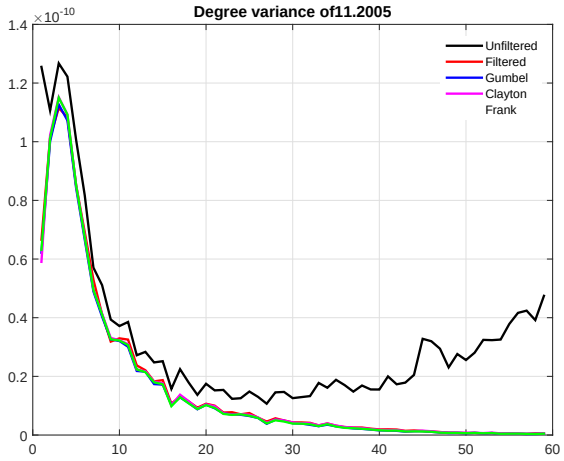

(c) November 2005

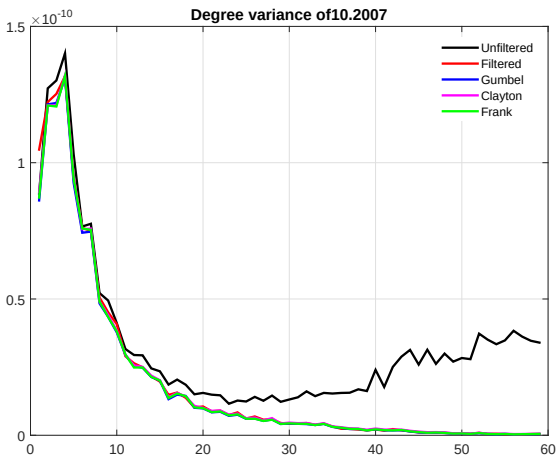

(d) October 2007

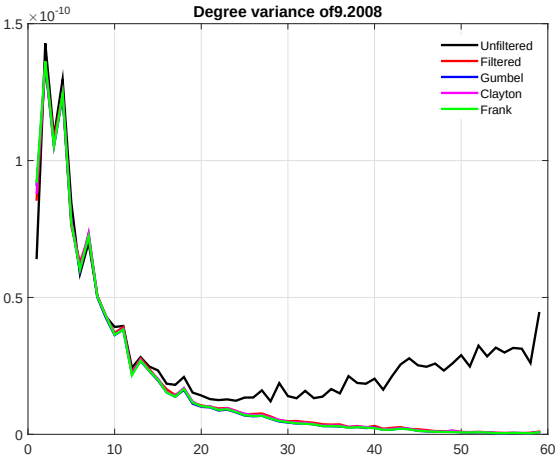

(e) September 2008

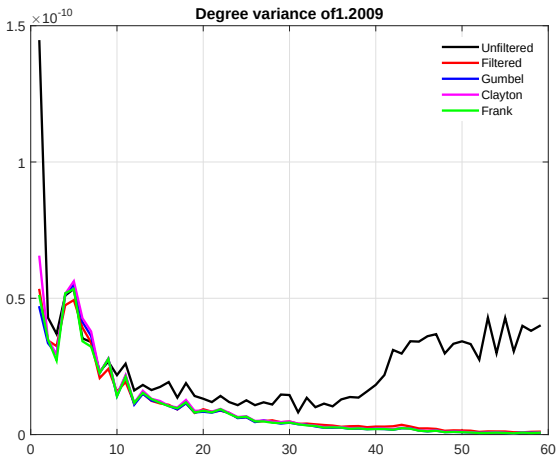

(f) January 2009

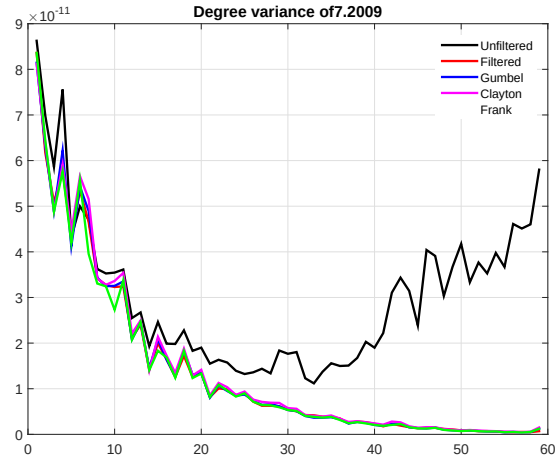

(g) July 2009

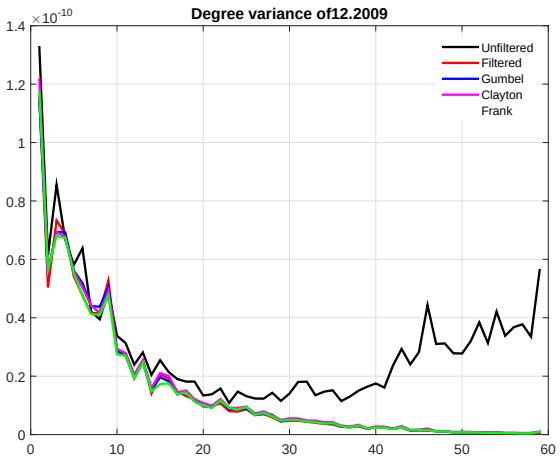

(h) December 2009

Figure 4.15: *Degree variance unfiltered and filtered* GRACE *data and Copula filtered data.*

As it can be seen in the Figure 4.15 the degree variance of unfiltered data (black) falls sharply until to degree 25 to 30, then there is a slight increase up to degree of 60. The red line shows filtered data which decreases contentiously. The Copula-based derived random data from Gumbel Copula is in blue, Clayton Copula is purple, and Frank Copula is in green. They decrease sharply up to degree 60. This Copula-based random data show very good agreement with the original (filtered GRACE) data. Figure 4.15 (a) shows degree variance of data for March 2005. A difference can be seen in lower degrees between filtered GRACE and the Copula-based derived random data. However, after degree 3 they show the same degree variance up to degree of 60.

Figure 4.15 (b) and (f) show the degree variance of data for July 2005. The lines indicate that although unfiltered (black) shows higher degree variance in degree 2 and

3, it does not affect the Copula-based derived random data. The results are completely matched to original filtered data.

Figure 4.15 (c) presents the degree variance of data for November 2005. A big gap is shown in lower degrees between the unfiltered and filtered data. The Copula-based random data are agreed very well to filtered data, their degree variances increase up to degree 4, and then the degree variance decreased sharply from degree 4 to degree 60.

Figure 4.15 (d), (e), (h), and (g) show the same degree variance for the unfiltered, filtered, Gumbel, Clayton, and Frank Copula up to degree 10. Then the filtered and Copula-based derived random data decrease until the degree 60.

4.3.2 Residual

One way to analyze the performance of Copula-based derived random data are computing the residual map between the Copula-based simulated data and filtered GRACE data. In this case, the residual plot can be computed by subtracting filtered GRACE data from the data that are simulated by the Copula-based approach.

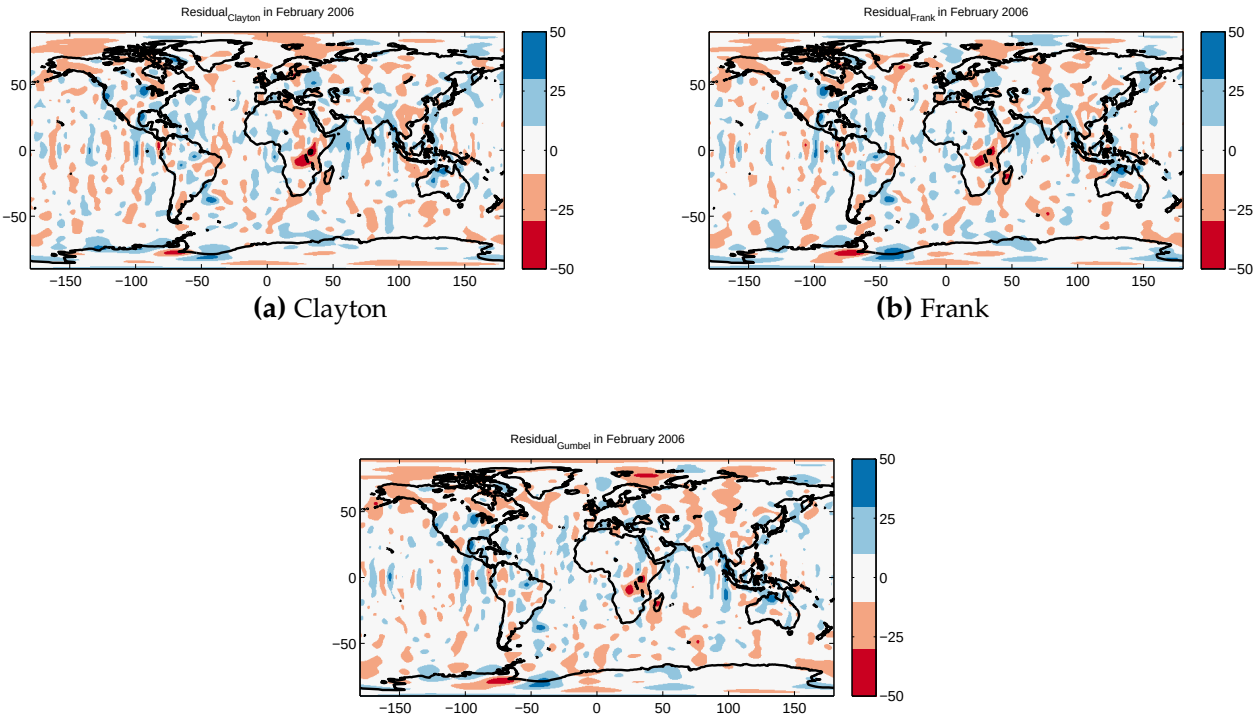

(a) Clayton

(b) Frank

(c) Gumbel

Figure 4.16: *Residual of simulated data using Archimedean Copula a) Clayton Copula, b) Frank Copula, c) Gumbel Copula in February 2006 [mm].*

The results are shown in Figure 4.16. In these figures, the color bar has been changed to ± 50 mm. The residual maps show mainly random patterns, which seem similar to typical GRACE-type North-South stripes. However, some regions also show some physical patterns, e.g. over central Africa. Furthermore, all three maps show similar features. They show the same pattern, but the magnitudes of the patterns are different. Errors are shown randomly, overestimation and underestimation in simulated data can also be observed. However, in the south part of Africa, an overestimation in simulated random data appears in all residual maps for February 2006. The other months look very similar, but these are not shown further here.

4.3.3 Analysing time series in different area and their RMS

In this subsection, three major river basins that are well-distributed over the globe are chosen. The river basins are Amazon, Mississippi, and Ganges. Each basin has a time series for 60 months. In Figure 4.17 (a), the water storage anomaly is shown from January 2005 to December 2009 in Amazon. The time series of Copula-based random data derived from Gumbel Copula, Frank Copula, and Clayton Copula agree well with the filtered GRACE data. While, the time series of Gumbel Copula shows better performance. For most of the months, the results of Gumbel Copula is relatively agreed with filtered GRACE data.

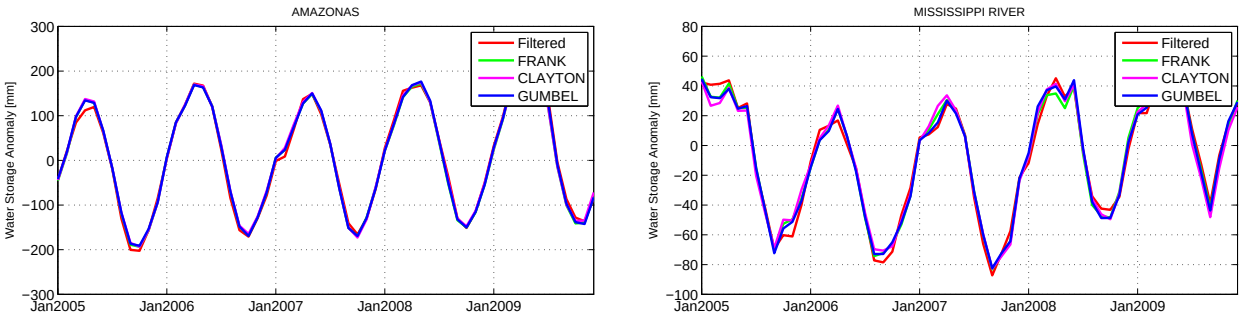

(a) Amazon

(b) Mississippi

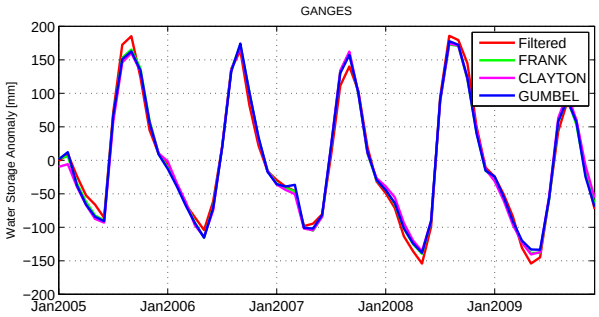

(c) Ganges

Figure 4.17: *Time series of filtered data and Copula derived random data in Amazon, Mississippi, and Ganges*

As it can be seen in the Figure 4.17(b) in Mississippi River, data that are simulated by Copula-based approach show a similar trend and dynamic as filtered data. During most months (except for the peaks and troughs), the data derived from the Gumbel

Copula, Frank Copula, and Clayton Copula agrees well with the filtered GRACE data. The figure implies that Copula-based approach can maintain the dynamic behaviour of the data in Mississippi. However, Copula-based data show a difference of around 20 mm in September 2005 or March 2009.

Figure 4.17(c) indicates time series of GRACE filtered data and Copula-based random data (Clayton, Frank, and Gumbel Copula) in the Ganges. The data derived from the Gumbel Copula, Frank Copula, and Clayton Copula agree well with the filtered GRACE data.

Table 4.1: RMS *of filtered* GRACE *data, Clayton, Gumbel, and Frank Copula in Amazon, Mississipi and Ganges*

RMS [mm]	Filtered	Clayton	Gumbel	Frank
Amazon	123.95	121.17	122.49	121.41
Mississippi	40.58	39.68	40.07	40.07
Ganges	93.28	91.78	91.73	92.16

The RMS of the signal for the filtered GRACE data and the Copula-based random data derived from Clayton Copula, Gumbel Copula, and Frank Copula are shown for Amazon, Mississippi, and Ganges. For all of them the RMS of the conditional random data from derived dependency structure from the Copula-based approach are the same power as filtered GRACE data. The results of the RMS show that Copula-based approach will maintain the power of the signal.

Table 4.2: *Correlation of Clayton, Gumbel, and Frank Copula with filtered* GRACE *data in Amazon, Mississipi and Ganges*

Correlation with filtered	Clayton	Gumbel	Frank
Amazon	0.99	0.99	0.99
Mississippi	0.98	0.99	0.99
Ganges	0.99	0.99	0.99

The correlation between random data with filtered GRACE data are shown in Table 4.2. The correlation is equal to 0.99 for all Copula-based random data (Clayton Copula, Gumbel Copula, and Frank Copula). Therefore, Copula-based approach maintains the dynamic of filtered behaviour.

The results in spectral and spatial domains show that Copula-based approach successfully captured the dependency structure of filtered and unfiltered GRACE data.

Chapter 5

Prediction of water storage changes from precipitation

5.1 Introduction

In this Chapter, the idea of predicting the water storage anomalies from precipitation data is studied as an application of the Copula-based method. For this purpose, the monthly filtered GRACE data and monthly precipitation data from January 2005 to December 2009 are analysed.

The left flowchart 5.1 shows an overview of fitting the theoretical Copula to empirical Copula. The processing steps are similar to Chapter 4. However, instead of unfiltered GRACE data, now the precipitation data are used. At first, precipitation and filtered GRACE data are transformed to the rank space. Then, the empirical Copula between the precipitation and filtered GRACE data are computed. Finally, the three Archimedean Copula are fitted to the empirical Copula.

The shown flowchart in 5.1 (right) presents how the water storage anomalies are predicted from precipitation using Copula-based approaches. The theoretical Copula is fitted to the empirical Copula. One thousand random data are drawn from derived conditional Copula-based approach. These drawn data is transformed to the data space. These Copulas derived random data are expected to be the water storage anomalies. Therefore, the Copula-based data are compared with water storage anomalies which is derived from filtered GRACE data.

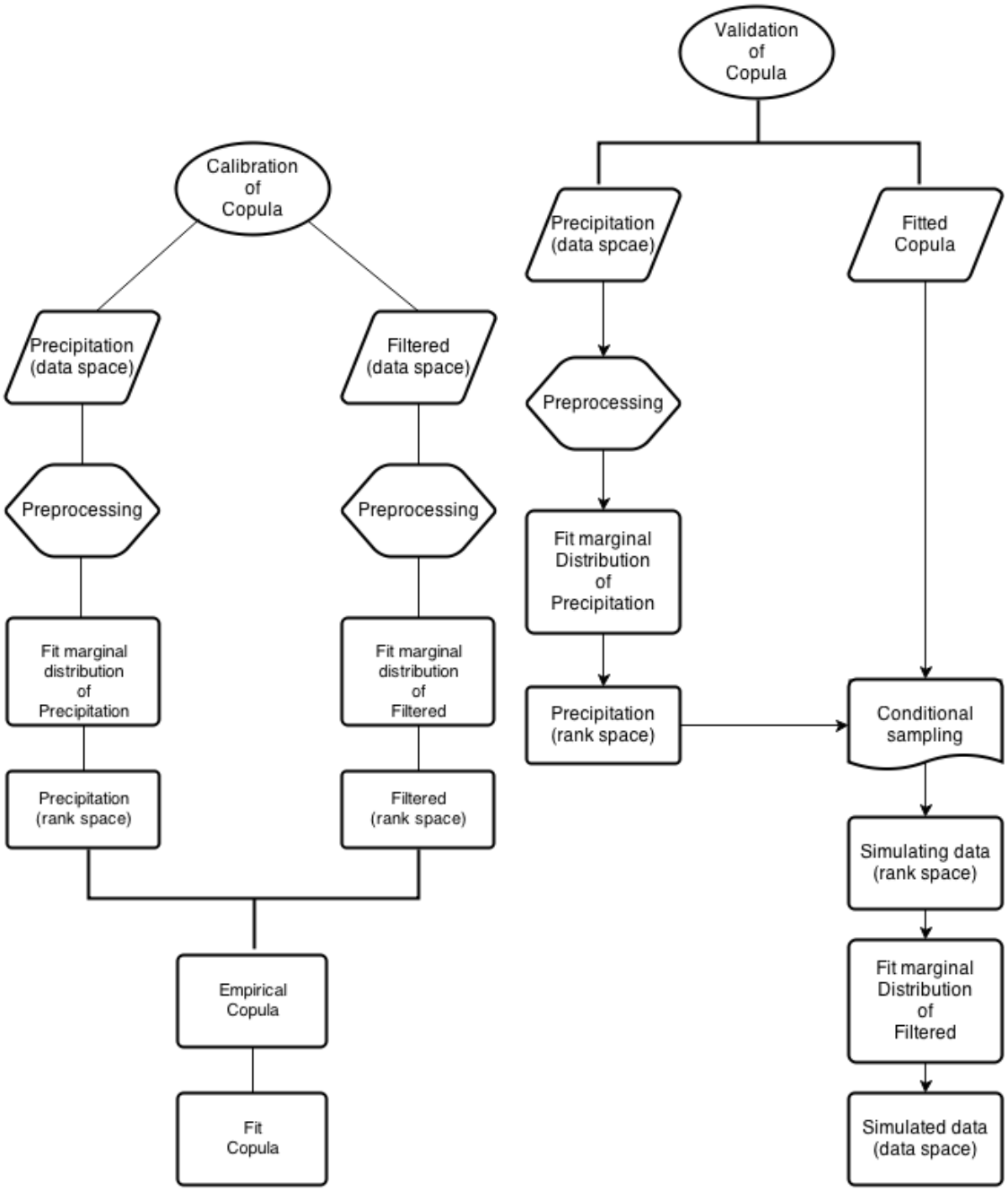

Figure 5.1: *Overview of fitting Copula to bivariate data and simulating data using Copula-based approaches for precipitation and filtered* GRACE *data.*

5.2 Prediction of water storage anomalies from precipitation using Copula-based approach

Figure 5.2 represents a sample of Copula-based approach application. We want to find out if the Copula-based methods are able to capture the dependency structure between precipitation and filtered GRACE data.

The color bar is not the same because the magnitude of the water storage anomalies and precipitation is different. Furthermore, the maps are shown different patterns of precipitation and water storage anomalies. The red circle points that the patterns are totally different in South America.

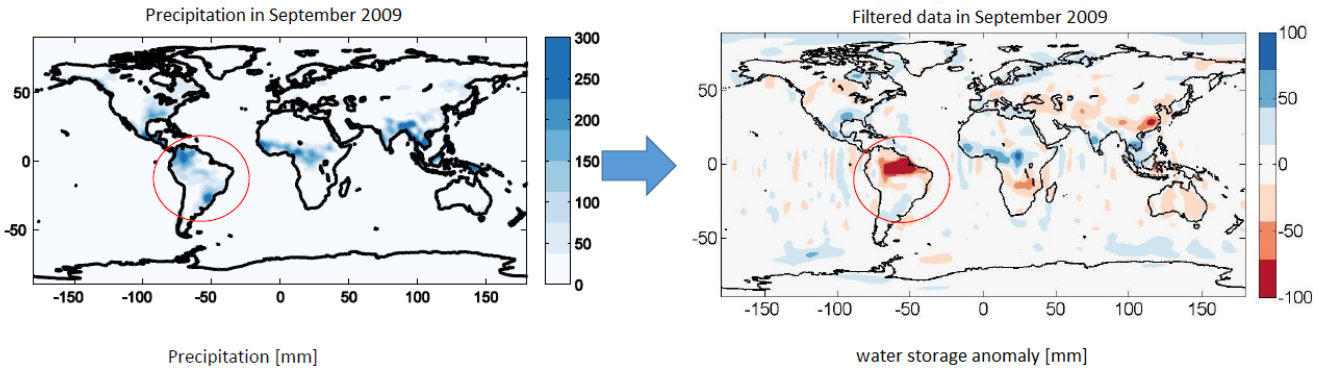

Figure 5.2: *Overview of Copula-based approach application, the prediction of water storage anomalies from precipitation data using Copula-based techniques. Precipitation is shown on the left, and the water storage anomalies data is on the right side in September 2009 [mm]. As it can be seen, different patterns are shown in South-America specified by a red circle.*

As a result, all the processes mentioned in chapter 4 are applied to find out the relation between the filtered GRACE and precipitation data.

5.2.1 Transforming data into rank space

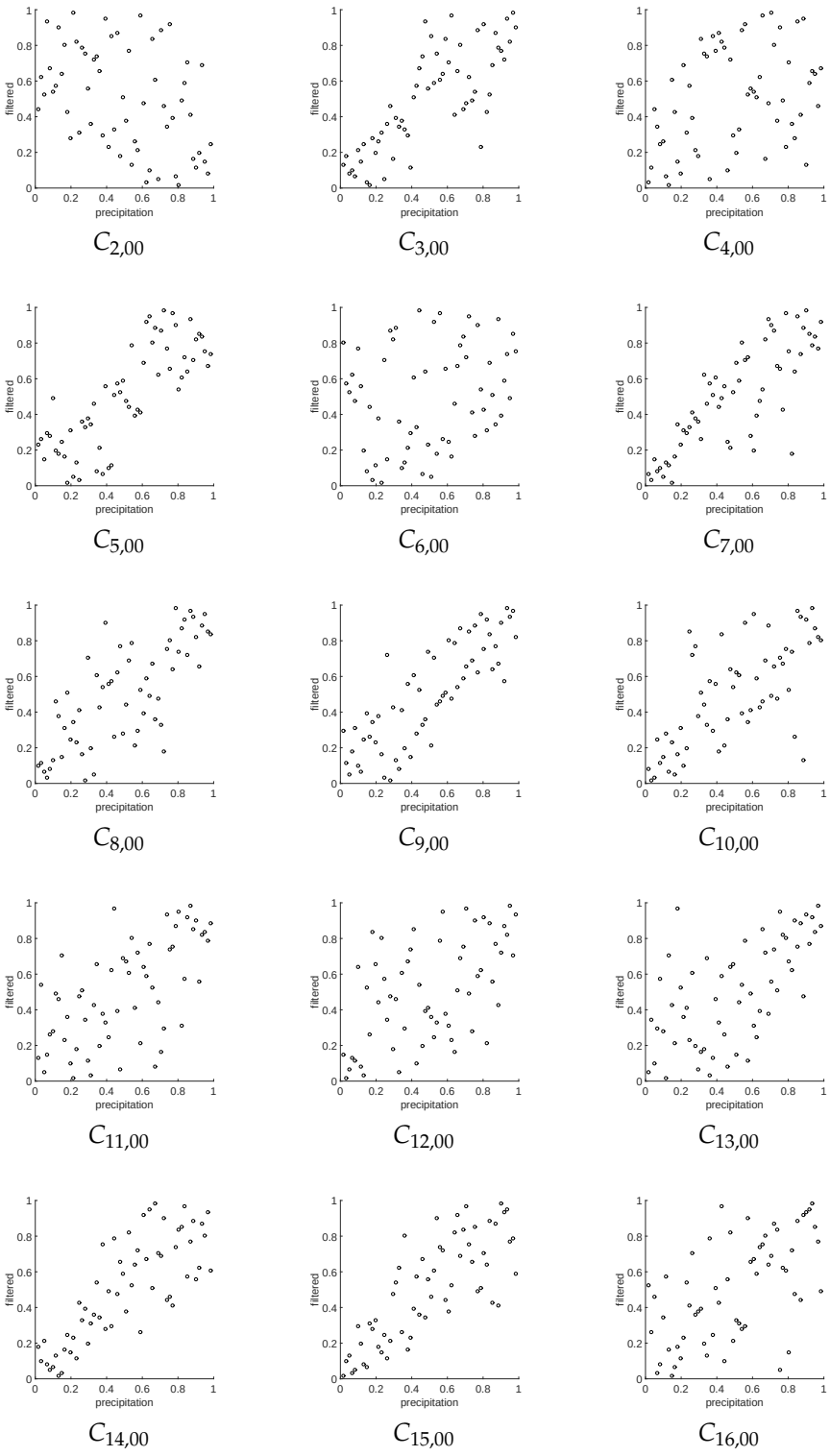

Figure 5.3: *Precipitation and filtered* GRACE *coefficients. Degree 2–16 and order 0.*

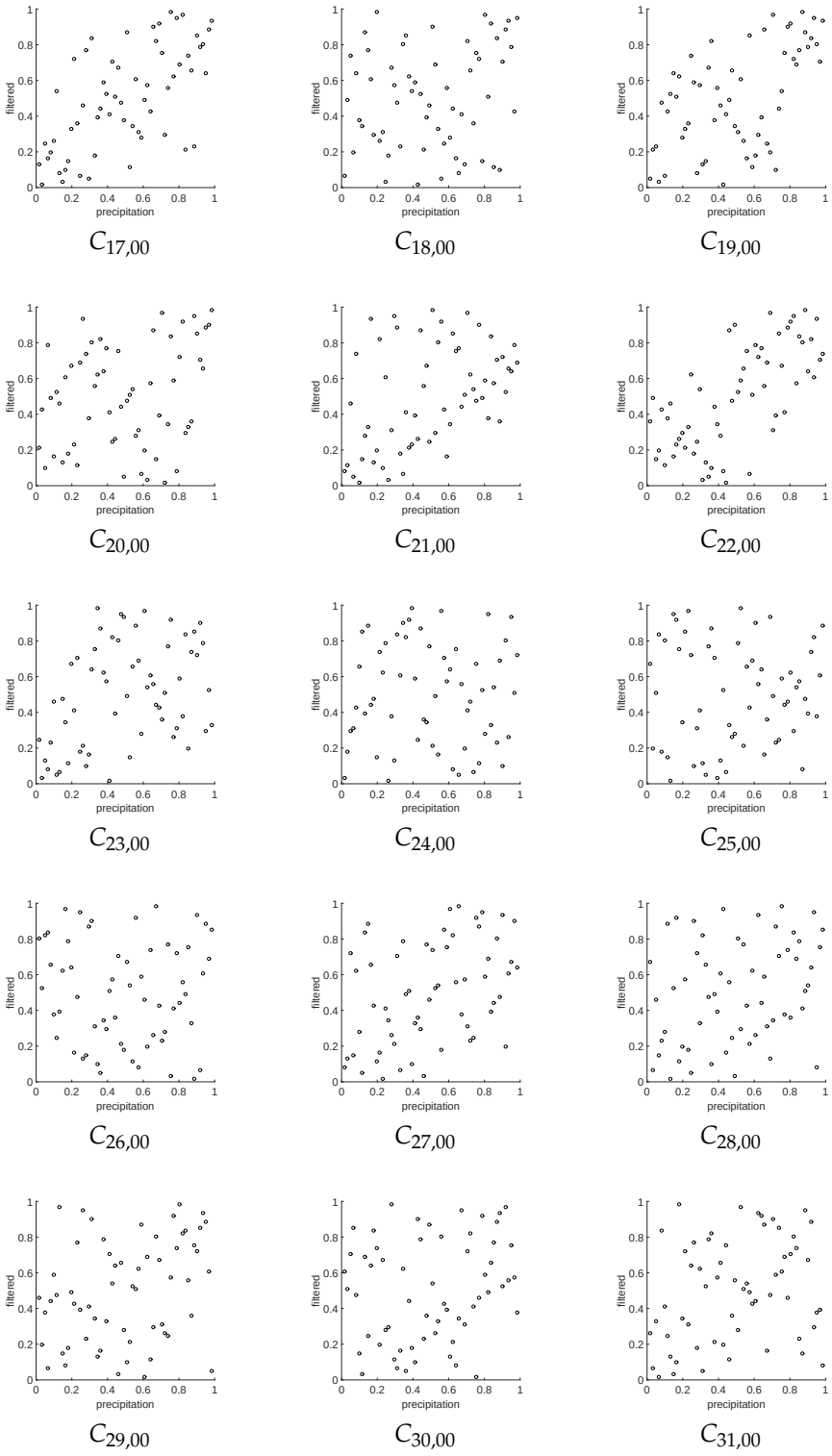

Figure 5.4: *Precipitation and filtered* GRACE *coefficients. Degree 17–31 and order 0.*

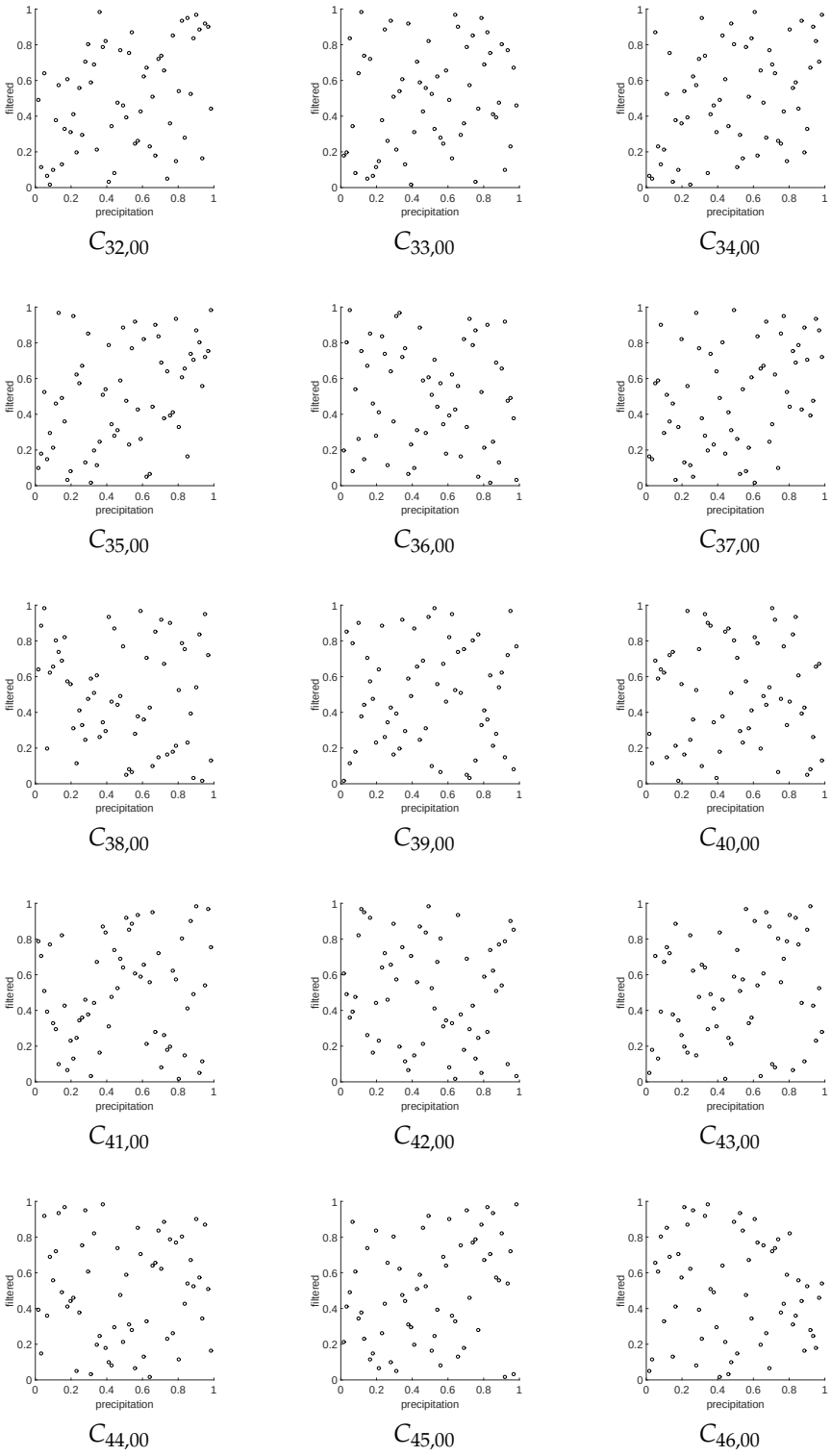

Figure 5.5: *Precipitation and filtered* GRACE *coefficients. Degree 32–46 and order 0.*

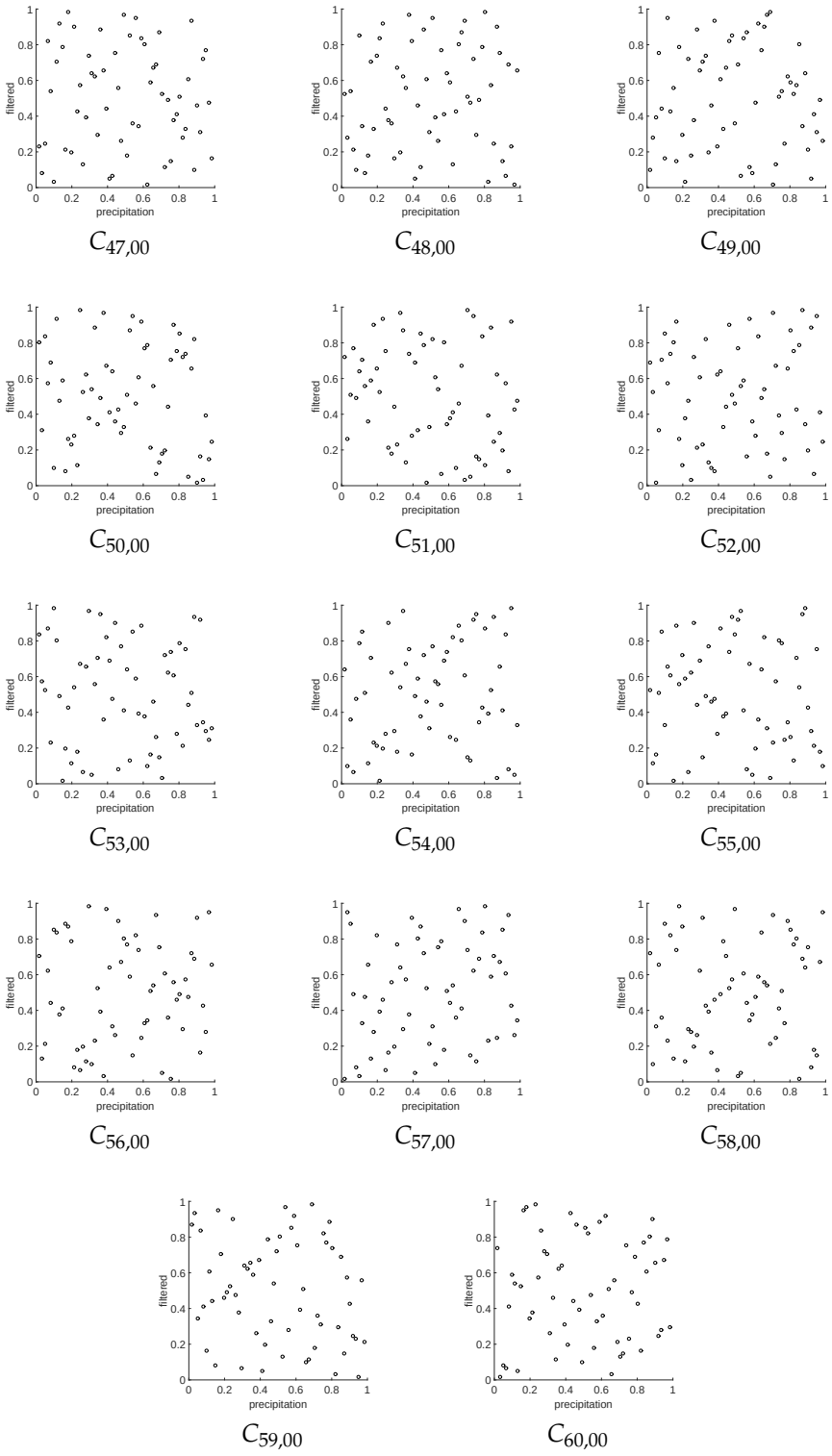

Figure 5.6: *Precipitation and filtered* GRACE *coefficients. Degree 47–60 and order 0.*

Figure 5.3, 5.4, 5.5, and 5.6 show a linear dependency between the precipitation and filtered data from degree 2 to degree 22 while it is more scattered in the higher degrees. However, for some coefficients, it is completely independence. For instance, $C_{36,00}$ show the total random distribution, and it can be assumed that the Copula-based approach is not able to capture the dependency structure for this coefficient.

5.2.2 Computing Copula parameter

The Copula parameters for the precipitation and filtered GRACE data are computed. The results are as follows.

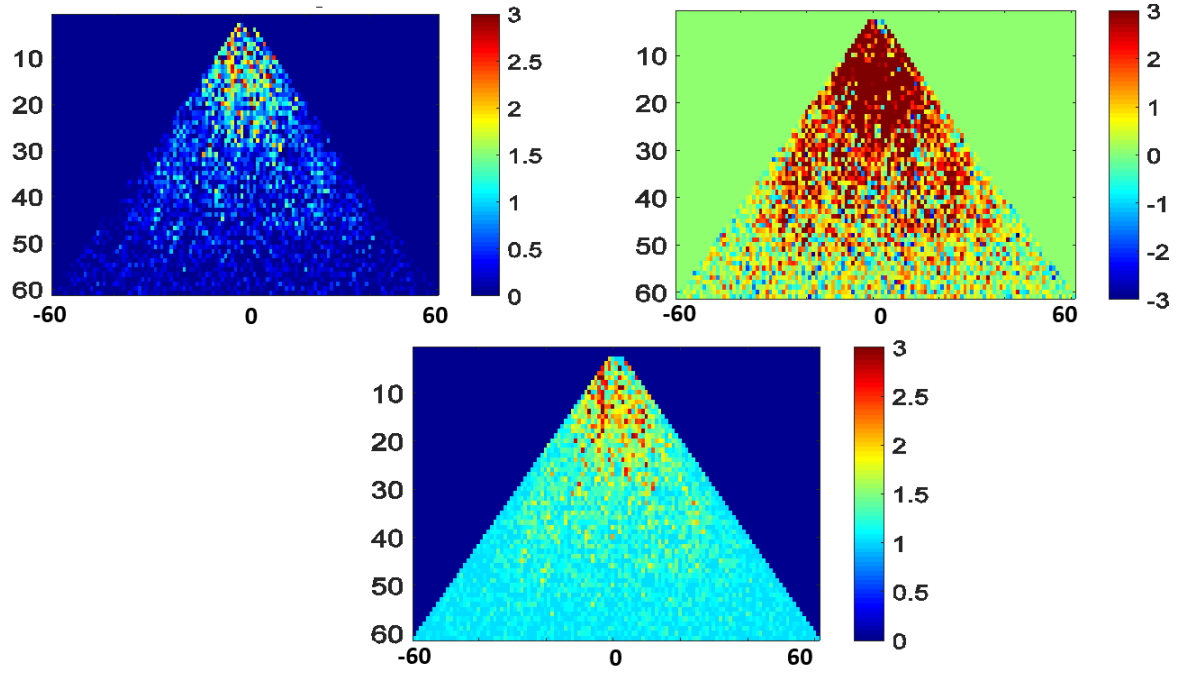

Figure 5.7: *Copula parameters for each coefficient. The vertical axis shows the degree and horizontal displays the order of coefficients. Clayton Copula parameters are on the top-left, Frank Copula parameter is located on the top-right, and Gumbel Copula parameters are shown on the bottom. Note the Copula parameters of these three Archimedean Copulas should not be compared to each other, because different Copula has a different range of possibility of Copula parameter. Higher parameters indicate higher dependency which can be concluded from the Copula parameter and the rank correlation Kendall's τ, see Table C.1.*

Figure 5.7 shows the Clayton Copula parameters on the top-left, Frank Copula parameters on the top-right, and the Gumbel Copula parameters on the bottom. Even the parameter are different for all three Archimedean Copulas, the dependency is high in the lower part of the spectrum, and lower dependency can be observed in higher degrees. For instance, Figure 5.7 (top-right) show high dependency up to degree 50. However, these parameters show very weak dependency for the coefficients that are higher than degree 50.

5.3 Fitting theoretical Copula to dependency structure

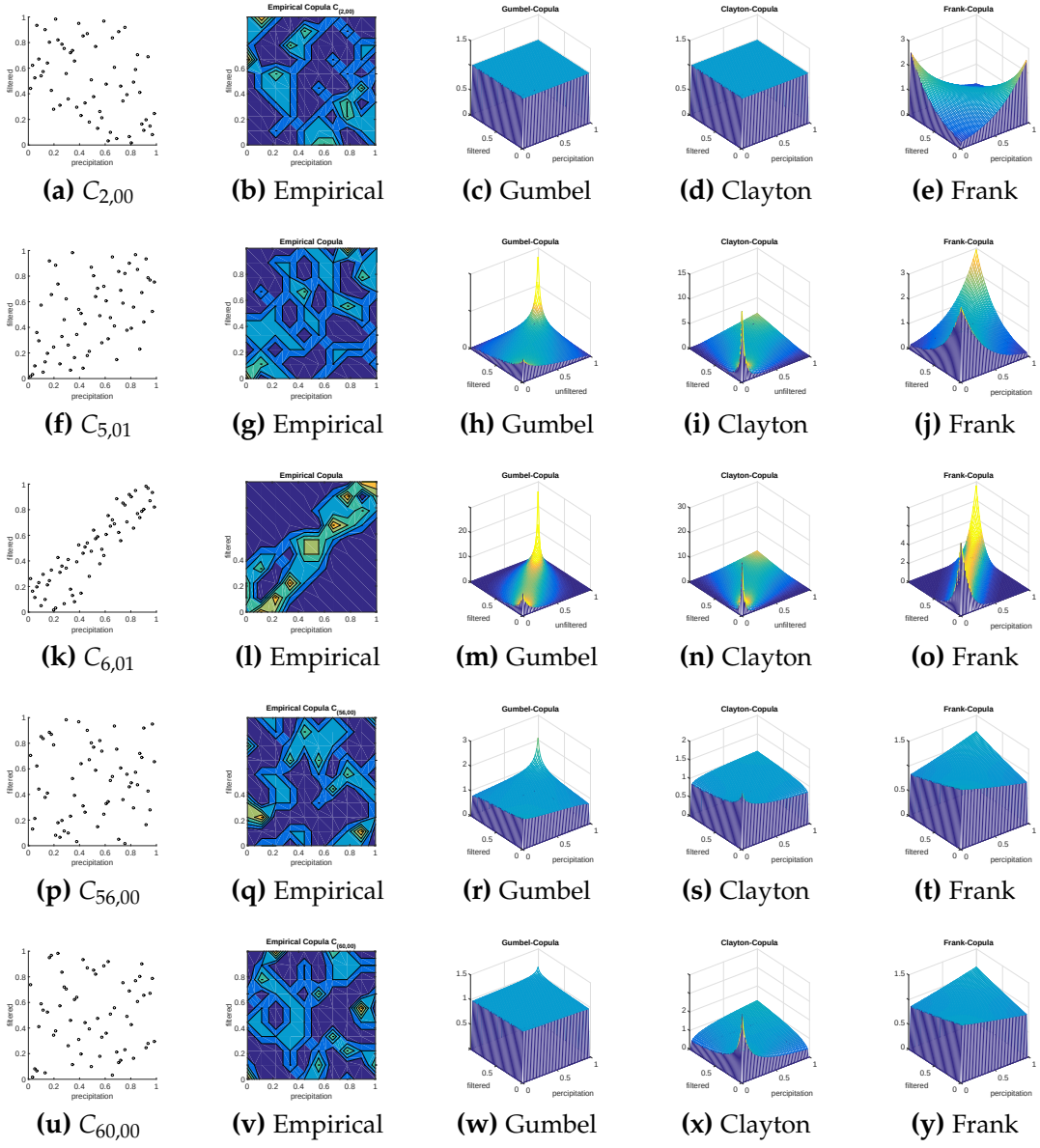

(a) $C_{2,00}$ **(b)** Empirical **(c)** Gumbel **(d)** Clayton **(e)** Frank

(f) $C_{5,01}$ **(g)** Empirical **(h)** Gumbel **(i)** Clayton **(j)** Frank

(k) $C_{6,01}$ **(l)** Empirical **(m)** Gumbel **(n)** Clayton **(o)** Frank

(p) $C_{56,00}$ **(q)** Empirical **(r)** Gumbel **(s)** Clayton **(t)** Frank

(u) $C_{60,00}$ **(v)** Empirical **(w)** Gumbel **(x)** Clayton **(y)** Frank

Figure 5.8: *Fitting the Archimedean Copula to dependency structure between filtered and precipitation data.*

The top row of the Figure 5.8 shows a negative linear dependency for the coefficient $C_{2,00}$ which can only be represented by Frank Copula. For the coefficients, $C_{5,01}$ and $C_{6,01}$ all the three Copula models can capture the dependency structure between the precipitation and filtered GRACE coefficients. However, for higher degrees a weak dependency can be observed e.g. $C_{56,00}$ and $C_{60,00}$ show a very weak dependency.

5.3.1 Comparison

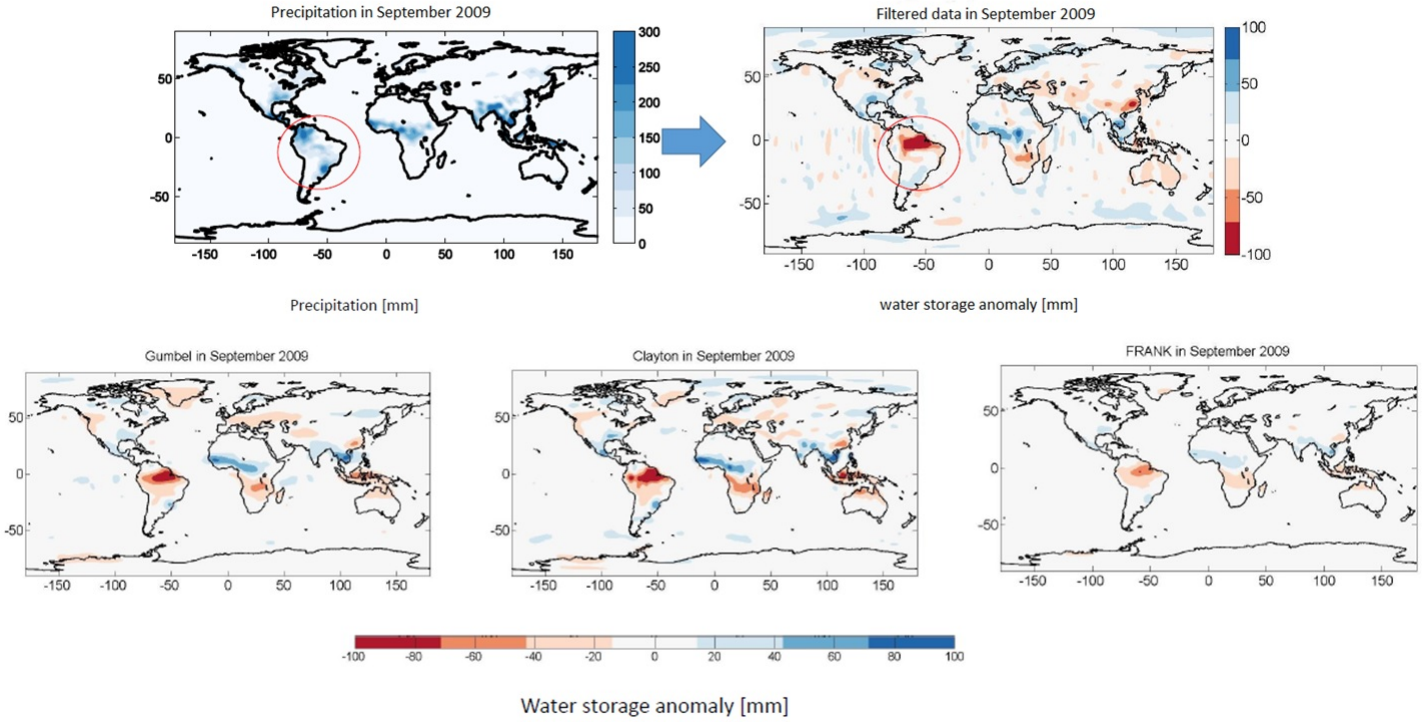

Figure 5.9: *The water storage anomalies are predicted from precipitation data using the Copula-based approach in September 2009.*

Figure 5.9 shows the results of three different Archimedean Copula in September 2009. Precipitation is used as input data on the top-left. Also water storage anomalies (top-right) is presented as reference map to compare with the simulated data. The results of three different Archimedean Copula, Gumbel Copula (left), Clayton Copula (center), and Frank Copula (right) show very similar patterns compared to filtered GRACE data. However, the patterns of the results of Gumbel Copula and Clayton Copula show a higher magnitude.

For validation the results, the degree variance, the residual, and catchment analyses are studied as follows.

5.3.2 Degree variance

The total spectral power of the signal per degree is computed for precipitation, unfiltered and filtered GRACE data, and the Copula-based data derived from the dependency structure between the precipitation and filtered GRACE data. The degree variance implies whether the Copula-based approach can maintain the power of the signal.

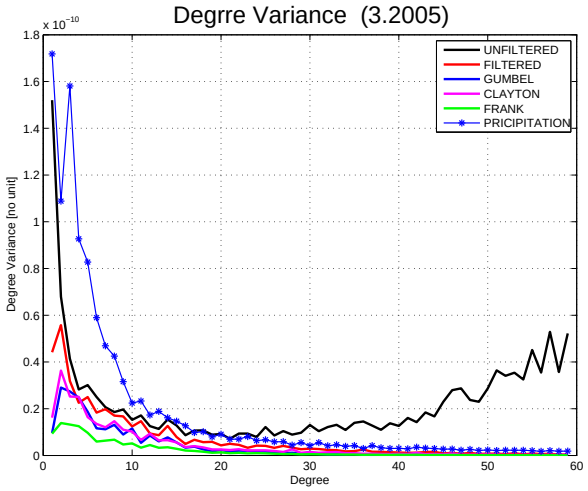

(a) March 2005

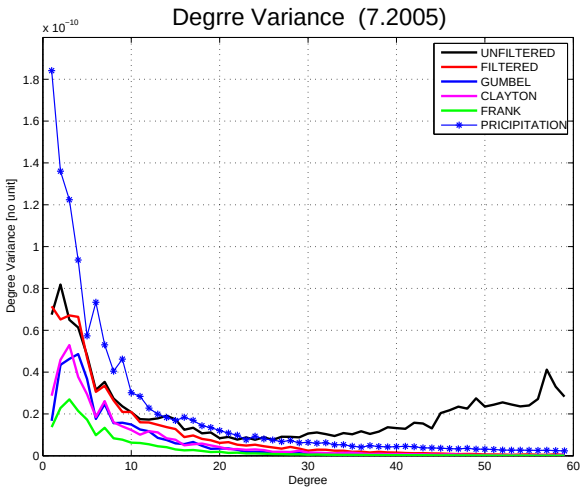

(b) July 2005

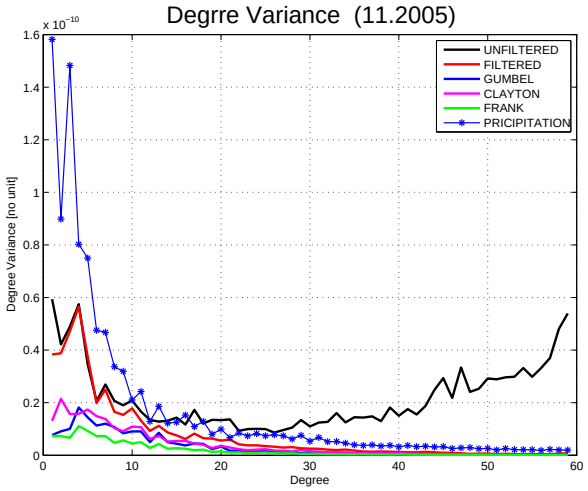

(c) November 2005

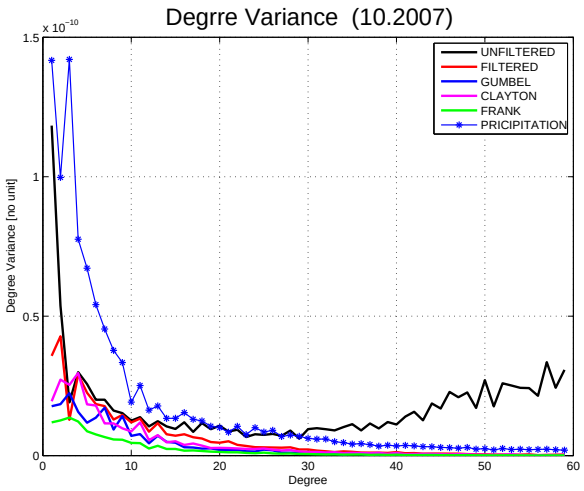

(d) October 2007

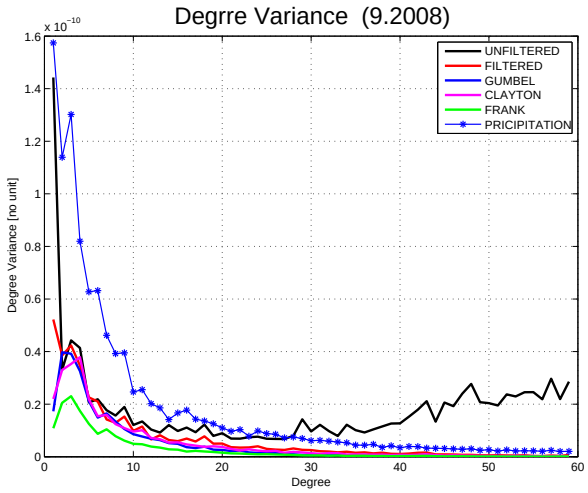

(e) September 2008

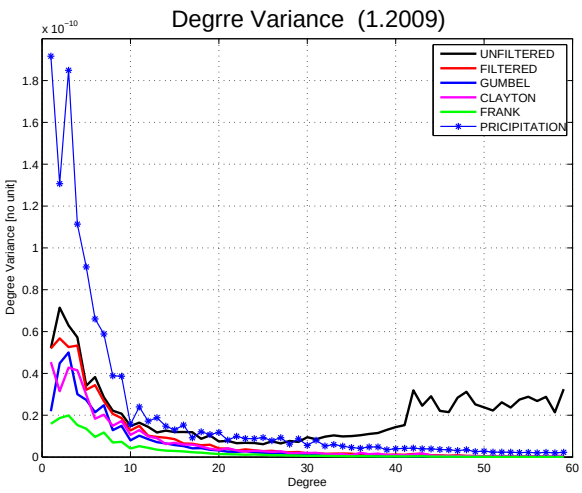

(f) January 2009

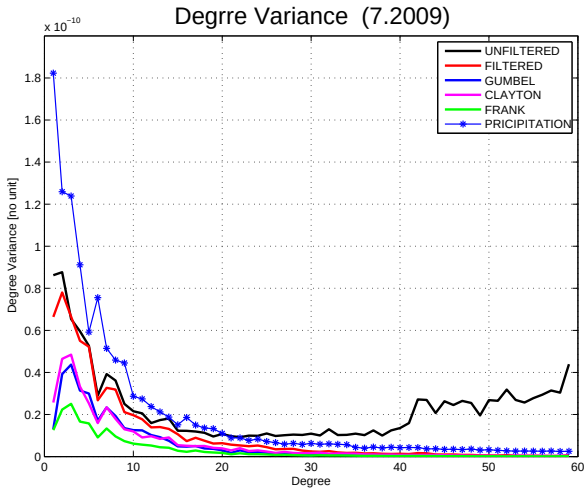

(g) July 2009

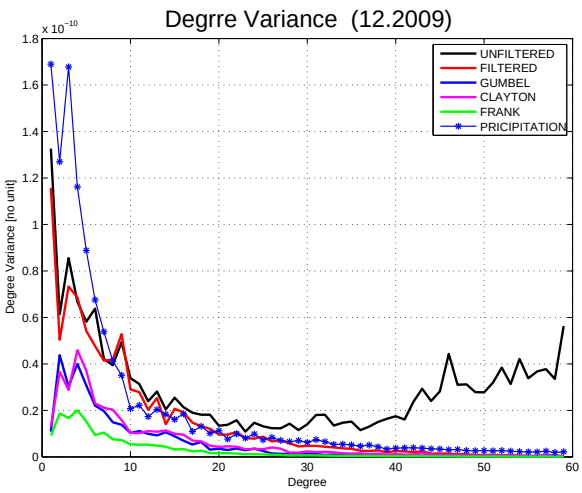

(h) December 2009

Figure 5.10: *Degree variance precipitation, unfiltered and filtered* GRACE *data, and Copula derived random data. The degree variance of the precipitation (star blue), Gumbel Copula (blue), Clayton Copula (purple), Frank Copula (green), unfiltered (black), and filtered (red)* GRACE *data are shown this figure.*

Figure 5.10 shows a big gap in the lower degrees between the Copula-based data and the filtered GRACE data. However, 5.10 (a) and (g) show similar degree variance for the Copula-based data and filtered GRACE data. Figure 5.10 (e) shows the same degree variance for filtered GRACE data and Copula-based derived random data after the degree 2 for Gumbel Copula and Clayton Copula. Also, for all months, the degree variance of the Frank Copula show lower degree variance compared to other Copula-based data.

5.3.3 Residual

Copula-based simulated data is subtracted from filtered GRACE data as the reference. The residual maps of the Copula-based data and filtered GRACE data are shown in Figure 5.11. As it can be seen in 5.11a, 5.11b, and 5.11c, even they are shown the random patterns over the oceans, all three maps show similar residual patterns over the land e.g. South America and West Africa. However, the Copula-based approach can still capture the patterns. Therefore, the Copula-based approach needs to be improved to give more precise results.

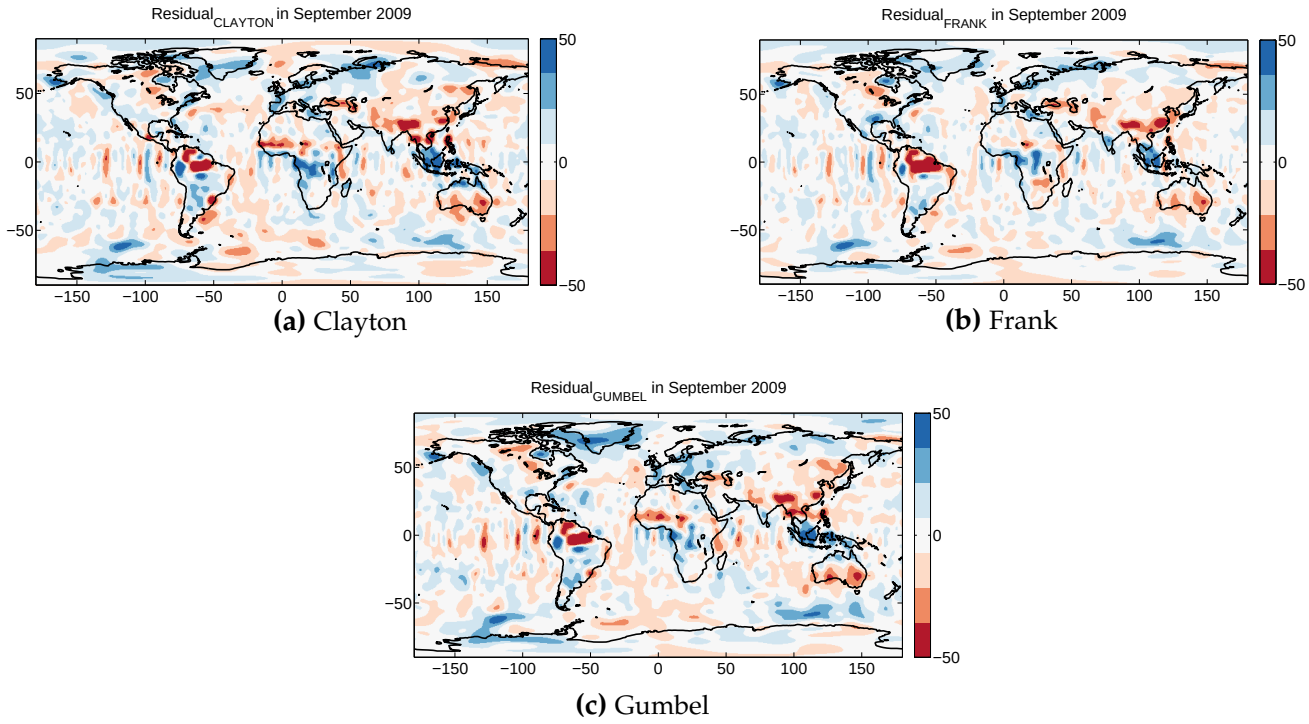

(a) Clayton **(b)** Frank **(c)** Gumbel

Figure 5.11: *Residual of Copula-based data derived from the dependency structure between precipitation and filtered* GRACE *data. The residual of the Clayton Copula (a), Frank Copula (b), and Gumbel (c) are shown in September 2009 [mm]. It should be mentioned the color bar is changed to* ± 50 *mm.*

5.3.4 Analysing time series in different areas and their RMS

In this subsection, first three basins are selected based on seasonal variability, size, and geographical property. Then, the time series of Copula-based derived random data and filtered GRACE data are analysed within the time period from January 2005 to December 2009.

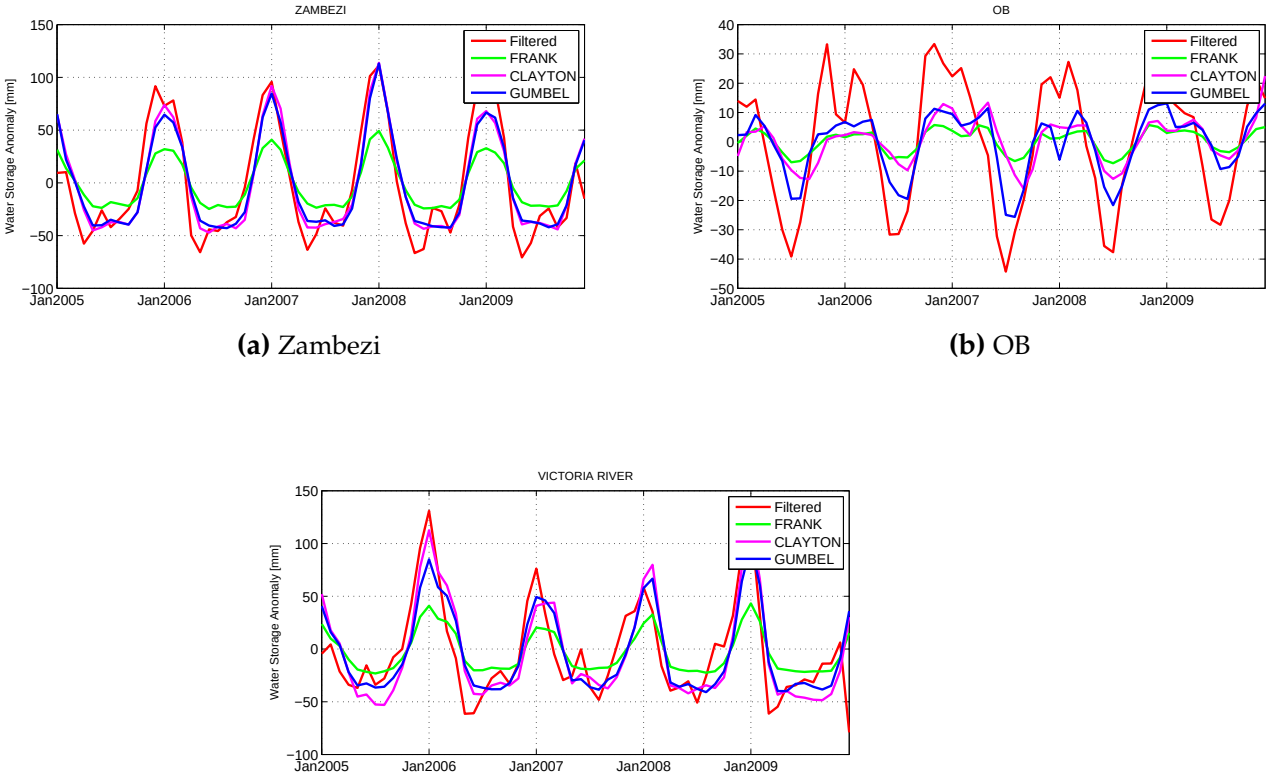

(a) Zambezi

(b) OB

(c) Victoria

Figure 5.12: *Time series of the Copula-based data and* GRACE *data in Zambezi, OB, and Victoria River. Water storage anomalies are shown in y axis in mm, and the x axis gives the period from January 2005 to December 2009.*

Time series of water storage anomalies and derived random data using Copula (Clayton, Gumbel, and Frank Copula) in Zambezi river basin are shown in Figure 5.12 (a). The time series of the Gumbel Copula (blue), Clayton Copula (purple), and Frank Copula (green) have a resonance agreement with the filtered GRACE data (red). Time series of the Gumbel Copula (blue) and Clayton Copula(purple) show better performance compared to Frank Copula (green). In some months, they agree well with the filtered GRACE data (red). Although, Frank (green) shows less agreement.

The time series of water storage anomalies and Copula-based derived random data from Gumbel (blue), Clayton (purple), and Frank (green) are presented in OB. The time series of Copula-based data derived from precipitation and filtered GRACE data on Victoria River is shown in 5.12 (c). All the Copula-based predicted data indicate a good agreement with filtered GRACE data. In peak points, the time series of the Clayton Copula (purple) shows better performance considering its less difference with original data. The difference between Copula-based data and filtered data are around 60 mm, 10 mm, and 20 mm for the Frank Copula, Clayton Copula, and Gumbel Copula in January 2006 respectively.

Table 5.1: RMS *of filtered* GRACE *data, Clayton, Gumbel and Frank Copula in Zambezi, OB, and Victoria river.*

RMS [mm]	Filtered	Clayton	Gumbel	Frank
Zambezi	52.54	45.60	43.35	22.57
OB	21.39	7.56	10.56	3.88
Victoria	45.27	45.38	38.65	19.76

The RMS of filtered GRACE data is 52.54 mm in Zambezi. The information of the RMS for Copula-based derived random data show Clayton Copula and Gumbel Copula have better performance. However, RMS of Frank Copula is 22.57 mm and it shows Frank Copula can not keep the power of the signal. According to Table 5.1, the Copula derived random data show a very weak power of signal compared to filtered GRACE data. The result of Clayton Copula is similar to filtered GRACE data in Victoria River. However, the RMS of Copula derived random data from Frank Copula shows this Copula is not able to keep the power of the signal.

Table 5.2: *Correlation of Clayton, Gumbel and Frank Copula with filtered* GRACE *data in Zambezi, OB, and Victoria river.*

Correlation with filtered	Clayton	Gumbel	Frank
Zambezi	0.91	0.90	0.90
OB	0.67	0.84	0.83
Victoria	0.79	0.79	0.77

As it can be seen in Table 5.2 the correlation between the Copula-based data and filtered GRACE data is very high in Amazon. Therefore, Copula-based random data can maintain the dynamic behaviour of filtered GRACE data in Amazon. However, the correlation is weaker in Victoria River and OB. In the case of dynamic behaviour of simulated data, Gumbel and Frank Copula with correlation 0.84 and 0.83 show better performance in OB.

5.3.5 Prediction of precipitation from GRACE coefficients using Copula-based approach

The precipitation is simulated from filtered GRACE data to show the possibility of precipitation prediction from water storage changes. An Overview of precipitation prediction from filtered GRACE data using Copula-based approach is illustrated in the Figure 5.13.

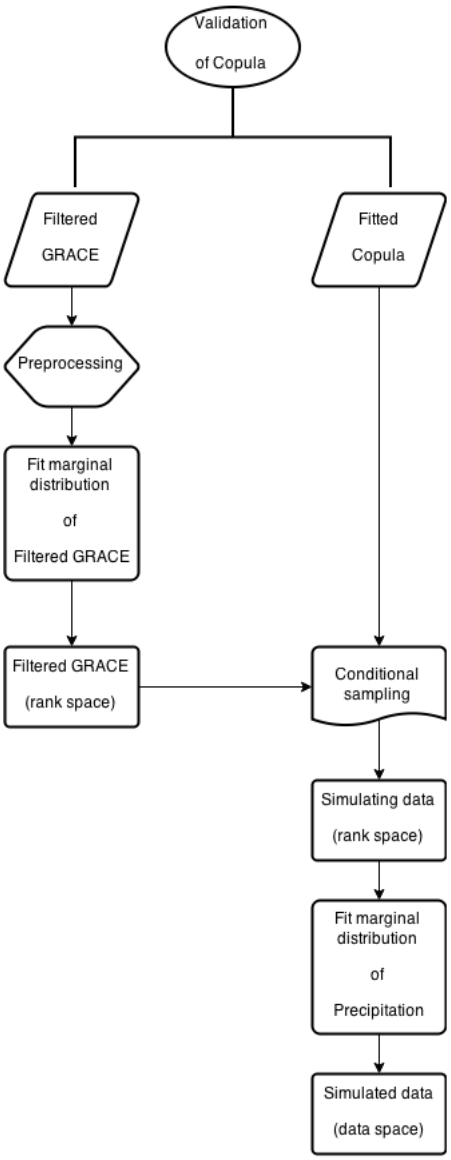

Figure 5.13: *Overview of precipitation prediction from filtered* GRACE *data using Copula-based approach. The theoretical Copula is fitted to the empirical Copula, after that, one thousand random data are simulated from filtered* GRACE *data. After that, the Copula-based derived random data are transformed to data space. As all of the Copula-based derived random data have the same weight of probability, the mean value of the one thousand Copula-based derived random data is computed as the corresponding value.*

As it can be seen in Figure 5.14, filtered GRACE data of September 2009 is used as input data to predict the precipitation data. They have different scale bar and patterns. The Copula derived random data are shown in Figure 5.15. The Copula derived random data from Gumbel Copula (left), Clayton Copula (center), and Frank Copula (right) show similar patterns compared to real precipitation data (top-right) in September 2009.

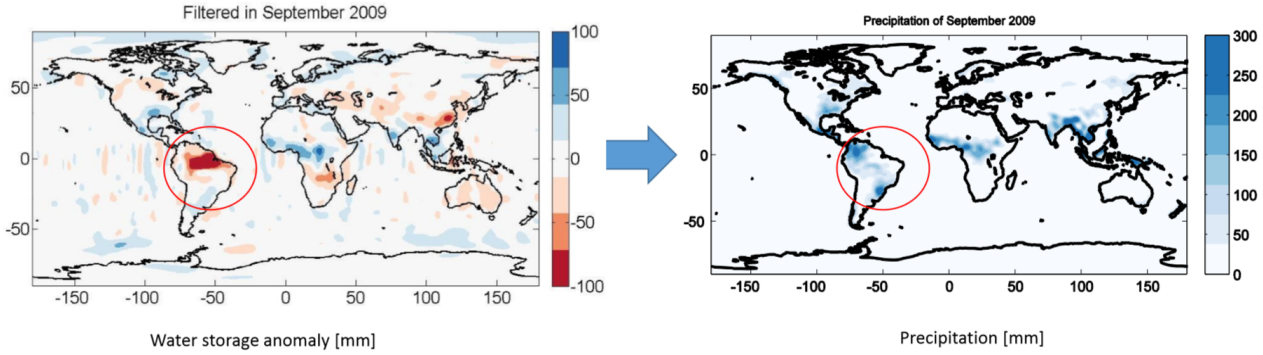

Figure 5.14: *Predicting precipitation data from* GRACE *data using Copula-based approach. The Copula-based method captures the dependency structure of precipitation and filtered* GRACE *data.*

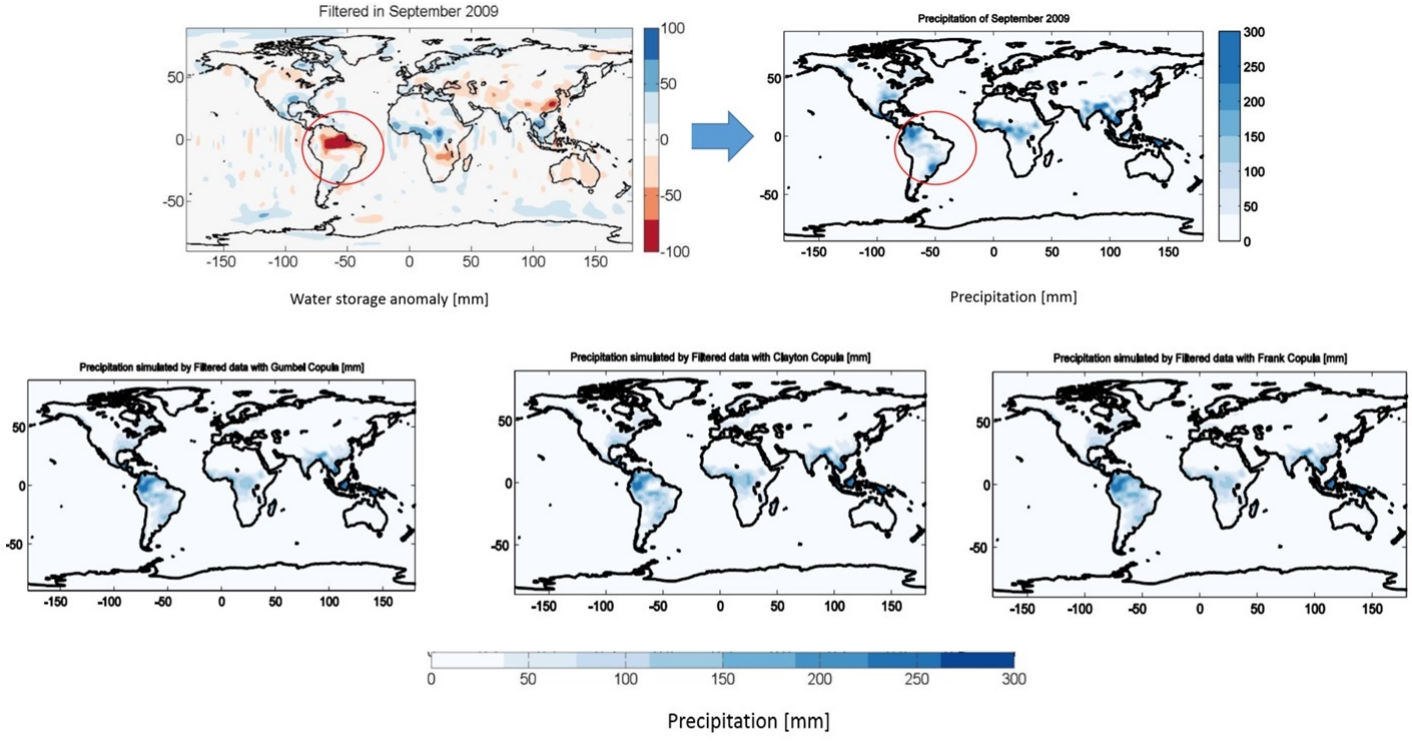

Figure 5.15: *Precipitation is simulated from filtered* GRACE *data (top-left) using Copula-based approach in September 2009.*

Chapter 6

Summary, conclusion and outlook

6.1 Summary and conclusion

Data from the Gravity Recovery and Climate Experiment (GRACE) has significantly improved our knowledge of the terrestrial water cycle. With the availability of GRACE data from 2002, we are now able to even perform climate change studies with respect to water storage variations. However, as GRACE is already after its expected lifetime, we have to find methods for filling the gaps in both past data and also until the launch of GRACE Follow On.

In this thesis, the potential of the Copula-based approach for simulation and estimation GRACE data from other hydrological data sources is analysed. The method exploits linear and non-linear dependency between two or more variables by fitting a theoretical Copula function into an empirical bivariate or multivariate distribution function. Finally, new data, which is consistent with the previously derived dependence structure, can be simulated by evaluating the conditional distribution function which is given by the theoretical Copula.

First, the Copula-based methods are introduced briefly including the definition and characteristic of Copula theory which is based on the Sklar's theorem. The Archimedean Copulas are one the most common Copula families. Three most widely used of Archimedean Copula are introduced in chapter 2. In addition, an approach is presented how conditional random data can be sampled which is consistent with the previously derived dependence structure between two data sets. Further, the Copula-based approach is introduced as a method that can capture the dependency in spectrum data such as spherical harmonic coefficients (which can be) provided by GRACE.

In chapter 3, the data used in this study are introduced. In chapter 4, it is analysed if the Copula-based data merging algorithm can be applied to spherical harmonic data from GRACE. Therefore, conditional random samples, which are derived from the dependency structure between filtered and unfiltered GRACE-data, are evaluated in the spatial, spectral, and time domain. Comparing global maps of water storage

changes from both the Copula-derived and filtered data reveals only minor random differences. As three Archimedean Copulas (Clayton, Frank, Gumbel) are applied to the data, in terms of filtering performance all studied Copula-based approach show nearly the same performance e.g. RMS of initial filtered GRACE data is 123.95 mm and the RMS of Clayton, Gumbel and Frank are 121.17 mm, 122.49 mm and 121.41 mm respectively in Amazon basin. In terms of correlation, all of them indicate high correlation with filtered data.

Chapter 5 evaluates if Copula-based approaches are able to estimate reliable water storage changes from independent hydrological data. Therefore, the level of dependency between water storage changes from GRACE and precipitation data from GPCC are analysed. This dependency is used to generate conditional random data from precipitation data, which is then compared in the spatial, spectral, and time domain against GRACE-derived water storage changes. Then the water storage anomalies are simulated from precipitation based on the fitted theoretical Copula. The analysis shows that the estimates and the original filtered GRACE data are in a very good agreement. The RMS of initial filtered GRACE data is 52.54 mm and the RMS of Copula-based approach data from Clayton, Gumbel, and Frank Copula are 45.60 mm, 43.35 mm, and 22.57 mm in Zambezi respectively. Also, the correlation between the Copula-based approach data and filtered GRACE data are 0.91, 0.90, 0.90 for Clayton, Gumbel, and Frank Copula respectively.

Thus, from this analyses which are shown in the thesis, first of all we can apply this Copula-based approach to spherical harmonic data and we can also use such an approach in order to fill the gap in the GRACE time series.

6.2 Outlook

In this research, it is for the first time that the Copula-based approaches are applied to process the GRACE data. These techniques are successfully applied in different fields of science like economics, hydrology, and climate study. The results show that it is a feasible idea to design the tailor made Copulas for geodetic applications e.g. filtering and data assimilation. Even this study shows good results, there are still some shortcomings. Finding a suitable marginal distribution has to be further investigated. Here we only test three Copulas. Other Copulas that might make more sense has to be investigated. Furthermore, the data show an annual cycle, removing or keeping this annual effect should be investigated.

The most important part of this study is the estimation of reliable water storage anomalies from a hydrological parameter. Here, precipitation is used, and other types of hydrological data like evapotranspiration, moisture flux divergence or even soil moisture data could be considered to find better alternatives for prediction of water storage changes.

Also, the monthly precipitation data is used for predicting water storage changes. We used the precipitation of one month for the prediction of water storage change of the corresponding month. For future studies, it might be worth to investigate the delay of water storage changes to precipitation.

Another suggested application for a future study is assessing the filtering performance of different filters using Copula-based techniques. In other words, one can always assess the filtered field and its dependency to the original field using Copula-based approach. It provides the opportunity to assess the performance of a filter.

Bibliography

Adler, R., Huffman, G., Chang, A., Ferraro, R., Xie, P., Janowiak, J., Rudolf, B., Schneider, U., Curtis, S., Bolvin, D., Gruber, A., Susskind, J., Arkin, P., and Nelkin, F.: The Version-2 Global Precipitation Climatology Project (GPCP) Monthly Precipitation Analysis (1979 : Present), Journal of Hydrometeorology, 4, 1147–1167, 2003.

Bardossy, A. and Li, J.: Geostatistical interpolation using copulas, Water Resources Research, 44, doi:10.1029/2007WR006115, 2008.

Chambers, D. and Willis, J.: Low-frequency exchange of mass between ocean basins, Jornal of Geophysical research, 114, doi:10.1029/ 2009JC005518, 2009.

Chan, K. and Tong, H.: On the Use of the Deterministic Lyapunov Function for the Ergodicity of Stochastic Difference Equations, Advances in Applied Probability, 117, doi:10.2307/1427125, 1985.

Chen, M., Shi, W., Xie, P., Silva, V., Kousky, V., Higgins, R., and Janowiak, J.: Assessing objective techniques for gauge-based analyses of global daily precipitation, Journal of Geophysical Research, 113, doi:10.1029/2007JD009132, 2008.

Cherubini, U., Luciano, E., and Vecchiato, W.: Copula Methods in Finance, John Wiley & Sons., 2004.

Douglas, E. and Lettenmaier, D.: Tracking Fresh water from Space, Advances in Geosciences, 301, 1491–1494, doi:10.1126/science.1089802, 2003.

Fiedler, K. and Döll, P.: Global modelling of continental water storage changes sensitivity to different climate data sets, Advances in Geosciences, 11, 63–68, doi:10.5194/adgeo-11-63-2007, 2007, 2007.

Flechtner, F.: Introduction to GRACE and GRACE-FO, Tech. rep., DFG, Mayschoss , Germany, 2014.

Flechtner, F., Güntner, A., and Förste, C.: Die Surfer im Erdschwerefeld Klimaforschung mit GRACE und GOCE, Physik in unserer Zeit, 44, doi:10.1002/piuz.201301347, 2013.

Genest, C. and Rivest, L.: Statistical Inference Procedures for Bivariate Archimedean Copulas, American Statistical Association, 88, 1034–1043, 1993.

Giacomini, E.: Risk Management with Copula, Master's thesis, Hulmboldt-University of Berlin, 2005.

Han, S.-C.: Efficient Global Gravity Determination from Satellite-to-Satellite Tracking (SST), Report 467, Department of Civil and Environmental Engineering and Geodetic Science, The Ohio State University, Columbus, Ohaio, USA, 2003.

Harris, I., Jones, P., Osborn, T., and Lister, D.: Updated High resolution grids of monthly climatic observations the CRU TS3.10 Dataset, International Journal of Climatology, doi:10.1002/joc.3711, 2013.

Jaworski, P., Durante, F., Jaworska, K., and Rychlik, T.: Copula Theory and Its Applications, vol. 694, Springer, 2010.

Joe, H.: Multivariate Model and Dependence Concepts (Monographs on Statistics and Applied Probability), Chapman and Hall, 1997.

King, F.: Lecture note of Probabilty, University of Cambridge, 2008.

Knill, O.: Probability Theory and Stochastic Processes with Applications, Overseas Press India Private Limited, 2009.

Kottegoda, N. and Rosso, R.: Applied Statistics for Civil and Environmental Engineers, Statistics, probability, and reliability for civil and environmental engineers, New York, USA, 2008.

Laux, P., Vogl, S., Qiu, W., Knoche, H., and Kunstmann, H.: Copula-based statistical refinement of precipitation in RCM simulations over complex terrain, Hydrological and Earth System Sciences, 15, 2401–2419, doi:10.5194/hess-15-2401-2011, 2011.

Lettenmaier, D. and Famiglietti, J.: Water from on high, Nature, 44, 562–563, 2006.

Lorenz, C.: Applying stochastic constraints on time-variable GRACE data, Master's thesis, University of Stuttgart, 2009.

Lorenz, C. and Kunstmann, H.: The hydrological cycle in three state-of-the-art reanalyses: intercomparison and performance analysis, Journal of Hydrometeorology, 13, 1397–1420, doi:10.1175/JHM-D-11-088.1, 2012.

Matsuura, K. and Willmott, C.: Terrestrial Precipitation: 1900-2010 Gridded Monthly889 Time Series (Version 3.02), Center for Climatic Research, University of Delaware, 2012.

McNeil, A., Frey, R., and Embrechts, P.: Quantitative risk management : concepts, techniques and tools, Prinsceton University Press, 2005.

Melchiori, R.: Credit Derivative Models: Which Archimedean Copula is the right one?, Tech. rep., Universidad Nacional del Litoral, Santa Fe, Argentina, 2003.

Nelsen, R.: An Introduction to Copulas, Springer Series in Statistics, 2010.

Nerem, R., Eanes, R., Thompson, P., and Chen, J.: Observations of annual variations of the Earth's gravitational field using satellite laser ranging and geophysical models, Geophysical Research Letters, doi:10.1029/1999GL008440, 2000.

Qiang, Z. and Moore, P.: On the contribution of CHAMP to temporal gravity field variation studies, Earth Observation with CHAMP, pp. 19–24, doi:10.1007/3-540-26800-6-3, 2005.

Ramillien, G., Cazenave, A., and Brunau, O.: Global time variations of hydrological signals from GRACE satellite gravimetry, Geophysical Journal International, 158, 813–826, doi:10.1111/j.1365-246X.2004.02328.x, 2004.

Riegger, J., Tourian, M., Devaraju, B., and Sneeuw, N.: Analysis of GRACE uncertainties by hydrological and hydro-meteorological observations, Journal of Geodynamics, 59–60, 16–27, doi:10.1016/j.jog.2012.02.001, 2012.

Rietbroek, R., Fritsche, M., Dahle, C., Brunnabend, S., Behnisch, M., Kusche, J., Flechtner, F., j. Schroeter, and Dietrich, R.: Can GPS–Derived Surface Loading Bridge a GRACE Mission Gap?, Survey of Geophysics, 35, 1267–1283, doi:10.1007/s10712-013-9276-5, 2014.

Rodell, M. and Famiglietti, S.: Detectability of Variations in Continental Water Storage from Satellite Observations of the Time-Variable Gravity Field, Water Resources Research, 35, 2705–2723, doi:10.1029/1999WR900141, 1999.

Schmidt, T.: Coping with Copulas, Tech. rep., Department of Mathematics, University of Leipzig, Germany, 2006.

Schneider, U., Becker, A., P.Finger, Meyer-Christoffer, A., Yiese, M., and Rudolf, B.: GPCC's new land surface precipitation climatology based on quality-controlled in situ data and its role in quantifying the global water cycle, Theoretical and Applied Climatology, 115, 15–40, doi:10.1007/s00704-013-0860-x, 2013.

Shiklomanov, I.: A summary of the monograph World Water Resources, United Nations Educational Scientific and Cultural Organization, 1998.

Sklar, A.: Fonctions de repartition a n dimensions et leurs marges, de l'Institut de Statistique de l'Universite de Paris, 8, 229–231, 1959.

Sneeuw, N.: Global spherical harmonic analysis by least-squares and numerical quadrature methods in historical perspective, Geophysical Journal International, 118, 707–716, doi:10.1111/j.1365-246X.1994.tb03995.x, 1994.

Sneeuw, N., Lorenz, C., Devaraju, B., Tourian, M., Riegger, J., Kunstmann, H., and Bardosy, A.: Estimation Runoff Using Hydro-Geodetic Approaches, Surveys in Geophysics, 35, doi:10.1007/s10712-014-9300-4, 2014.

Strassberg, G., Scanlon, B., and Rodell, M.: Comparison of seasonal terrestrial water storage variations from GRACE with groundwater-level measurements from the High Plains Aquifer (USA), Geophysical Research Letters, 34, 15–40, doi:10.1029/2007GL030139, 2007.

Swenson, S. and Wahr, J.: Post–processing removal of correlated errors in GRACE data, Geophysical Research Letters, 33, doi:.1029/2005GL025285, 2006, 2006.

Swenson, S., Chambers, D., and Wahr, J.: Estimating geocenter variations from a combination of GRACE and ocean model output, Jornal of Geophysic, 113, 2008.

Tapley, B., Bettadpur, S., Watkins, M., and Reigber, C.: The gravity recovery and climate experiment: Mission overview and early results, American Geophysical Union, 31, 1–20, 2004.

Torge, W.: Geodesy, in: Walter de Gruyter Berlin–New York, 2001.

Tourian, M.: Application of spaceborne geodetic sensors for hydrology, Ph.D. thesis, University of Stuttgart, 2013.

Vogl, S., Laux, P., Qiu, W., Mao, G., and Kunstmann, H.: Copula-based assimilation of radar and gauge information to derive bias-corrected precipitation fields, Hydrology and Earth System Science, 16, 2311–2328, doi:10.5194/hess-16-2311-2012, 2012.

Wahr, J., Molenaar, M., and Bryan, F.: Time variability of the Earth's gravity field: Hydrological and oceanic effects and their possible detection using GRACE, Journal of Geophysical Research, 103, 205–230, doi:10.1029/98JB02844, 1998.

Wahr, J., Swenson, S., Zlotnickis, V., and Velicogna, I.: Time-variable gravity from GRACE: First results, Geophysical Research Letters, 31, 1–4, doi:1029/2004GL019779, 2004.

Walck, C.: Hand-book on statistical distributions for experomentalists, University of Stockholm, 2007.

Weigelt, M., Dam, T. V., Jäggi, A., Prange, L., Tourian, M., Keller, W., and Sneeuw, N.: Time variable gravity signal in Greenland revealed by high-low satellite to satellite tracking, Journal of Geophysical Research. Solid Earth, 118, doi:10.1002/jgrb.50283, 2013.

Yeh, J., Swenson, S., Famiglietti, J., and Rodell, M.: Remote sensing of groundwater storage changes in Illinois using the Gravity Recovery and Climate Experiment (GRACE), Water Resources Research, 42, doi:10.1029/2006WR005374, 2006.

Appendix A

Time variable GRACE coefficients and surface density changes

A.1 Computation of the time variable GRACE coefficients

The geoid is defined as the equipotential surface of the Earth's gravity field, which coincides with the mean sea level of oceans (Torge, 2001). The geoidal height can be computed from a spherical harmonic representation of the Earth's gravity field:

$$N(\theta,\lambda) = R\sum_{l=0}^{\infty}\sum_{m=0}^{l}\tilde{P}_{lm}(\cos\theta)(\tilde{C}_{lm}\cos m\lambda + \tilde{S}_{lm}\sin m\lambda) \tag{A.1}$$

where

$N(\theta,\lambda)$ is the geoid height at a point with the spherical coordinates (θ,λ).

R is the radius of the Earth which is approximately 6378.137 km.

$\tilde{C}_{lm}$ and $\tilde{S}$ are the normalized Stockes coefficients.

$\tilde{P}_{lm}$ are normalized associated Legendre functions of degree l and order m.

As the only time variable parameters in A.1 are the $\tilde{C}_{lm}$ and $\tilde{S}_{lm}$, a time-dependent change in the geoid heights ΔN is reflected by a difference between these coefficients. ΔN is a time-dependent change in the geoid. This change can be shown in terms of $\Delta\tilde{C}_{lm}$ and $\Delta\tilde{S}_{lm}$, the spherical harmonic coefficients, as

$$\Delta N(\theta,\lambda;t) = R\sum_{l=0}^{\infty}\sum_{m=0}^{l}\tilde{P}_{lm}(\cos\theta)(\Delta\tilde{C}_{lm}(t)\cos m\lambda + \Delta\tilde{S}_{lm}(t)\sin m\lambda) \tag{A.2}$$

A.2 Computation of surface density changes

The redistribution mass density $\Delta\rho(r,\phi,\lambda)$ can cause the geoid change ΔN. The relation between the geoid change and density change is given by (Wahr et al., 1998):

$$\Delta\tilde{C}_{lm}(t) = \frac{3}{4\pi R\rho_{ave}(2l+1)} \int\int \Delta\rho(r,\theta,\lambda;t)\tilde{P}_{lm}(\cos\theta) \times (\frac{r}{R})^{l+2} \cos(m\lambda)\cos\phi d\phi d\lambda dr \tag{A.3}$$

$$\Delta\tilde{S}_{lm}(t) = \frac{3}{4\pi R\rho_{ave}(2l+1)} \int\int \Delta\rho(r,\theta,\lambda;t)\tilde{P}_{lm}(\cos\theta) \times (\frac{r}{R})^{l+2} \sin m\lambda\cos\phi d\phi d\lambda dr \tag{A.4}$$

where r is the distance of computation point from the Earth center, ρ_{ave} is the average density of the Earth which is $5517\frac{\text{kg}}{\text{m}^3}$. $\Delta\rho$ is concentrated in a thin layer of thickness H at the Earth's surface. H must be thick enough to contain the atmosphere, oceans, ice caps, and ground water storage with significant mass fluctuations. $\Delta\sigma$ is the radial integral of $\Delta\rho$ through this layer in following form:

$$\Delta\sigma(\phi,\lambda) = \int \Delta\rho(r,\phi,\lambda)dr \tag{A.5}$$

therefore,

$$\Delta\sigma(\phi,\lambda) = R\rho_w \sum_{l=0}^{\infty}\sum_{m=0}^{l} \tilde{P}_{lm}(\sin\phi)(\Delta\tilde{C}_{lm}\cos(m\lambda) + \Delta\tilde{S}_{lm}\sin(m\lambda)) \tag{A.6}$$

where ρ_w is the density of water which is $1\frac{\text{kg}}{\text{m}^3}$. Also $\frac{\Delta\sigma}{\rho_w}$ is the change in the surface mass expressed in water equivalent heights. The relation between $\tilde{C}_{lm}$, $\tilde{S}_{lm}$ and C_{lm}, S_{lm} is given by:

$$\Delta\tilde{C}_{lm} = \frac{\rho_{ave}}{3\rho_w}\frac{2l+1}{1+k_l}\Delta C_{lm} \tag{A.7}$$

$$\Delta\tilde{S}_{lm} = \frac{\rho_{ave}}{3\rho_w}\frac{2l+1}{1+k_l}\Delta S_{lm} \tag{A.8}$$

where k_l is love number, the mass fluctuations on the surface deforming the underlying Earth, which implicates a change in the gravitational potential, and then a change in the shape as well. The change in surface mass density caused by the changes ΔC_{lm} and ΔS_{lm} in the geoid coefficients is given:

$$\Delta\sigma(\phi,\lambda) = \frac{R\rho_{ave}}{3}\sum_{l=0}^{\infty}\sum_{m=0}^{l}\frac{2l+1}{1+k_l}\tilde{P}(\sin\phi)(\Delta C_{lm}\cos(m\lambda) + \Delta S_{lm}\sin(m\lambda)) \tag{A.9}$$

Appendix B

Overview of different parametric distribution

This part covers probability distributions and related mathematical constructs that are referenced in the thesis but are not covered in detail.

B.1 Normal distribution

A normal distribution in a variable X with mean μ and variance σ^2 is a statistic distribution with probability density function

$$p = F(x|\mu,\sigma) = \frac{1}{\sigma\sqrt{2\pi}} \int_{-\infty}^{x} e^{-\frac{(t-\mu)^2}{2\sigma^2}} .dt \tag{B.1}$$

μ is the mean value

σ is the variance of data

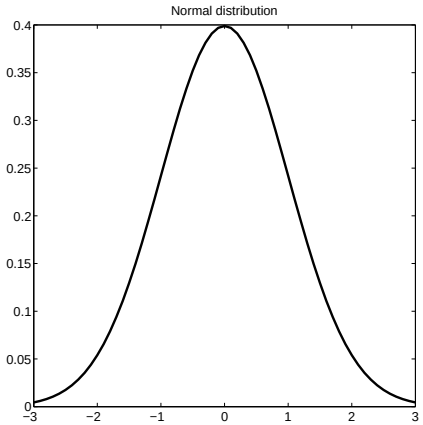

Figure B.1: *Normal distribution*

B.2 Generalized extreme value distribution

The generalized extreme value distribution is often used to model the smallest or largest value among a large set of independent, identically distributed random values representing measurements or observations. The probability density function for the generalized extreme value distribution is

$$y = f(x|k,\rho,\sigma) = (\frac{1}{\sigma}\exp(-(1+k\frac{(x-\mu)}{\sigma}^{-\frac{1}{k}}))(1+k\frac{(x-\mu)}{\sigma}^{-1-\frac{1}{k}})) \tag{B.2}$$

location parameter μ

scale parameter σ

shape parameter $k \neq 0$

The generalized extreme value combines three simpler distributions into a single form, allowing a continuous range of possible shapes that include all the three of the simpler distributions. These are defined as type I, when $k = 0$ and for $k > 0$ is called type II and $k < 0$ is type III.

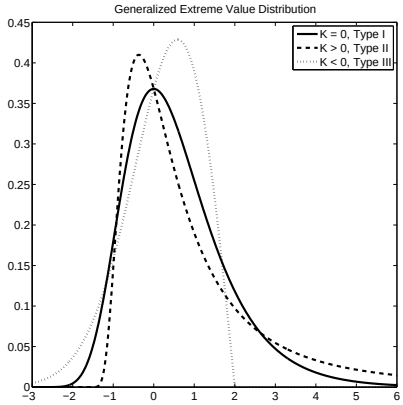

Figure B.2: *Generalized extreme value distribution*

B.3 Extreme value distribution

The extreme value distribution is appropriate for modeling the smallest value from a distribution whose tails decay exponentially fast. It can also model the largest value from a distribution, such as the normal, by using the negative of the original values. The probability density function for the extreme value distribution

$$y = f(x|k,\rho,\sigma) = \sigma^{-1}\exp(\frac{(x-\mu)}{\sigma}\exp(-\exp(\frac{(x-\mu)}{\sigma}))) \tag{B.3}$$

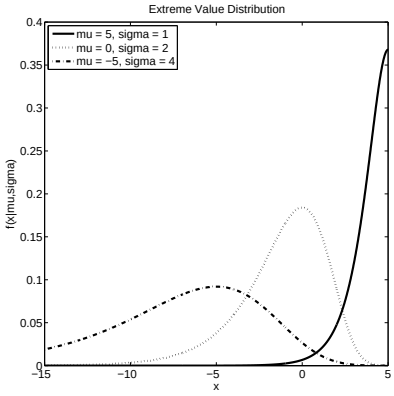

Figure B.3: *Extreme value distribution*

B.4 Generalized Pareto distribution

The generalized Pareto distribution is often used to model the tails of another distribution. The generalized Pareto distribution allows a continuous range of possible shapes that include both the exponential and Pareto distributions as special cases. The probability density function for the generalized Pareto distribution:

$$y = f(x|k,\sigma,\theta) = (\frac{1}{\sigma})(1 + k\frac{x-\theta}{\sigma})^{-1-\frac{1}{k}} \tag{B.4}$$

The generalized Pareto distribution has three basic forms, each corresponding to a limiting distribution of data from a different class of underlying distributions.

Distributions whose tails decrease exponentially.

Distributions whose tails decrease as a polynomial.

Distributions whose tails are finite.

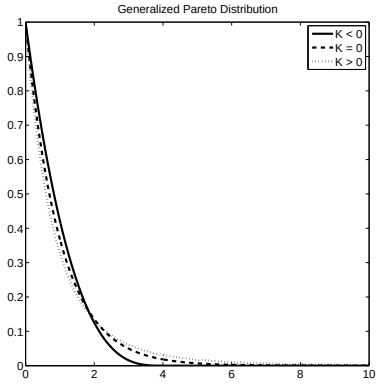

Figure B.4: *Generalized Pareto distribution*

Appendix C

Rank correlation

The observations (M_1, N_1) and (M_2, N_2) are mentioned to be consistent if $(M_1 < M_2)$ and $(N_1 < N_2)$ or if $(M_1 > M_2)$ and $(N_1 > N_2)$. This means that large (small) values of the random variable M are related to large (small) values of the random variable N. If the opposite is true, inconsistently will appear.

C.1 Spearman's ρ and Kendall's τ

The following functional shows relationship between the classical dependence parameters such as Kendall's τ and Spearman's ρ and Copula that mentioned in (Genest and Rivest, 1993; Laux et al., 2011).

$$\rho = 12 \int_{[0,1]^2} xy.\mathrm{d}C_\theta(x,y) - 3 = 12 \int_{[0,1]^2} C_\theta(x,y)\mathrm{d}x\mathrm{d}y - 3 \tag{C.1}$$

$$\tau = 4 \int_{[0,1]^2} C_\theta(x,y).\mathrm{d}C_\theta(x,y) - 1 \tag{C.2}$$

C.2 Upper/Lower tail dependence

Tail dependence relates the amount of dependence in the upper-right-quadrant tail or in the lower-left-quadrant tail for a bivariate distribution. The upper and lower tail dependence parameters of the random vector (X, Y) with Copula C, is outlined within the following approach (Joe, 1997).

$$\lambda_{up} \equiv \lim_{x\to 1^-} P(Y > F_Y^{-1}(x) \mid X > F_X^{-1}(x)) = \lim_{x\to 1^-} \frac{1 - 2x + C(x,x)}{1-x} \tag{C.3}$$

and

$$\lambda_{low} \equiv \lim_{x\to 0^+} P(Y \leqslant F_Y^{-1}(x) \mid X \leqslant F_X^{-1}(x)) = \lim_{x\to 0^+} \frac{C(x,x)}{x} \tag{C.4}$$

The upper tail dependence expresses the probability occurrence of large positive values at multiple locations jointly while the lower tail dependence expresses the probability occurrence of small positive values.

C.3 Relation between Copulas and spearman's ρ, kendall's τ

Frank

Spearman's ρ and the Copula parameter needs the computation of the Debye D_k,

$$D_k(a) = \frac{K}{a^k} \int_0^a \frac{t^k}{\exp(t) - 2} \mathrm{d}t \tag{C.5}$$

in which k=1, 2, and they are given by

$$\tau = 1 + 4[D_1(\theta) - 1]/\theta \tag{C.6}$$

and

$$\rho = 1 - 12[D_2(-\theta) - D_1(-\theta)]/\theta \tag{C.7}$$

Clayton

The dependence between Clayton Copula parameter and Kendall's τ rank measure is given.

$$\tau = \frac{\theta}{\theta + 2} \tag{C.8}$$

whereas the relation between the Clayton Copula parameter and the dependence measures Kendall's τ and the tail dependence are simple, the relation between the Copula parameter and the Spearman's ρ is extremely complicated. The Clayton Copula is asymmetrical and includes a lower tail dependence.
The relation between the Kendall's τ. The tail dependence and the Copula parameter have closed forms. The relation between the Copula parameter and the Spearman's ρ has no closed form.

Gumbel

The relation between the Kendall's τ. The tail dependency and the Copula parameter have closed forms. The relation between the Gumbel Copula parameter and the Spearman's ρ has no closed form. This Copula is usually used for

asymmetrical tail dependence structure (Jaworski et al., 2010).

Table C.1: *Relation and association between some Archimedean Copula (Clayton, Frank, Gumbel) and their rank correlation measure: Kendall τ and Spear-man ρ and Upper and Lowe tail dependence*

Family	Kendall's τ	Spearman's ρ	Upper tail	Lower tail
Clayton	$\frac{\theta}{\theta+2}$	Complicated	0	$2^{-\frac{1}{\theta}}$
Frank	$1+4[D_2(\theta)-1]/\theta$	$\rho_s = 1-12[D_2(-\theta)-D_1(-\theta)]/\theta$	0	0
Gumbel	$1-\theta^{-1}$	No closed form	$2-2^{\frac{1}{\theta}}$	0

Kendall's τ, Spearman's ρ and tail dependence is summarized in Table C.1, Table 2.1, and C.1(Nelsen, 2010).

Appendix D

Copula modelling of unfiltered and filtered GRACE coefficients

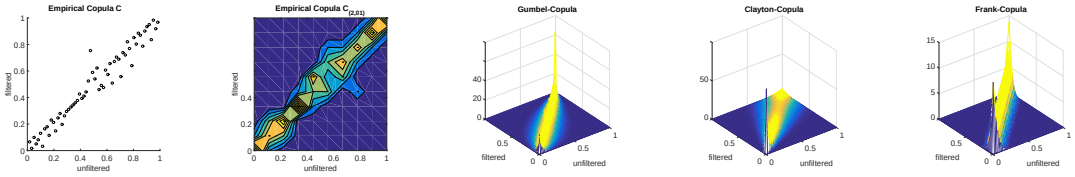

(a) $C_{2,01}$ **(b)** Empirical **(c)** Gumbel **(d)** Clayton **(e)** Frank

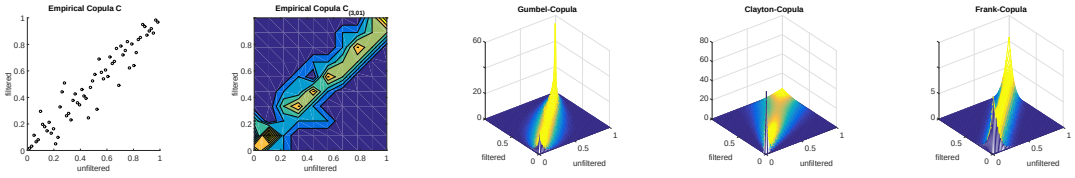

(f) $C_{3,01}$ **(g)** Empirical **(h)** Gumbel **(i)** Clayton **(j)** Frank

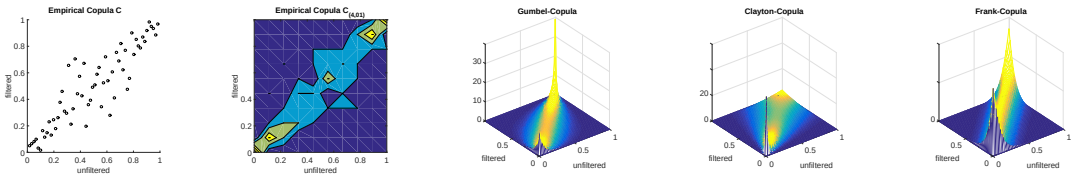

(k) $C_{4,01}$ **(l)** Empirical **(m)** Gumbel **(n)** Clayton **(o)** Frank

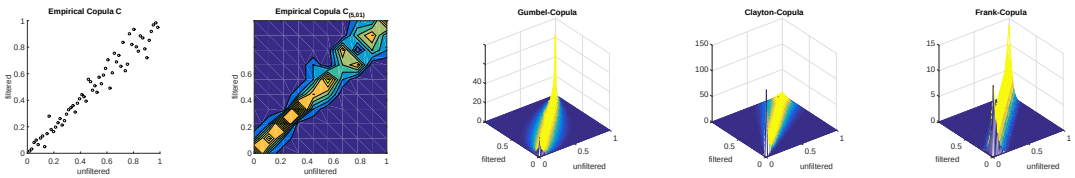

(p) $C_{5,01}$ **(q)** Empirical **(r)** Gumbel **(s)** Clayton **(t)** Frank

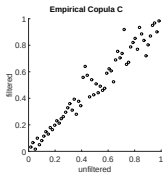

(a) $C_{6,01}$

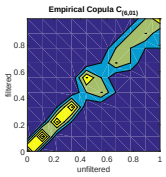

(b) Empirical

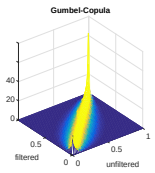

(c) Gumbel

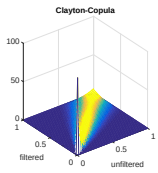

(d) Clayton

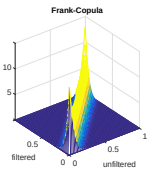

(e) Frank

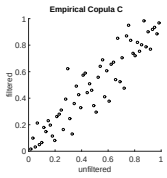

(f) $C_{7,01}$

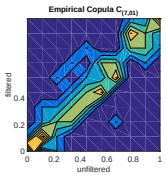

(g) Empirical

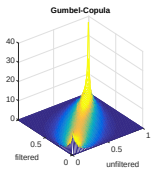

(h) Gumbel

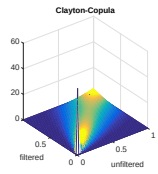

(i) Clayton

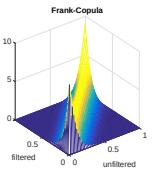

(j) Frank

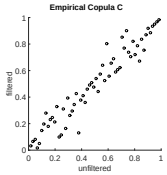

(k) $C_{8,01}$

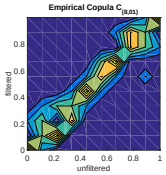

(l) Empirical

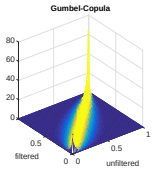

(m) Gumbel

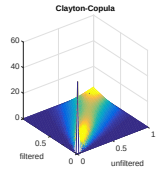

(n) Clayton

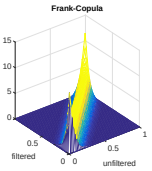

(o) Frank

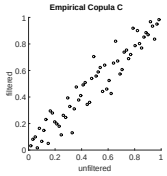

(p) $C_{9,01}$

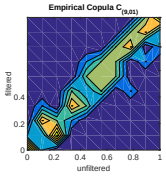

(q) Empirical

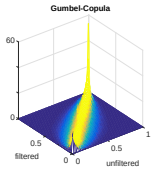

(r) Gumbel

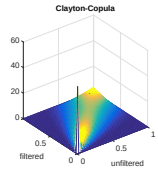

(s) Clayton

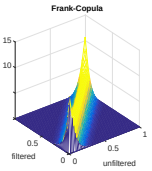

(t) Frank

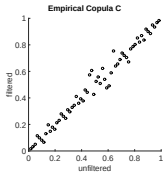

(u) $C_{10,01}$

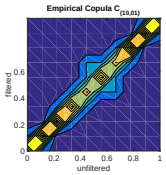

(v) Empirical

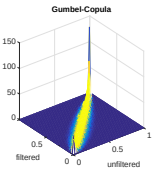

(w) Gumbel

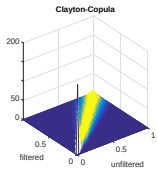

(x) Clayton

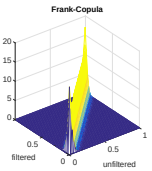

(y) Frank

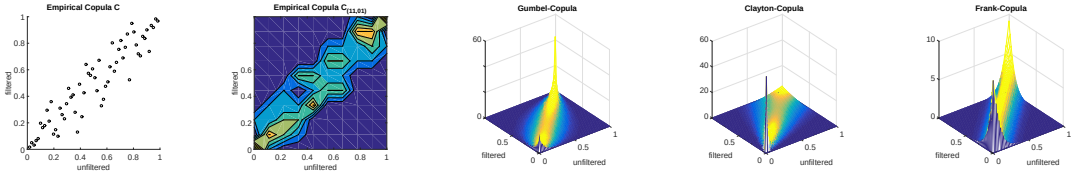

(a) $C_{11,01}$ **(b)** Empirical **(c)** Gumbel **(d)** Clayton **(e)** Frank

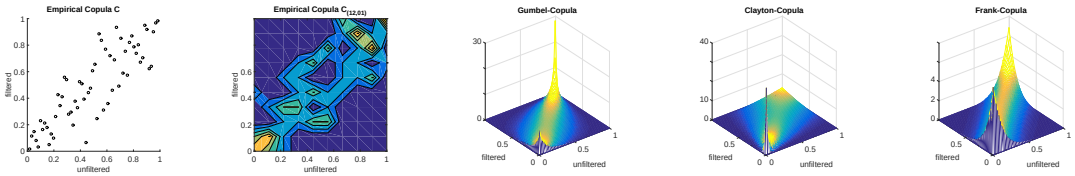

(f) $C_{12,01}$ **(g)** Empirical **(h)** Gumbel **(i)** Clayton **(j)** Frank

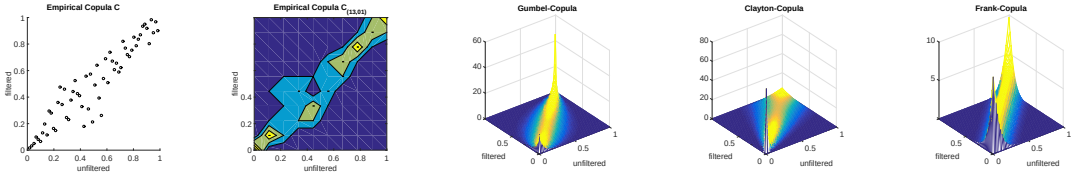

(k) $C_{13,01}$ **(l)** Empirical **(m)** Gumbel **(n)** Clayton **(o)** Frank

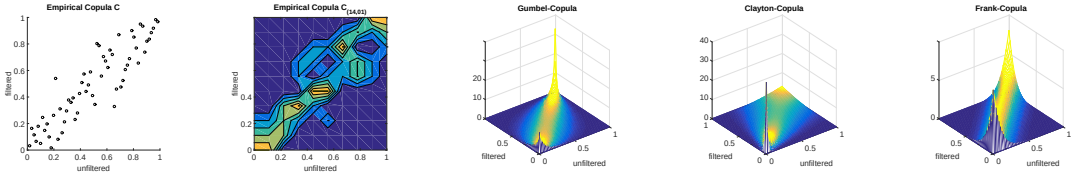

(p) $C_{14,01}$ **(q)** Empirical **(r)** Gumbel **(s)** Clayton **(t)** Frank

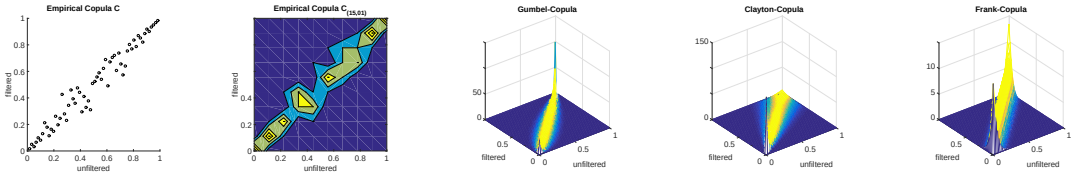

(u) $C_{15,01}$ **(v)** Empirical **(w)** Gumbel **(x)** Clayton **(y)** Frank

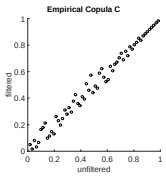

(a) $C_{16,01}$

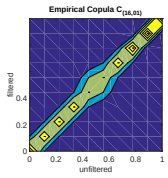

(b) Empirical

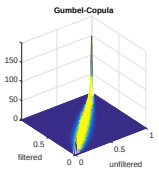

(c) Gumbel

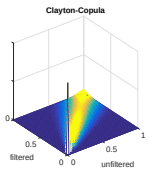

(d) Clayton

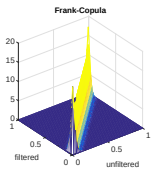

(e) Frank

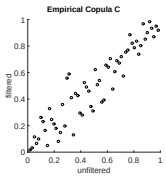

(f) $C_{17,01}$

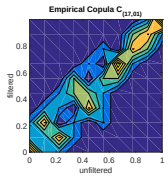

(g) Empirical

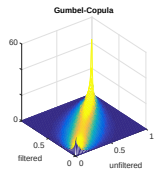

(h) Gumbel

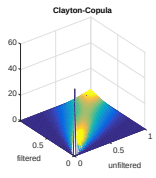

(i) Clayton

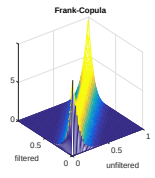

(j) Frank

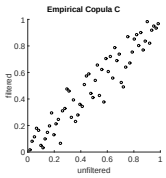

(k) $C_{18,01}$

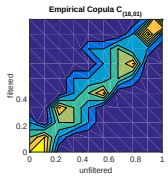

(l) Empirical

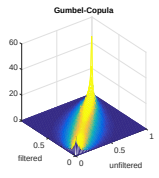

(m) Gumbel

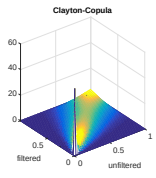

(n) Clayton

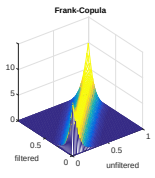

(o) Frank

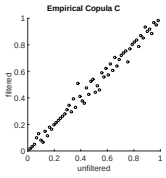

(p) $C_{19,01}$

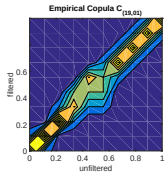

(q) Empirical

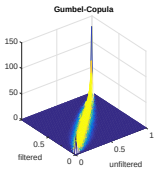

(r) Gumbel

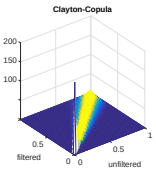

(s) Clayton

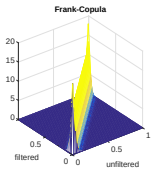

(t) Frank

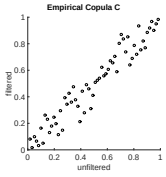

(u) $C_{20,01}$

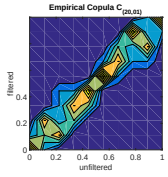

(v) Empirical

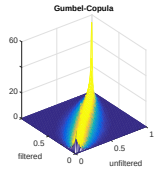

(w) Gumbel

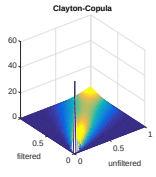

(x) Clayton

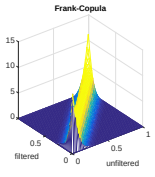

(y) Frank

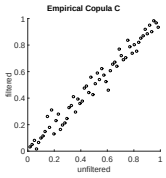

(a) $C_{21,01}$

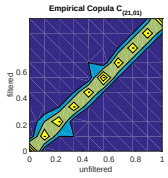

(b) Empirical

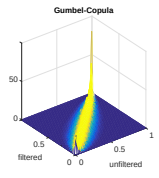

(c) Gumbel

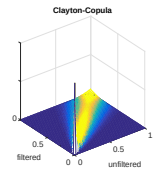

(d) Clayton

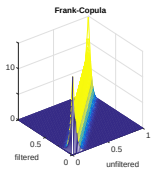

(e) Frank

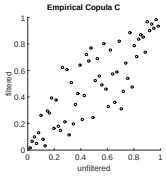

(f) $C_{22,01}$

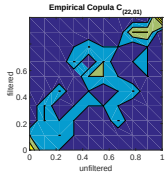

(g) Empirical

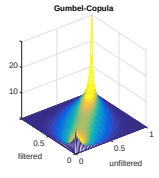

(h) Gumbel

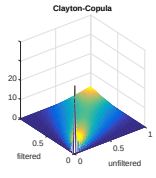

(i) Clayton

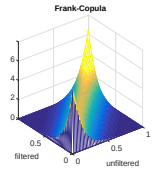

(j) Frank

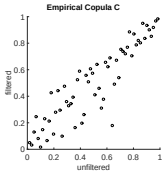

(a) $C_{23,01}$

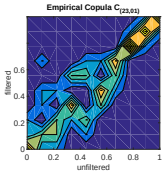

(b) Empirical

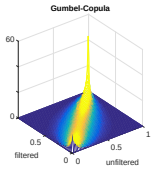

(c) Gumbel

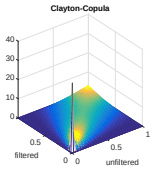

(d) Clayton

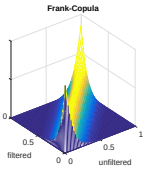

(e) Frank

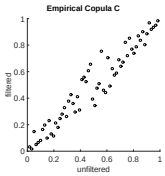

(f) $C_{24,01}$

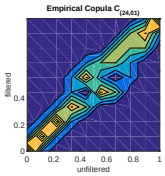

(g) Empirical

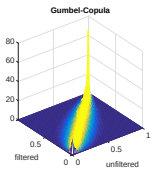

(h) Gumbel

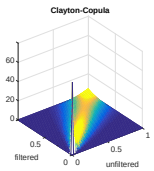

(i) Clayton

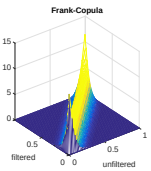

(j) Frank

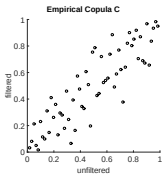

(k) $C_{25,01}$

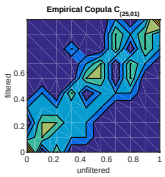

(l) Empirical

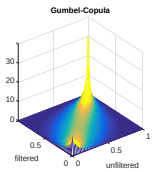

(m) Gumbel

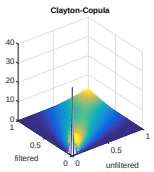

(n) Clayton

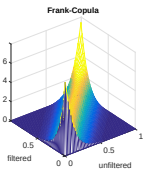

(o) Frank

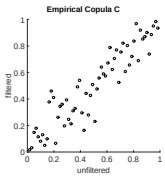

(p) $C_{26,01}$

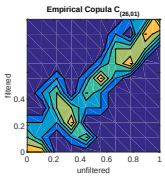

(q) Empirical

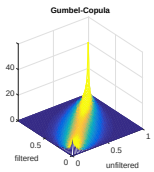

(r) Gumbel

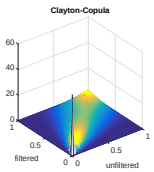

(s) Clayton

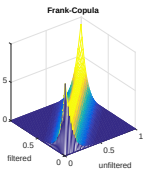

(t) Frank

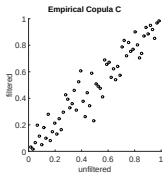

(a) $C_{27,01}$

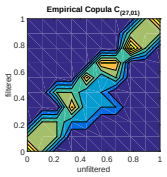

(b) Empirical

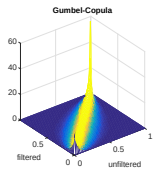

(c) Gumbel

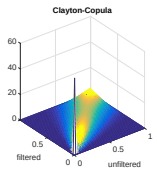

(d) Clayton

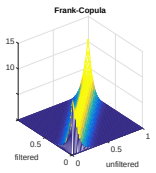

(e) Frank

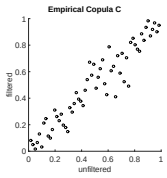

(f) $C_{28,01}$

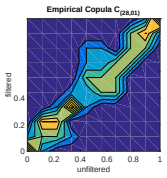

(g) Empirical

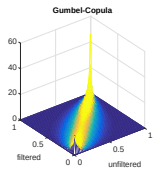

(h) Gumbel

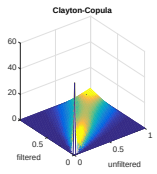

(i) Clayton

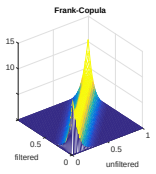

(j) Frank

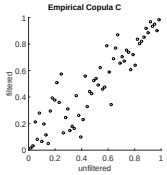

(k) $C_{29,01}$

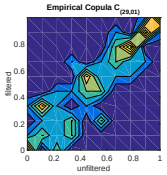

(l) Empirical

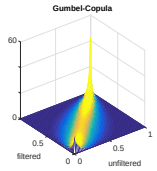

(m) Gumbel

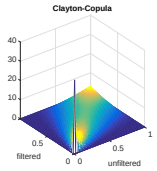

(n) Clayton

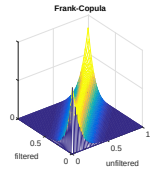

(o) Frank

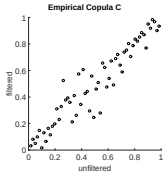

(p) $C_{30,01}$

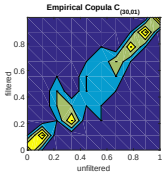

(q) Empirical

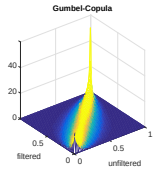

(r) Gumbel

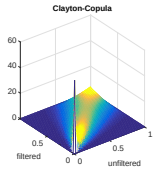

(s) Clayton

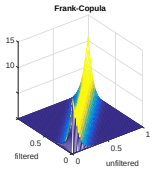

(t) Frank

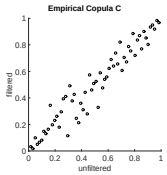

(u) $C_{31,01}$

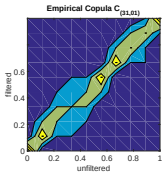

(v) Empirical

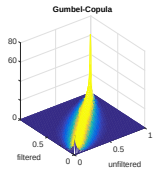

(w) Gumbel

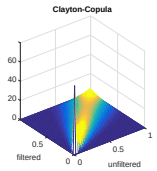

(x) Clayton

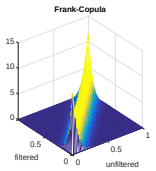

(y) Frank

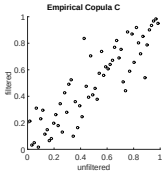

(a) $C_{32,01}$

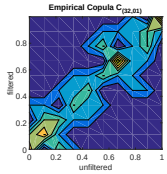

(b) Empirical

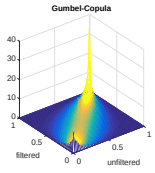

(c) Gumbel

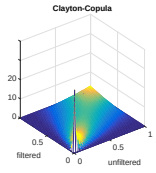

(d) Clayton

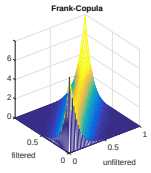

(e) Frank

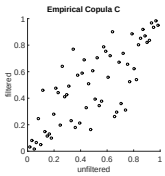

(f) $C_{33,01}$

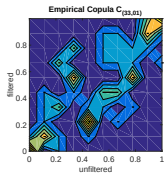

(g) Empirical

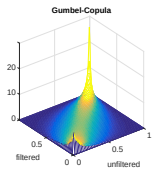

(h) Gumbel

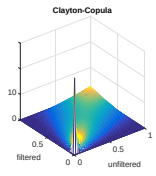

(i) Clayton

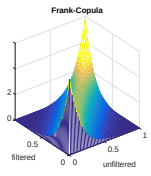

(j) Frank

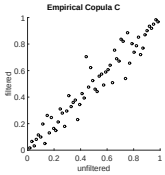

(k) $C_{34,01}$

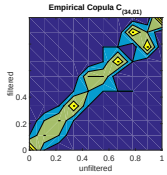

(l) Empirical

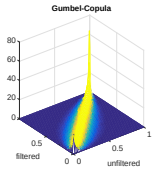

(m) Gumbel

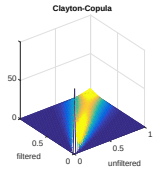

(n) Clayton

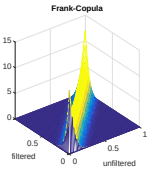

(o) Frank

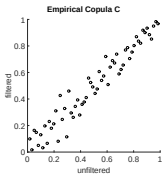

(p) $C_{35,01}$

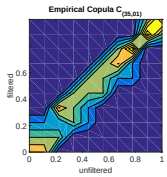

(q) Empirical

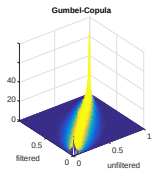

(r) Gumbel

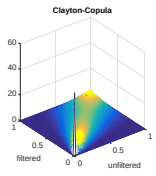

(s) Clayton

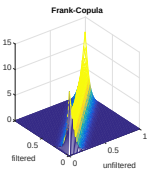

(t) Frank

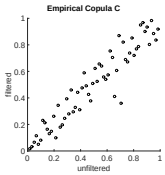

(u) $C_{36,01}$

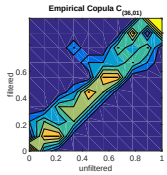

(v) Empirical

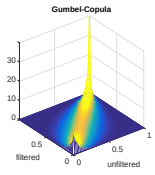

(w) Gumbel

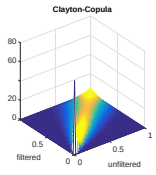

(x) Clayton

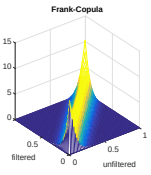

(y) Frank

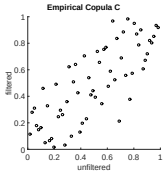

(a) $C_{37,01}$

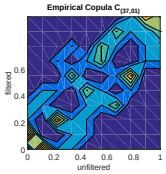

(b) Empirical

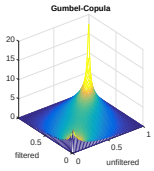

(c) Gumbel

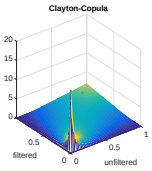

(d) Clayton

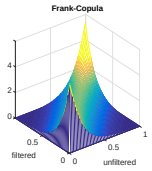

(e) Frank

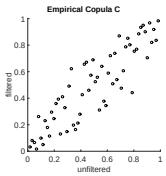

(f) $C_{38,01}$

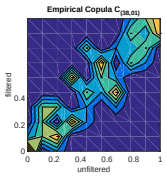

(g) Empirical

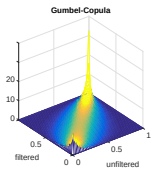

(h) Gumbel

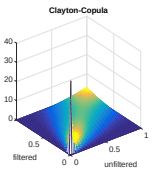

(i) Clayton

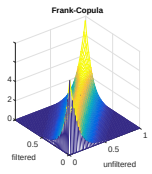

(j) Frank

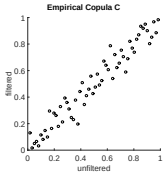

(k) $C_{39,01}$

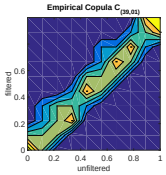

(l) Empirical

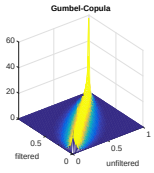

(m) Gumbel

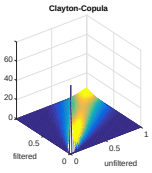

(n) Clayton

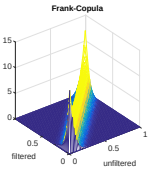

(o) Frank

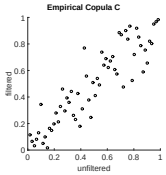

(p) $C_{40,01}$

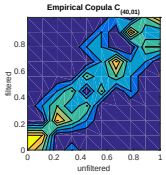

(q) Empirical

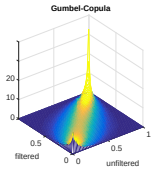

(r) Gumbel

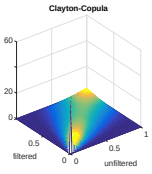

(s) Clayton

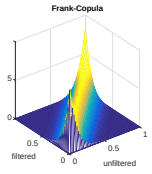

(t) Frank

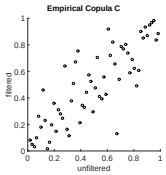

(u) $C_{41,01}$

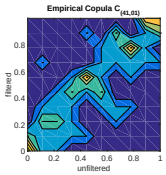

(v) Empirical

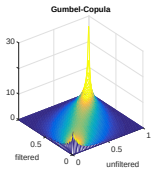

(w) Gumbel

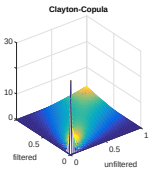

(x) Clayton

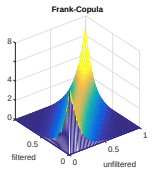

(y) Frank

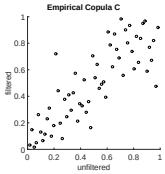

(a) $C_{42,01}$

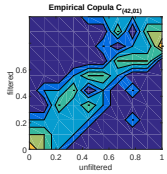

(b) Empirical

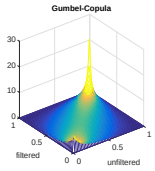

(c) Gumbel

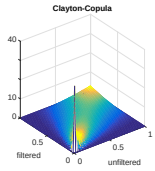

(d) Clayton

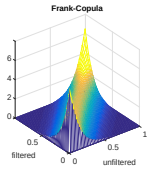

(e) Frank

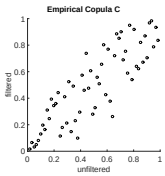

(f) $C_{43,01}$

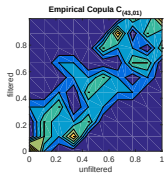

(g) Empirical

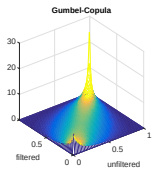

(h) Gumbel

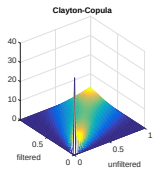

(i) Clayton

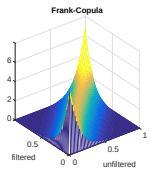

(j) Frank

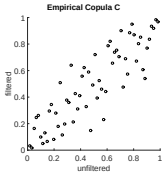

(k) $C_{44,01}$

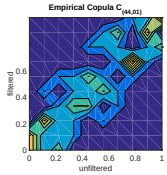

(l) Empirical

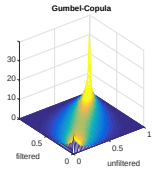

(m) Gumbel

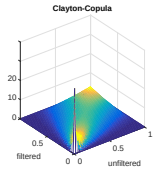

(n) Clayton

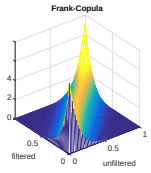

(o) Frank

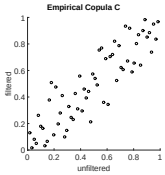

(p) $C_{45,01}$

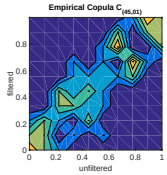

(q) Empirical

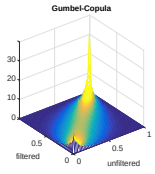

(r) Gumbel

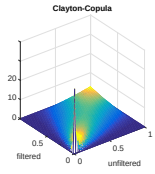

(s) Clayton

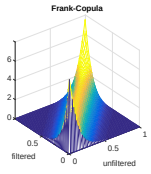

(t) Frank

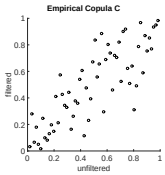

(u) $C_{46,01}$

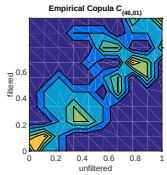

(v) Empirical

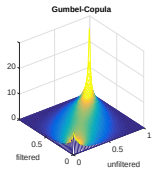

(w) Gumbel

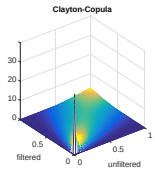

(x) Clayton

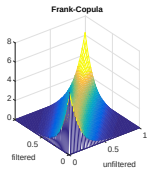

(y) Frank

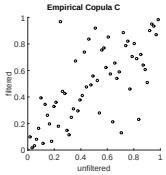

(a) $C_{47,01}$

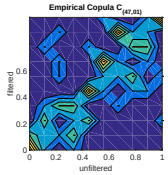

(b) Empirical

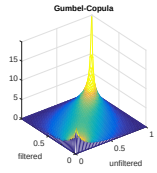

(c) Gumbel

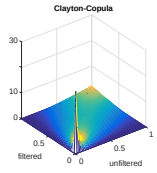

(d) Clayton

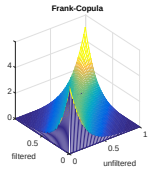

(e) Frank

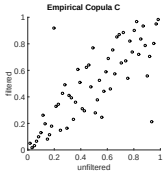

(f) $C_{48,01}$

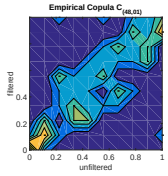

(g) Empirical

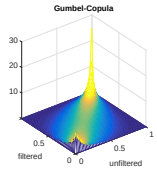

(h) Gumbel

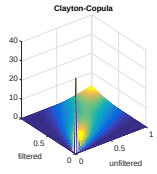

(i) Clayton

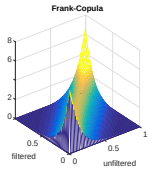

(j) Frank

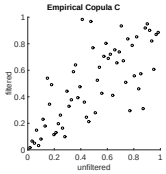

(k) $C_{49,01}$

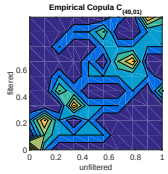

(l) Empirical

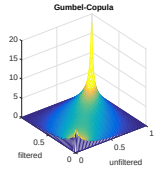

(m) Gumbel

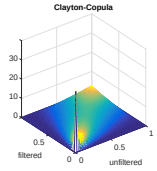

(n) Clayton

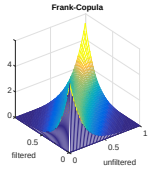

(o) Frank

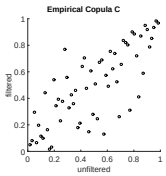

(p) $C_{50,01}$

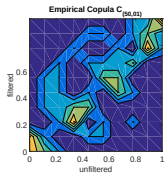

(q) Empirical

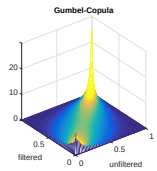

(r) Gumbel

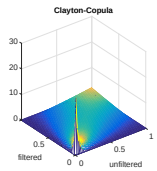

(s) Clayton

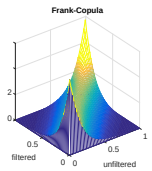

(t) Frank

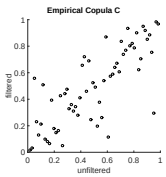

(u) $C_{51,01}$

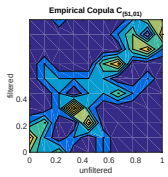

(v) Empirical

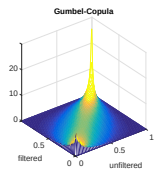

(w) Gumbel

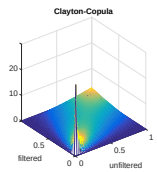

(x) Clayton

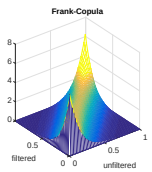

(y) Frank

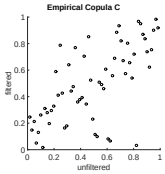

(a) $C_{52,01}$

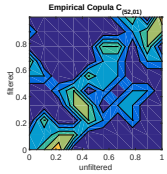

(b) Empirical

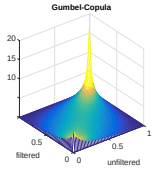

(c) Gumbel

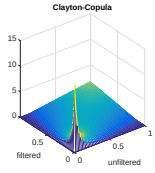

(d) Clayton

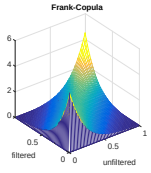

(e) Frank

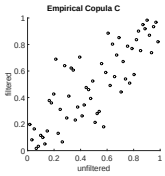

(f) $C_{53,01}$

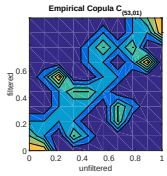

(g) Empirical

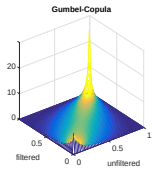

(h) Gumbel

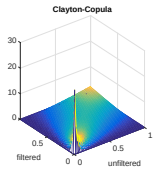

(i) Clayton

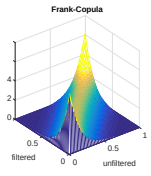

(j) Frank

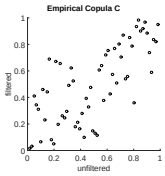

(k) $C_{54,01}$

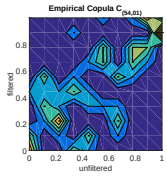

(l) Empirical

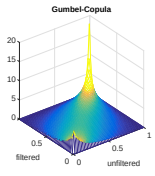

(m) Gumbel

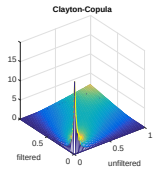

(n) Clayton

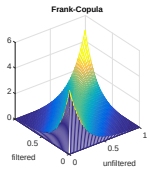

(o) Frank

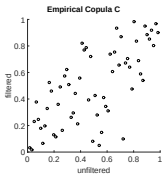

(p) $C_{55,01}$

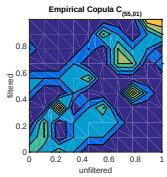

(q) Empirical

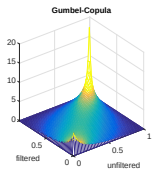

(r) Gumbel

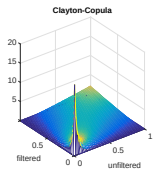

(s) Clayton

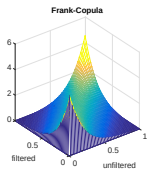

(t) Frank

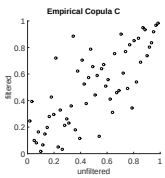

(u) $C_{56,01}$

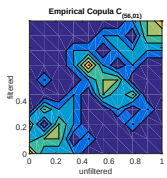

(v) Empirical

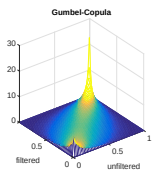

(w) Gumbel

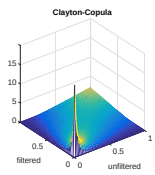

(x) Clayton

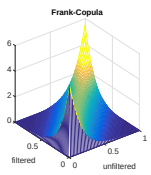

(y) Frank

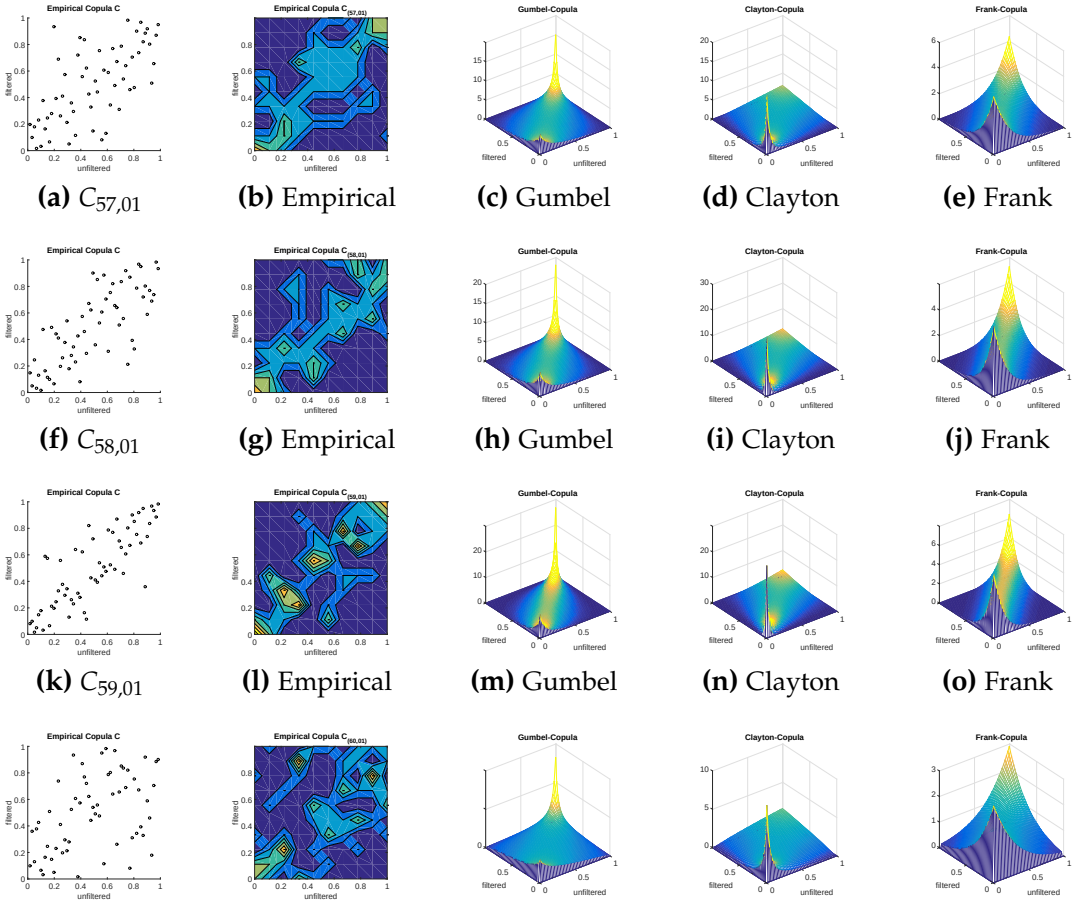

(a) $C_{57,01}$ **(b)** Empirical **(c)** Gumbel **(d)** Clayton **(e)** Frank

(f) $C_{58,01}$ **(g)** Empirical **(h)** Gumbel **(i)** Clayton **(j)** Frank

(k) $C_{59,01}$ **(l)** Empirical **(m)** Gumbel **(n)** Clayton **(o)** Frank

(p) $C_{60,01}$ **(q)** Empirical **(r)** Gumbel **(s)** Clayton **(t)** Frank

Figure D.1: *Dependency structure between unfiltered and filtered* GRACE *data for order 1.*

Appendix E

Copula modelling of precipitation and filtered GRACE coefficients

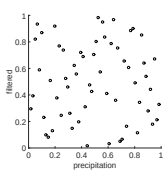

(a) $C_{2,01}$

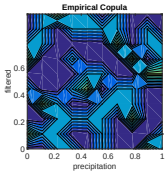

(b) Empirical

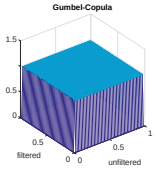

(c) Gumbel

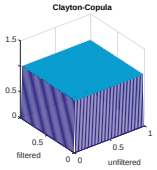

(d) Clayton

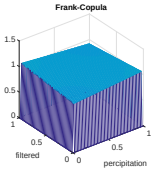

(e) Frank

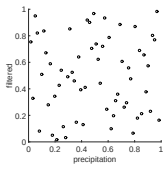

(f) $C_{3,01}$

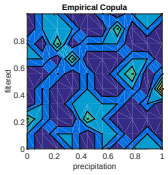

(g) Empirical

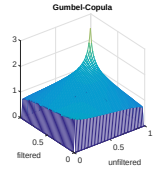

(h) Gumbel

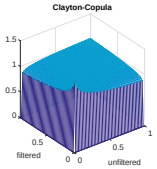

(i) Clayton

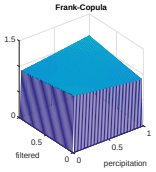

(j) Frank

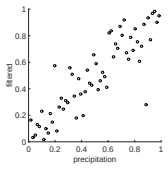

(k) $C_{4,01}$

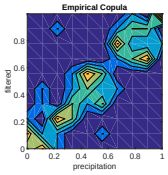

(l) Empirical

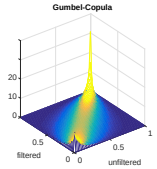

(m) Gumbel

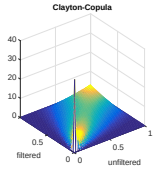

(n) Clayton

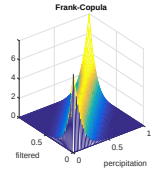

(o) Frank

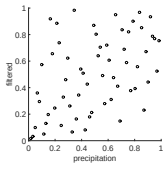

(p) $C_{5,01}$

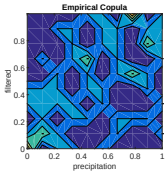

(q) Empirical

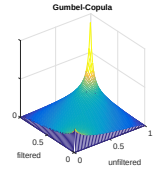

(r) Gumbel

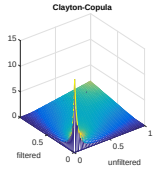

(s) Clayton

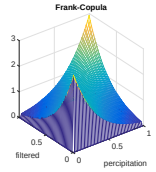

(t) Frank

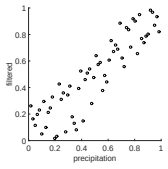

(u) $C_{6,01}$

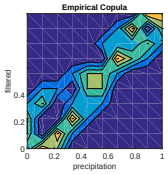

(v) Empirical

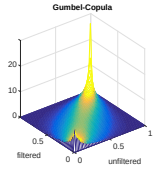

(w) Gumbel

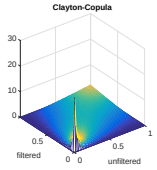

(x) Clayton

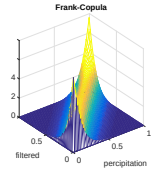

(y) Frank

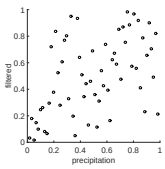

(a) $C_{7,01}$

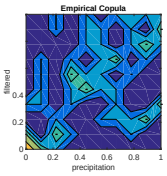

(b) Empirical

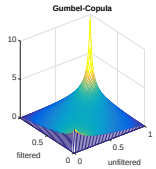

(c) Gumbel

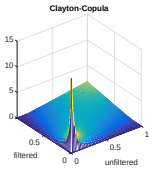

(d) Clayton

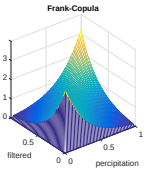

(e) Frank

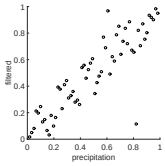

(f) $C_{8,01}$

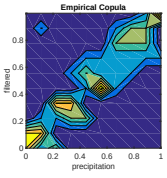

(g) Empirical

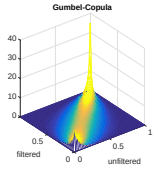

(h) Gumbel

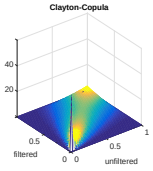

(i) Clayton

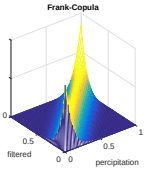

(j) Frank

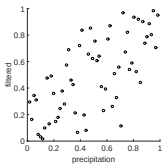

(k) $C_{9,01}$

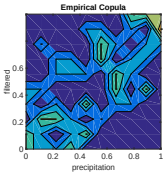

(l) Empirical

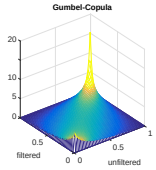

(m) Gumbel

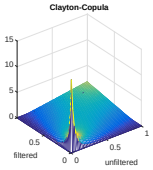

(n) Clayton

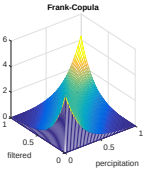

(o) Frank

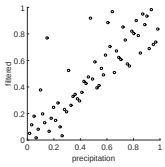

(p) $C_{10,01}$

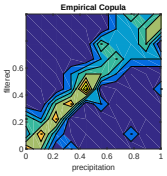

(q) Empirical

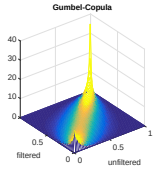

(r) Gumbel

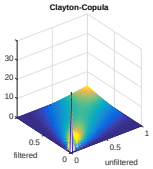

(s) Clayton

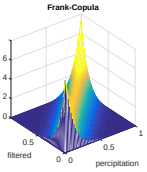

(t) Frank

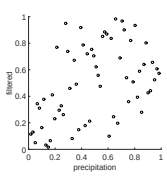

(a) $C_{11,01}$

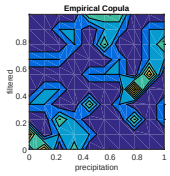

(b) Empirical

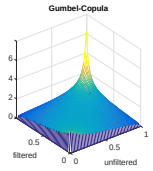

(c) Gumbel

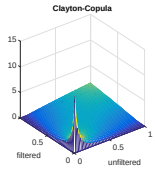

(d) Clayton

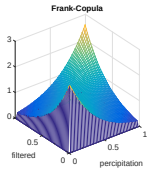

(e) Frank

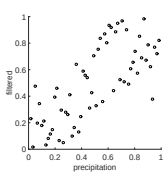

(f) $C_{12,01}$

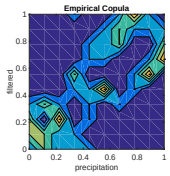

(g) Empirical

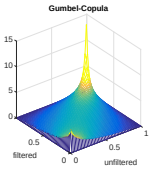

(h) Gumbel

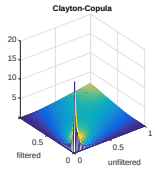

(i) Clayton

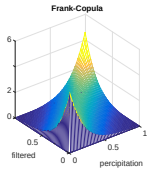

(j) Frank

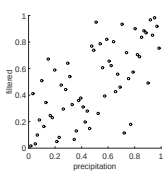

(k) $C_{13,01}$

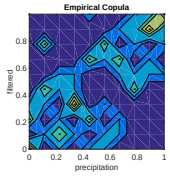

(l) Empirical

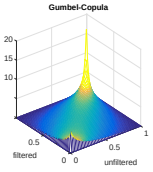

(m) Gumbel

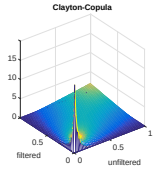

(n) Clayton

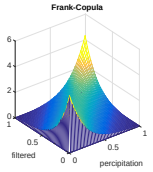

(o) Frank

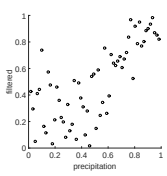

(p) $C_{14,01}$

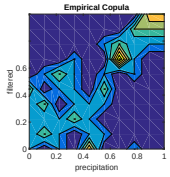

(q) Empirical

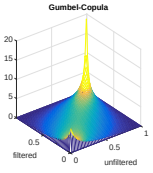

(r) Gumbel

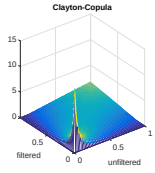

(s) Clayton

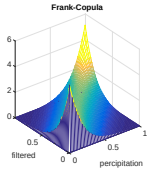

(t) Frank

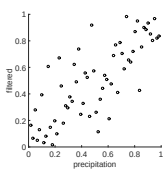

(u) $C_{15,01}$

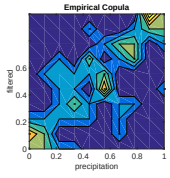

(v) Empirical

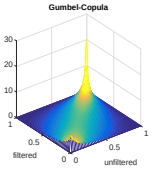

(w) Gumbel

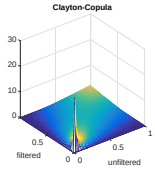

(x) Clayton

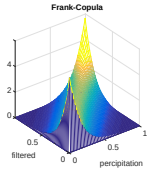

(y) Frank

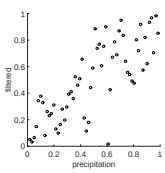

(a) $C_{16,01}$

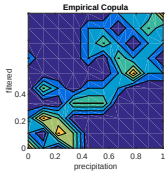

(b) Empirical

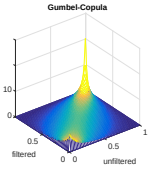

(c) Gumbel

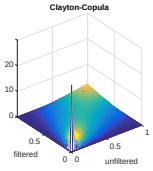

(d) Clayton

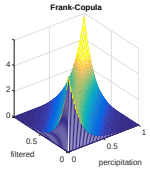

(e) Frank

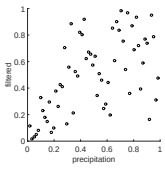

(f) $C_{17,01}$

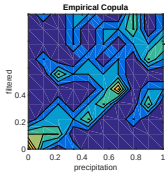

(g) Empirical

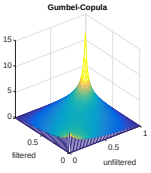

(h) Gumbel

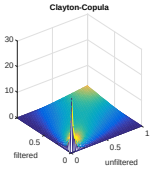

(i) Clayton

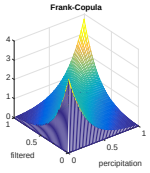

(j) Frank

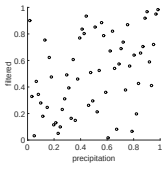

(k) $C_{18,01}$

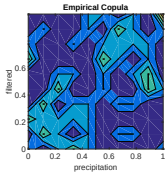

(l) Empirical

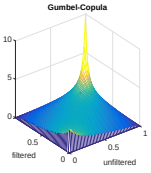

(m) Gumbel

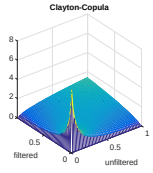

(n) Clayton

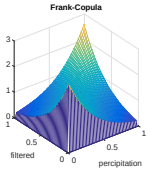

(o) Frank

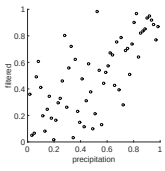

(p) $C_{19,01}$

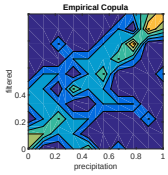

(q) Empirical

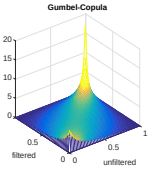

(r) Gumbel

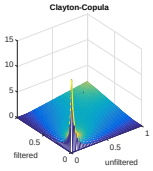

(s) Clayton

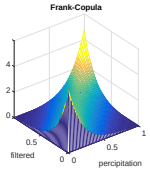

(t) Frank

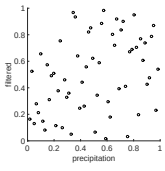

(u) $C_{20,01}$

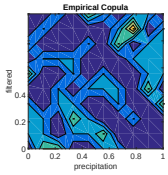

(v) Empirical

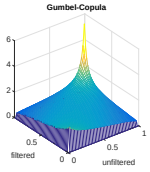

(w) Gumbel

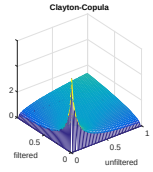

(x) Clayton

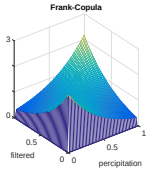

(y) Frank

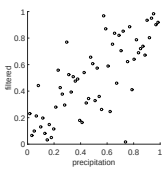

(a) $C_{21,01}$

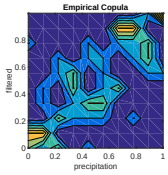

(b) Empirical

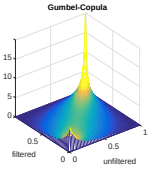

(c) Gumbel

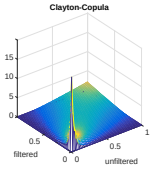

(d) Clayton

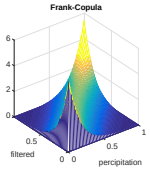

(e) Frank

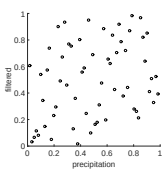

(f) $C_{22,01}$

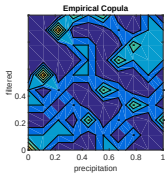

(g) Empirical

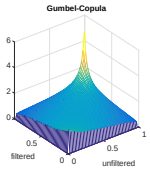

(h) Gumbel

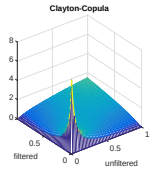

(i) Clayton

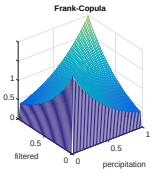

(j) Frank

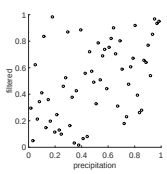

(a) $C_{23,01}$

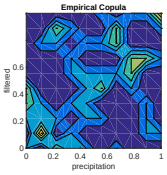

(b) Empirical

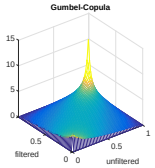

(c) Gumbel

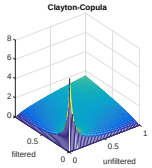

(d) Clayton

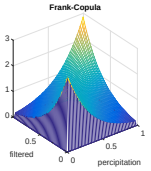

(e) Frank

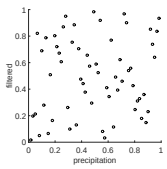

(f) $C_{24,01}$

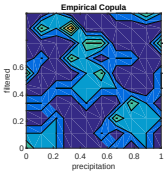

(g) Empirical

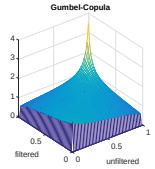

(h) Gumbel

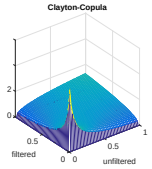

(i) Clayton

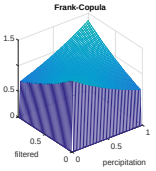

(j) Frank

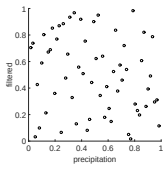

(k) $C_{25,01}$

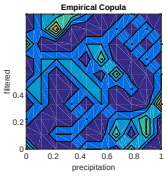

(l) Empirical

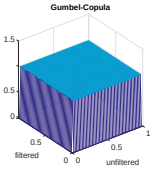

(m) Gumbel

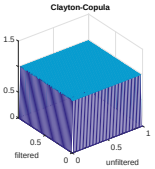

(n) Clayton

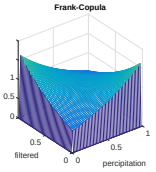

(o) Frank

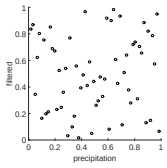

(p) $C_{26,01}$

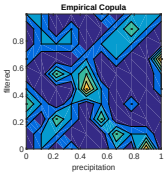

(q) Empirical

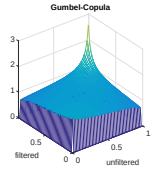

(r) Gumbel

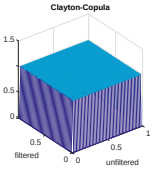

(s) Clayton

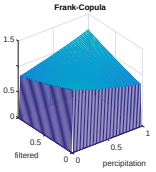

(t) Frank

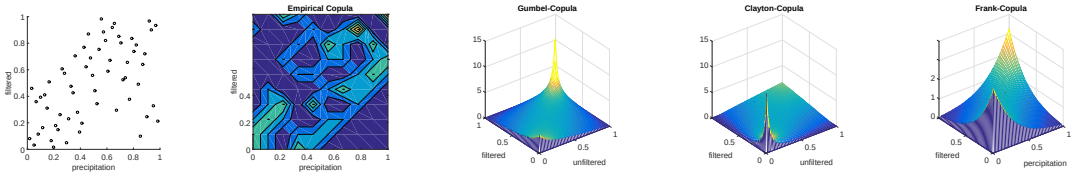

(a) $C_{27,01}$ **(b)** Empirical **(c)** Gumbel **(d)** Clayton **(e)** Frank

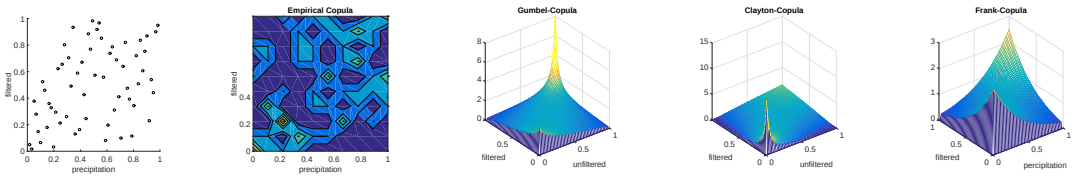

(f) $C_{28,01}$ **(g)** Empirical **(h)** Gumbel **(i)** Clayton **(j)** Frank

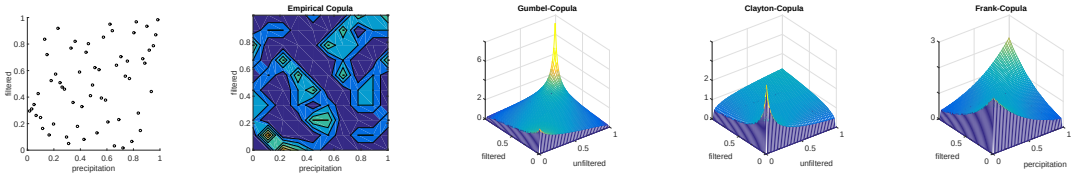

(k) $C_{29,01}$ **(l)** Empirical **(m)** Gumbel **(n)** Clayton **(o)** Frank

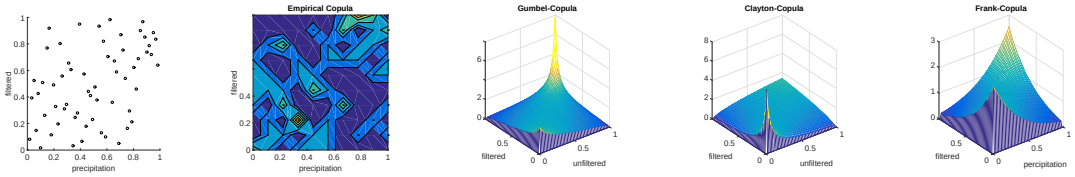

(p) $C_{30,01}$ **(q)** Empirical **(r)** Gumbel **(s)** Clayton **(t)** Frank

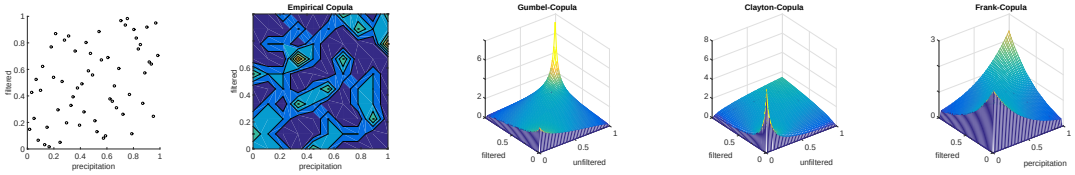

(u) $C_{31,01}$ **(v)** Empirical **(w)** Gumbel **(x)** Clayton **(y)** Frank

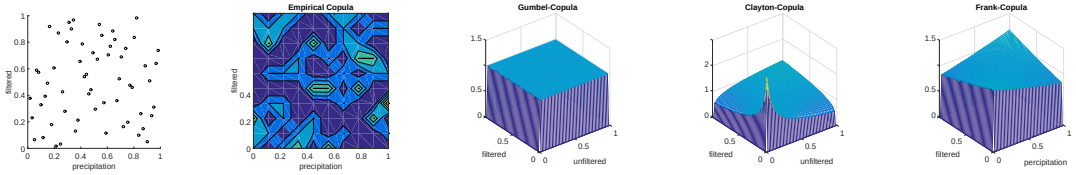

(a) $C_{32,01}$ **(b)** Empirical **(c)** Gumbel **(d)** Clayton **(e)** Frank

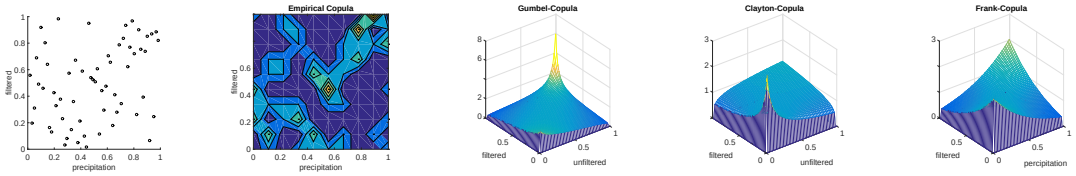

(f) $C_{33,01}$ **(g)** Empirical **(h)** Gumbel **(i)** Clayton **(j)** Frank

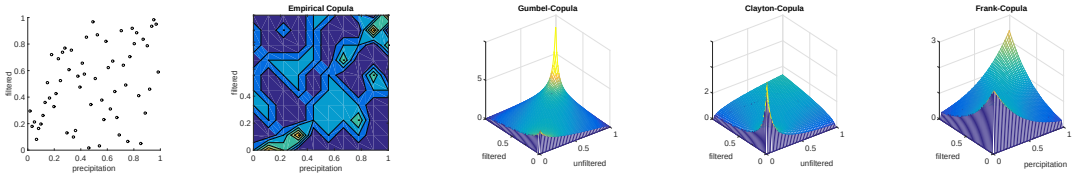

(k) $C_{34,01}$ **(l)** Empirical **(m)** Gumbel **(n)** Clayton **(o)** Frank

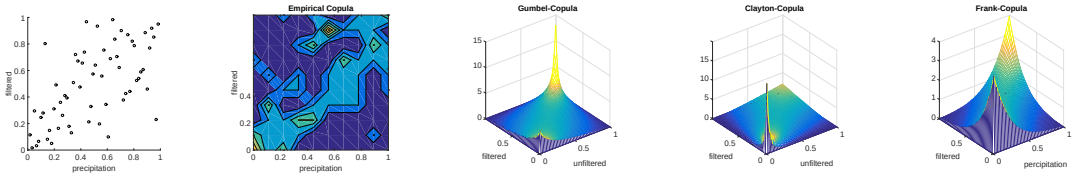

(p) $C_{35,01}$ **(q)** Empirical **(r)** Gumbel **(s)** Clayton **(t)** Frank

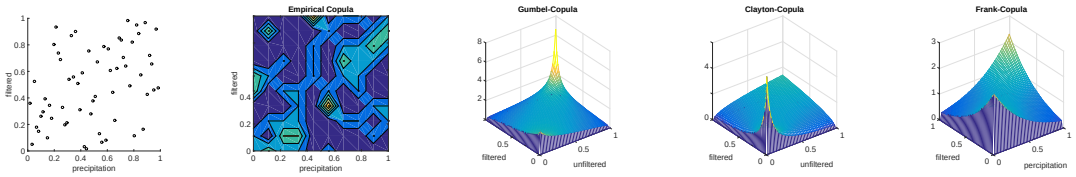

(u) $C_{36,01}$ **(v)** Empirical **(w)** Gumbel **(x)** Clayton **(y)** Frank

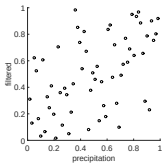

(a) $C_{37,01}$

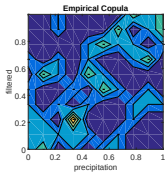

(b) Empirical

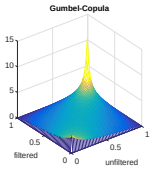

(c) Gumbel

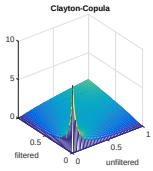

(d) Clayton

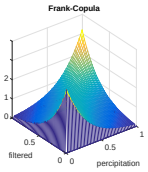

(e) Frank

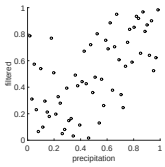

(f) $C_{38,01}$

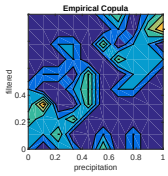

(g) Empirical

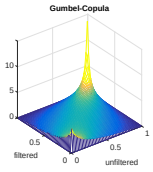

(h) Gumbel

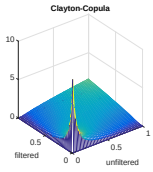

(i) Clayton

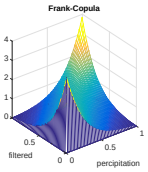

(j) Frank

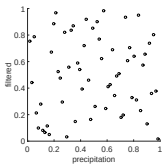

(k) $C_{39,01}$

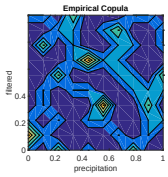

(l) Empirical

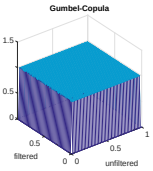

(m) Gumbel

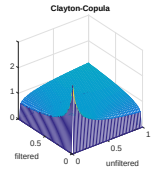

(n) Clayton

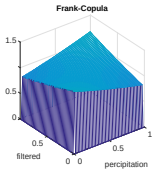

(o) Frank

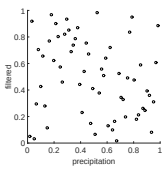

(p) $C_{40,01}$

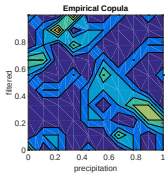

(q) Empirical

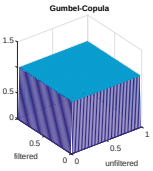

(r) Gumbel

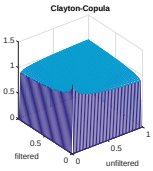

(s) Clayton

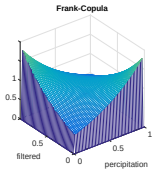

(t) Frank

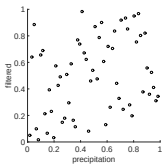

(u) $C_{41,01}$

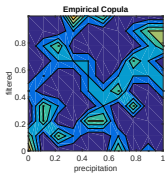

(v) Empirical

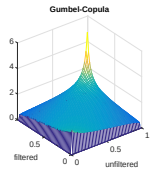

(w) Gumbel

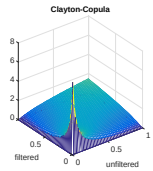

(x) Clayton

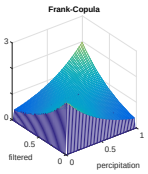

(y) Frank

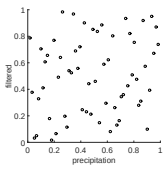

(a) $C_{42,01}$

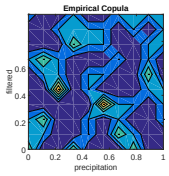

(b) Empirical

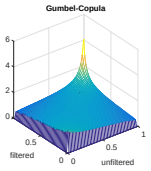

(c) Gumbel

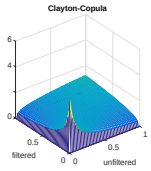

(d) Clayton

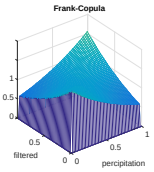

(e) Frank

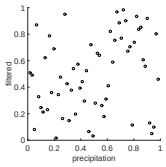

(f) $C_{43,01}$

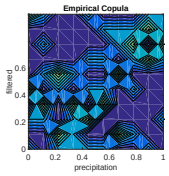

(g) Empirical

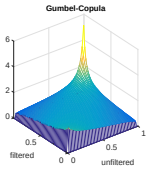

(h) Gumbel

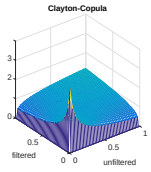

(i) Clayton

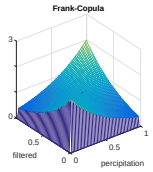

(j) Frank

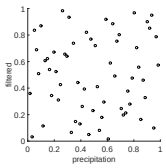

(k) $C_{44,01}$

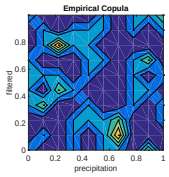

(l) Empirical

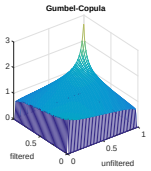

(m) Gumbel

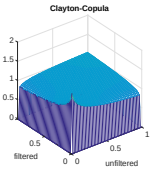

(n) Clayton

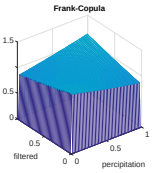

(o) Frank

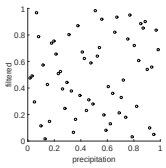

(p) $C_{45,01}$

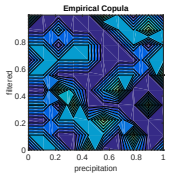

(q) Empirical

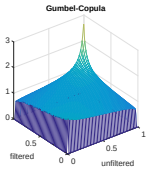

(r) Gumbel

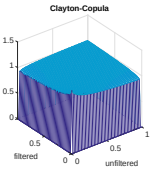

(s) Clayton

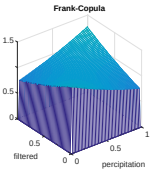

(t) Frank

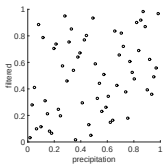

(u) $C_{46,01}$

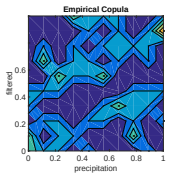

(v) Empirical

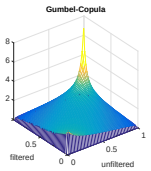

(w) Gumbel

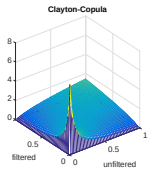

(x) Clayton

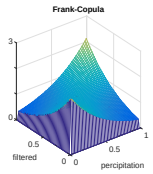

(y) Frank

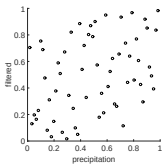

(a) $C_{47,01}$

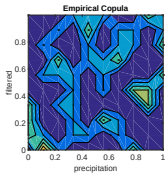

(b) Empirical

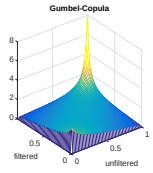

(c) Gumbel

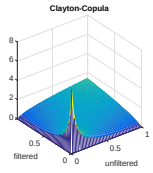

(d) Clayton

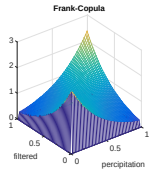

(e) Frank

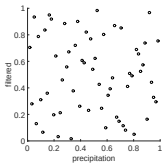

(f) $C_{48,01}$

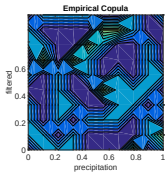

(g) Empirical

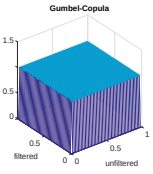

(h) Gumbel

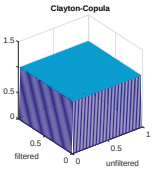

(i) Clayton

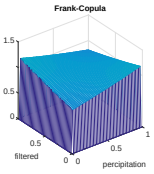

(j) Frank

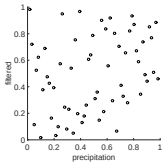

(k) $C_{49,01}$

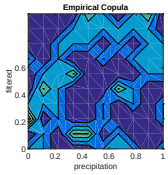

(l) Empirical

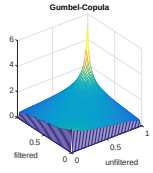

(m) Gumbel

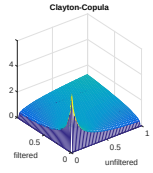

(n) Clayton

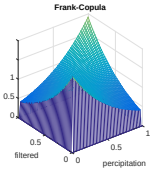

(o) Frank

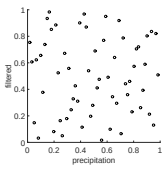

(p) $C_{50,01}$

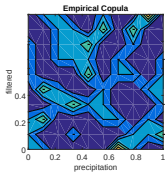

(q) Empirical

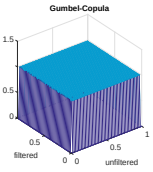

(r) Gumbel

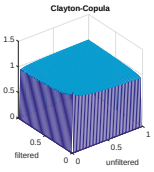

(s) Clayton

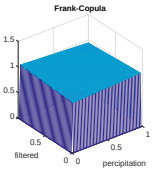

(t) Frank

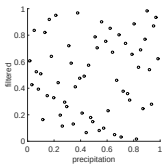

(u) $C_{51,01}$

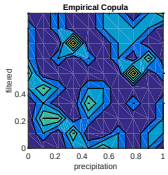

(v) Empirical

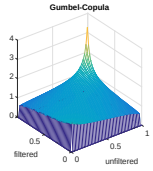

(w) Gumbel

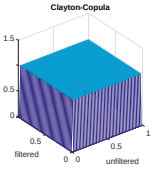

(x) Clayton

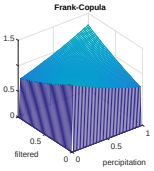

(y) Frank

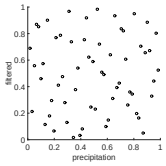

(a) $C_{52,01}$

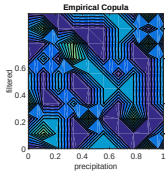

(b) Empirical

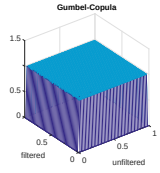

(c) Gumbel

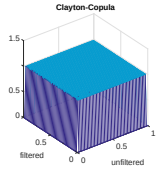

(d) Clayton

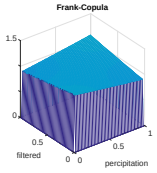

(e) Frank

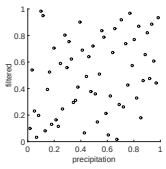

(f) $C_{53,01}$

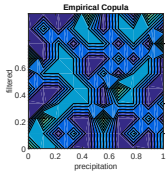

(g) Empirical

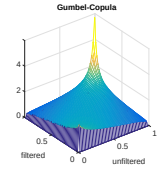

(h) Gumbel

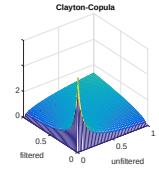

(i) Clayton

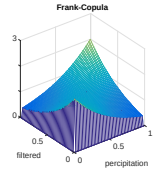

(j) Frank

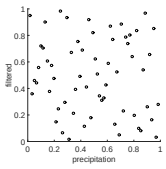

(k) $C_{54,01}$

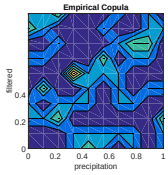

(l) Empirical

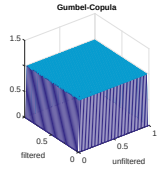

(m) Gumbel

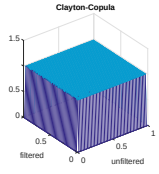

(n) Clayton

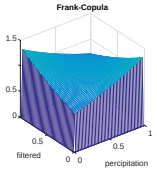

(o) Frank

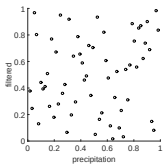

(p) $C_{55,01}$

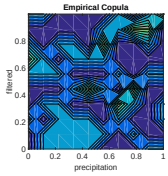

(q) Empirical

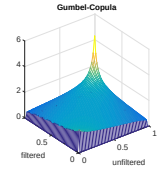

(r) Gumbel

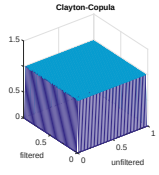

(s) Clayton

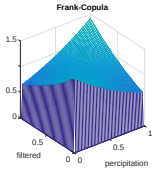

(t) Frank

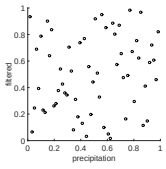

(u) $C_{56,01}$

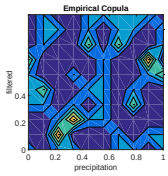

(v) Empirical

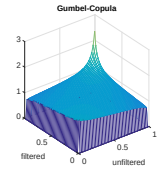

(w) Gumbel

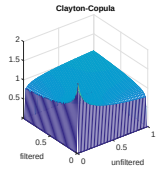

(x) Clayton

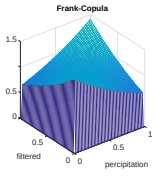

(y) Frank

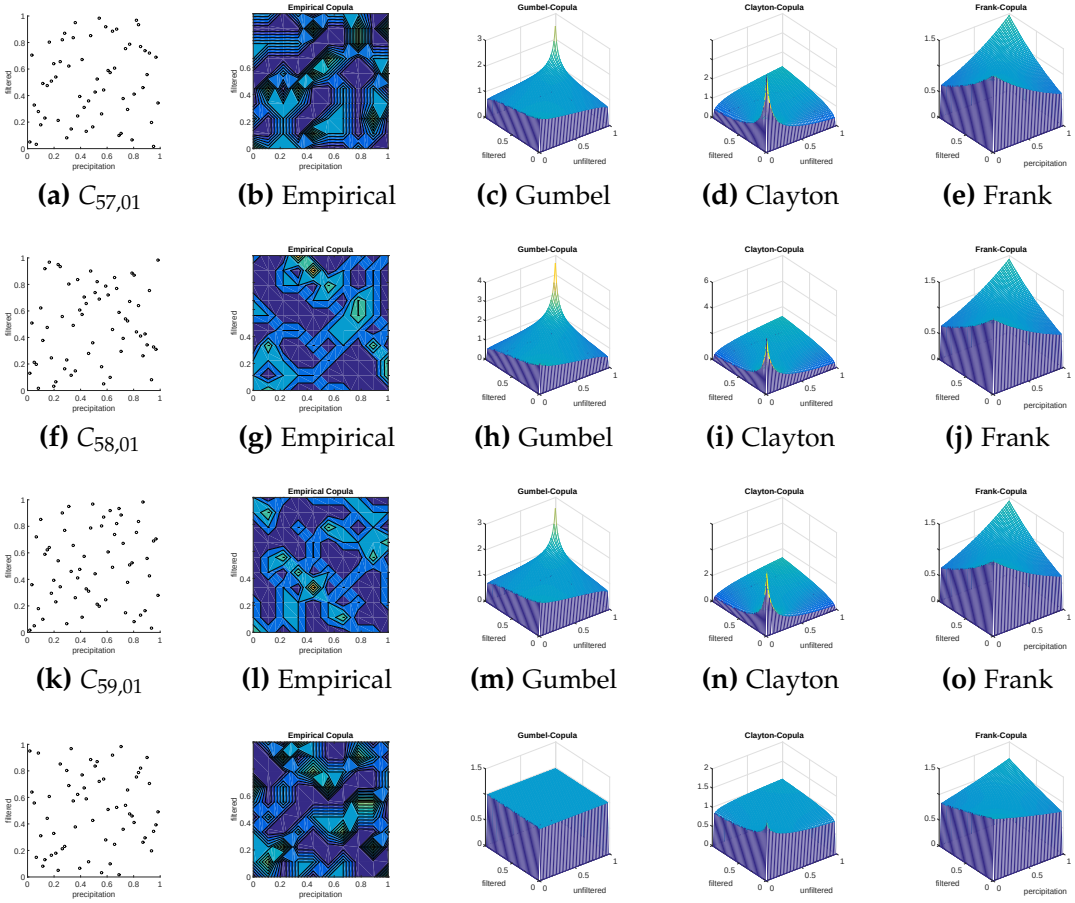

(a) $C_{57,01}$ **(b)** Empirical **(c)** Gumbel **(d)** Clayton **(e)** Frank

(f) $C_{58,01}$ **(g)** Empirical **(h)** Gumbel **(i)** Clayton **(j)** Frank

(k) $C_{59,01}$ **(l)** Empirical **(m)** Gumbel **(n)** Clayton **(o)** Frank

(p) $C_{60,01}$ **(q)** Empirical **(r)** Gumbel **(s)** Clayton **(t)** Frank

Figure E.1: *Dependency structure between precipitation and filtered* GRACE *data for order 1.*

Appendix F

Degree variance of Copula-based data and filtered GRACE

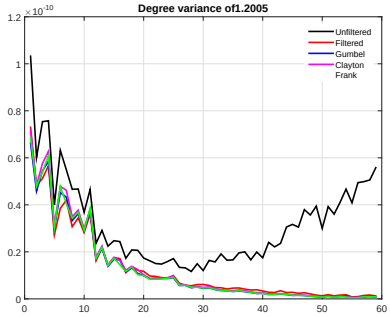

(a) January 2005

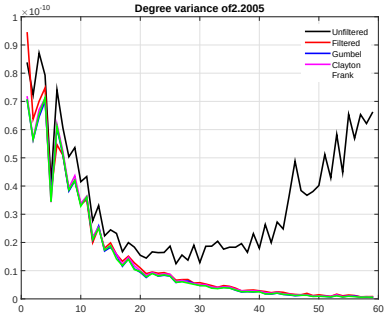

(b) February 2005

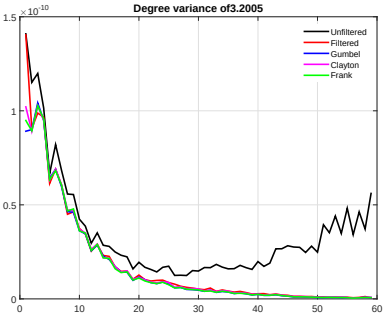

(c) March 2005

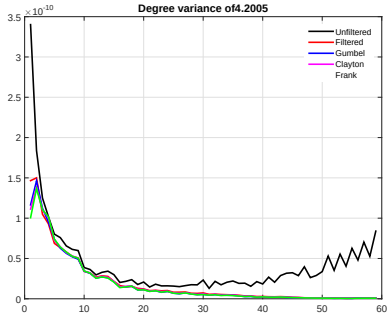

(d) April 2005

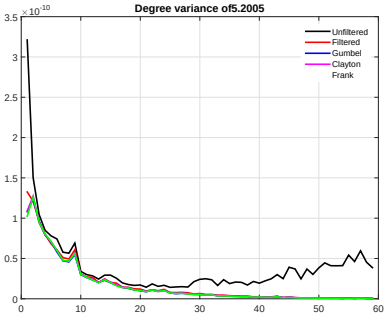

(e) May 2005

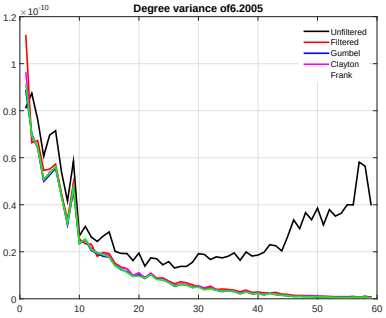

(f) June 2005

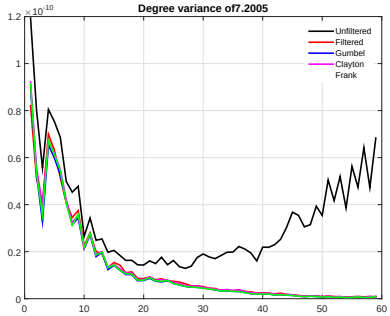

(g) July 2005

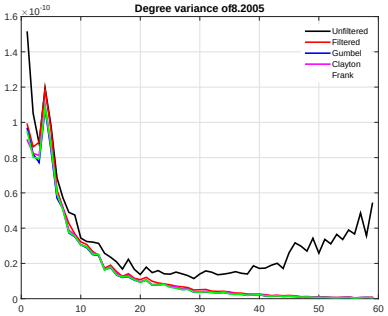

(h) August 2005

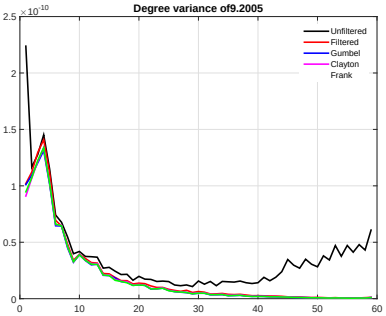

(i) September 2005

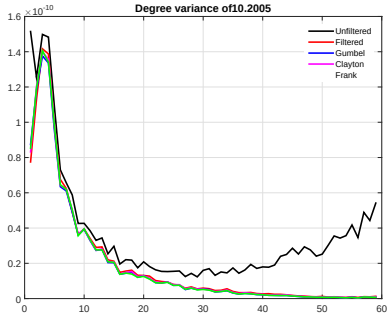

(j) October 2005

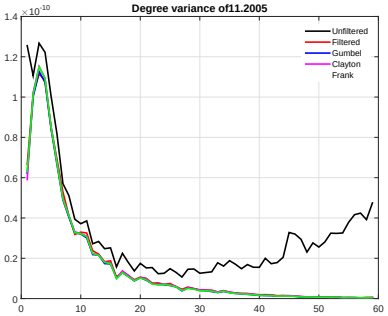

(k) November 2005

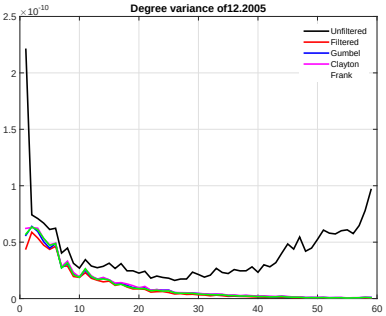

(l) December 2005

Figure F.1: *Degree variance of* GRACE *and Copula-based data 2005.*

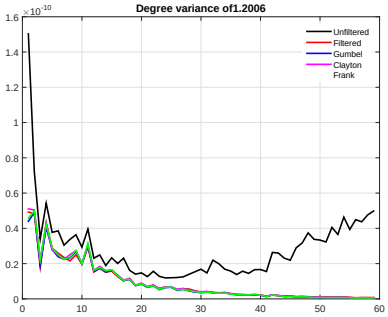

(a) January 2006

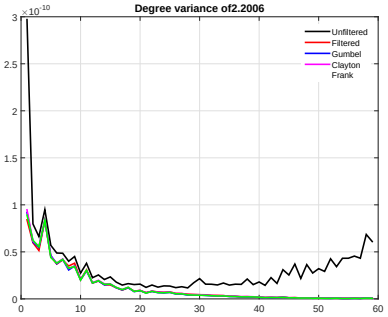

(b) February 2006

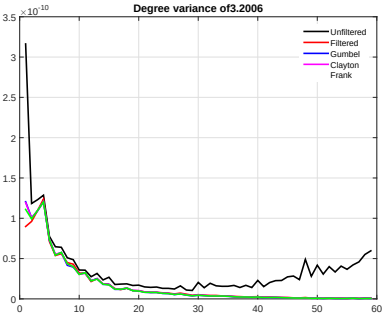

(c) March 2006

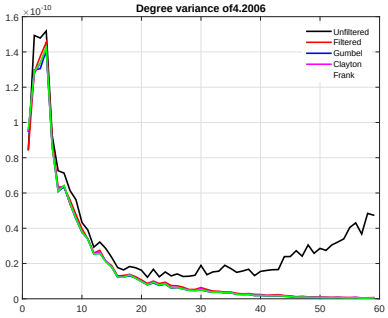

(d) April 2006

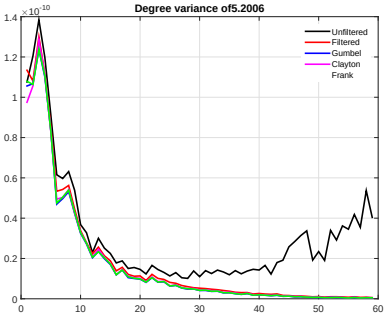

(e) May 2006

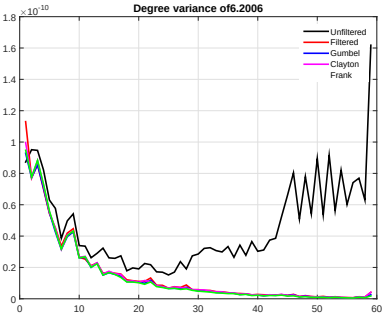

(f) June 2006

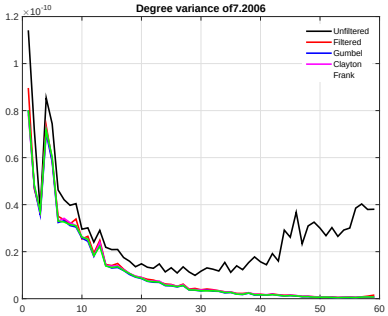

(g) July 2006

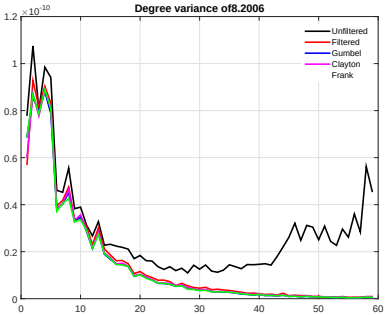

(h) August 2006

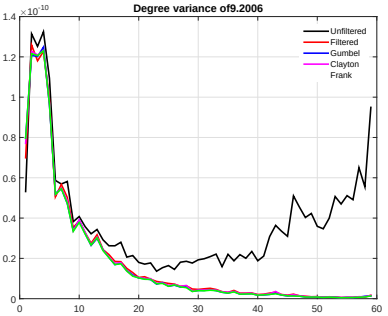

(i) September 2006

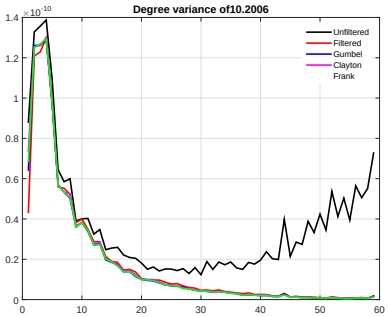

(j) October 2006

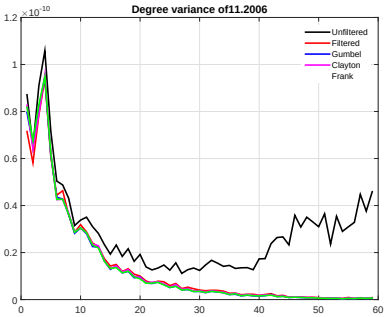

(k) November 2006

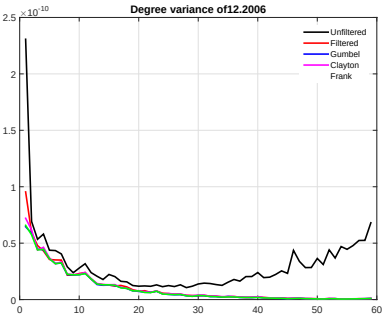

(l) December 2006

Figure F.2: *Degree variance of* GRACE *and Copula-based data 2006.*

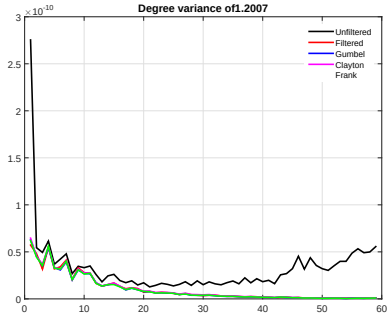

(a) January 2007

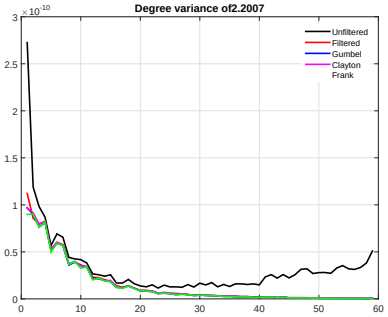

(b) February 2007

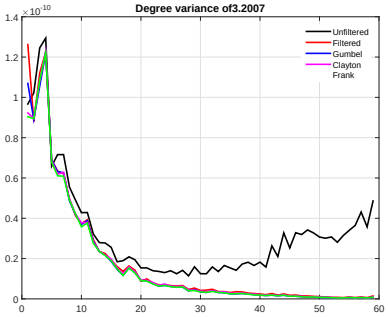

(c) March 2007

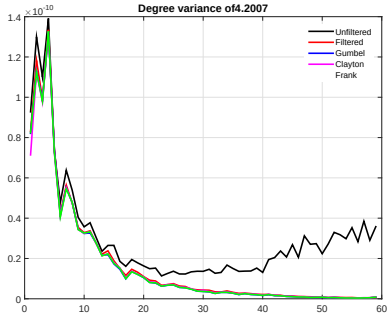

(d) April 2007

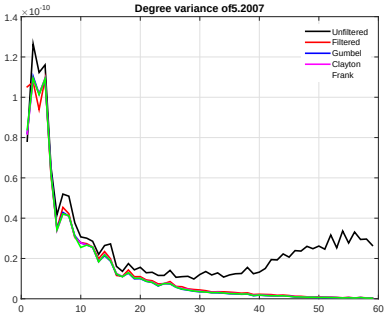

(e) May 2007

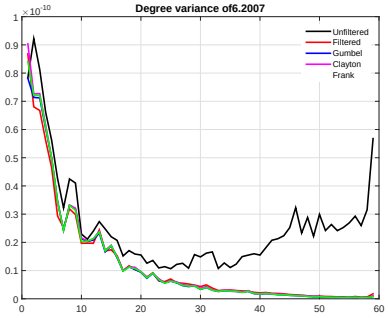

(f) June 2007

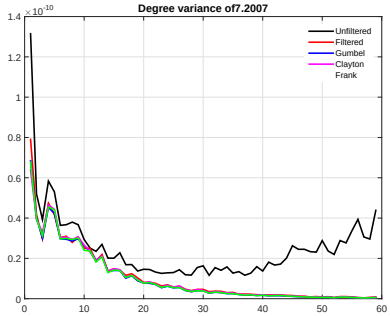

(g) July 2007

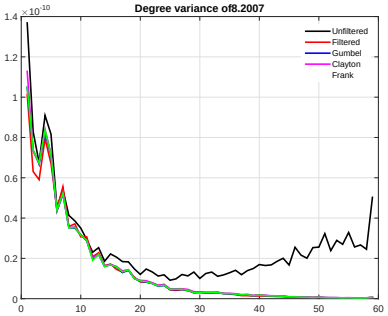

(h) August 2007

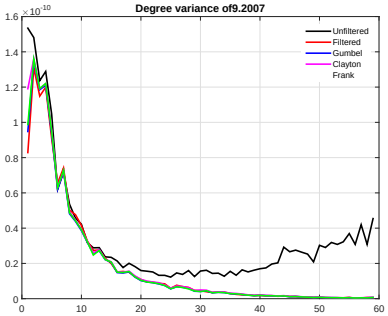

(i) September 2007

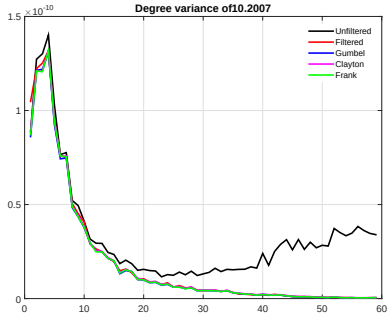

(j) October 2007

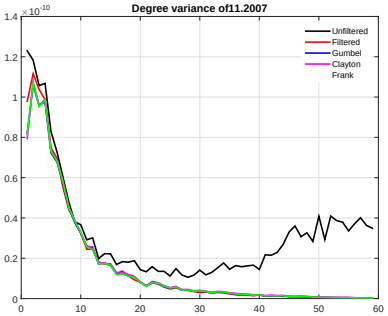

(k) November 2007

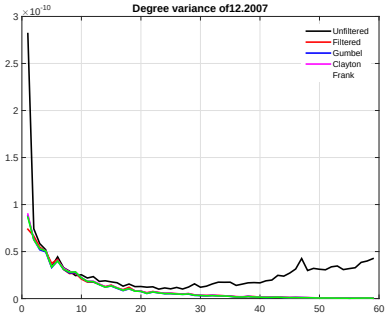

(l) December 2007

Figure F.3: *Degree variance of* GRACE *and Copula-based data 2007.*

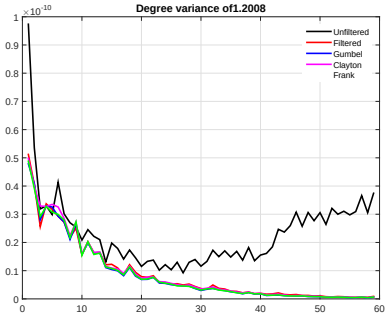

(a) January 2008

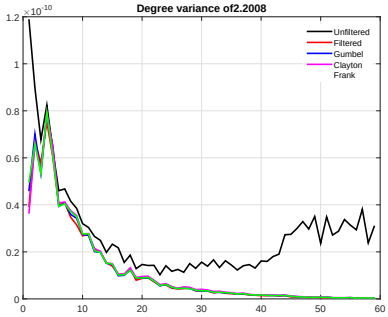

(b) February 2008

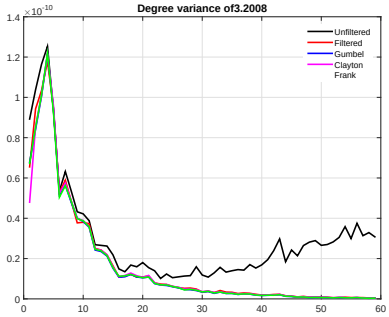

(c) March 2008

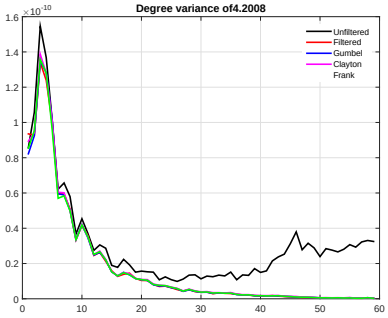

(d) April 2008

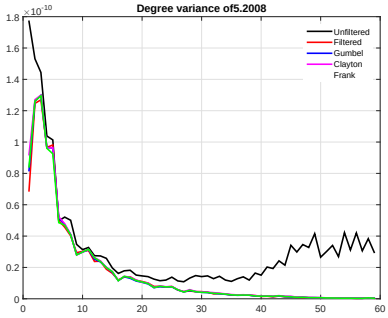

(e) May 2008

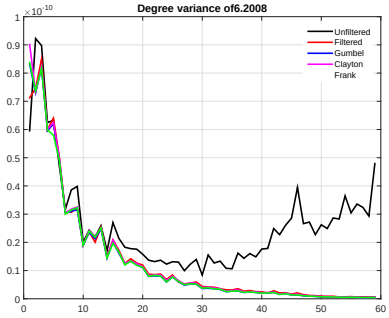

(f) June 2008

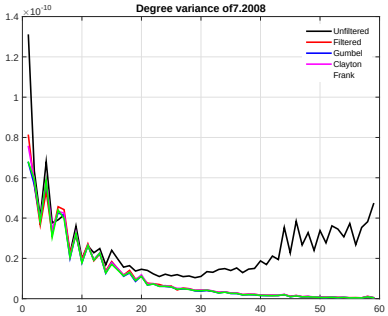

(g) July 2008

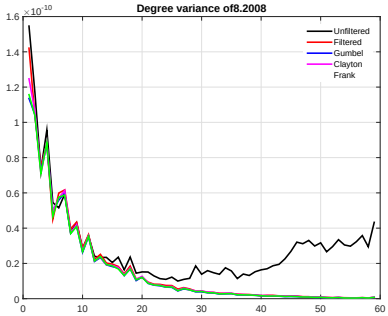

(h) August 2008

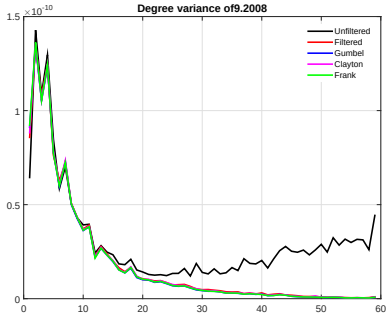

(i) September 2008

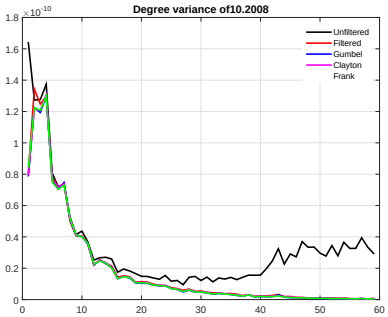

(j) October 2008

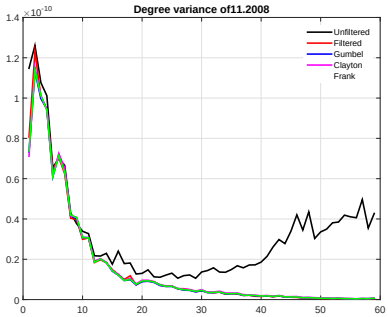

(k) November 2008

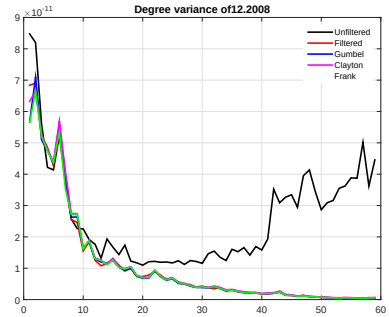

(l) December 2008

Figure F.4: *Degree variance of* GRACE *and Copula-based data 2008.*

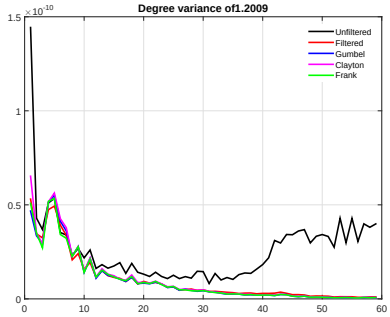

(a) January 2009

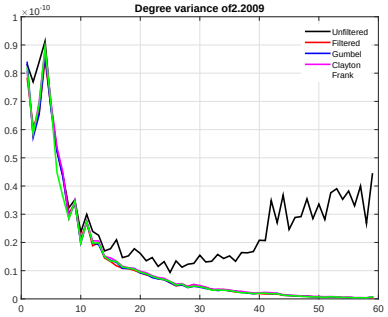

(b) February 2009

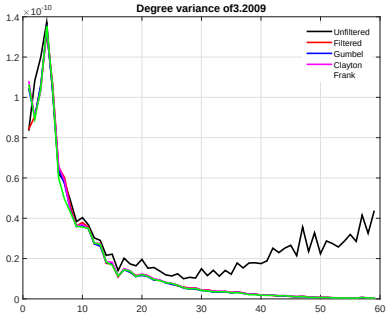

(c) March 2009

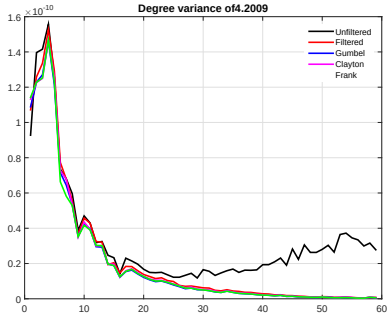

(d) April 2009

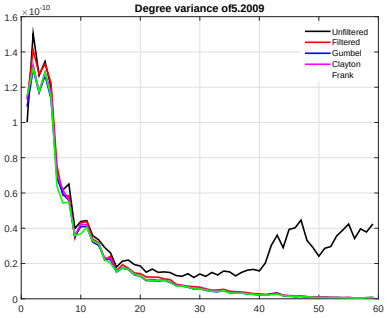

(e) May 2009

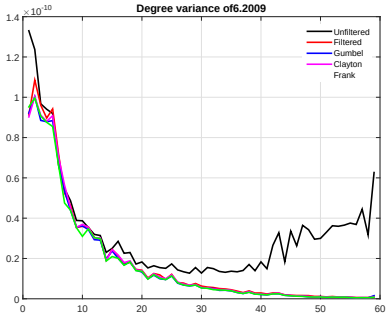

(f) June 2009

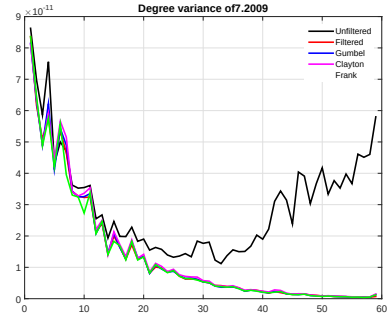

(g) July 2009

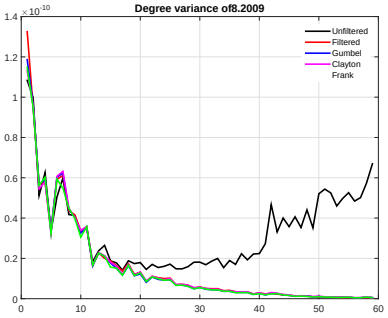

(h) August 2009

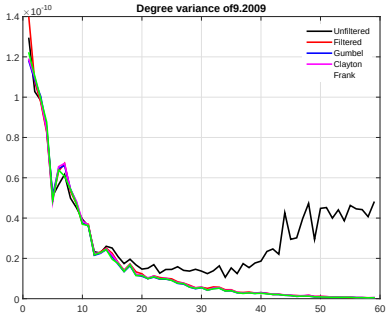

(i) September 2009

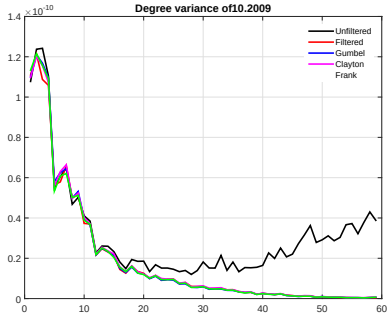

(j) October 2009

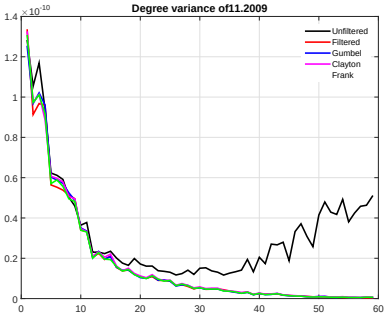

(k) November 2009

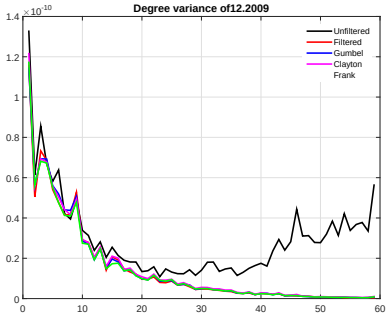

(l) December 2009

Figure F.5: *Degree variance of* GRACE *and Copula-based data 2009.*

Appendix G

Degree variance of Copula-based data and precipitation

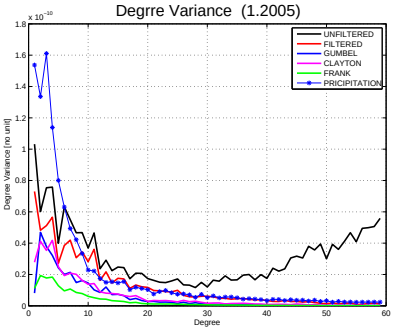

(a) January 2005

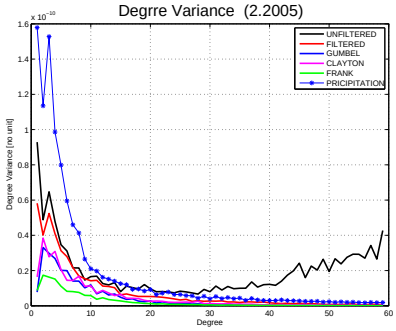

(b) February 2005

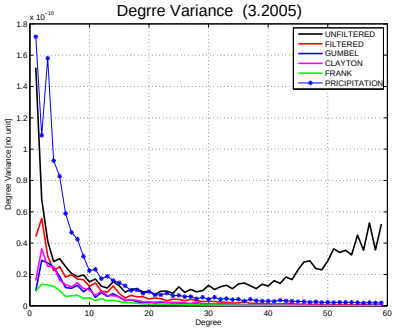

(c) March 2005

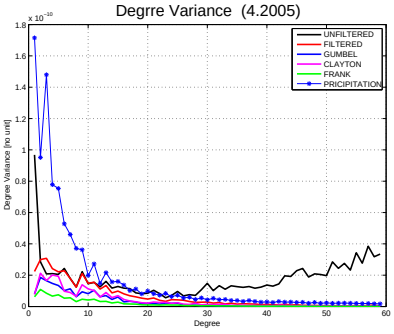

(d) April 2005

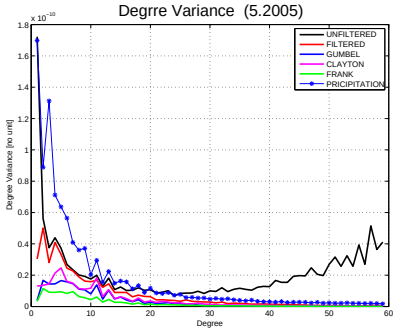

(e) May 2005

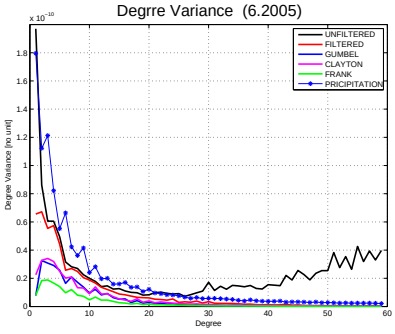

(f) June 2005

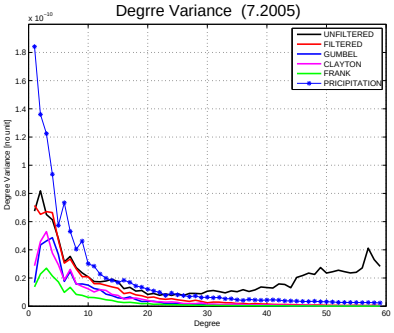

(g) July 2005

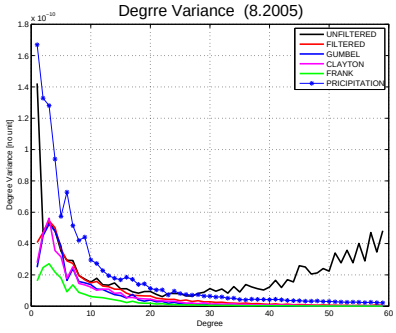

(h) August 2005

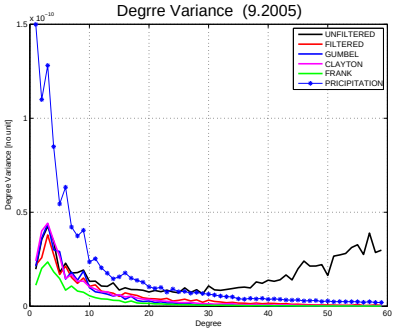

(i) September 2005

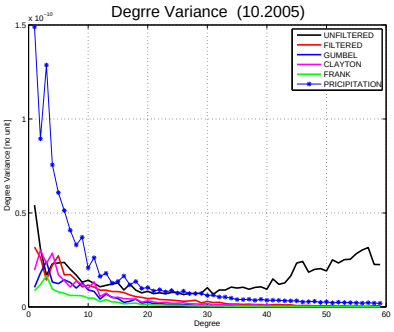

(j) October 2005

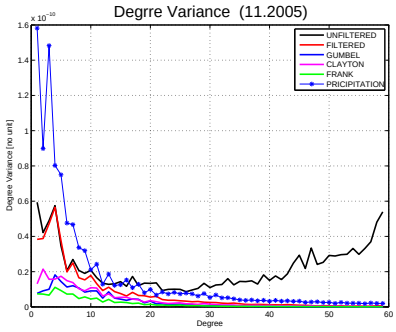

(k) November 2005

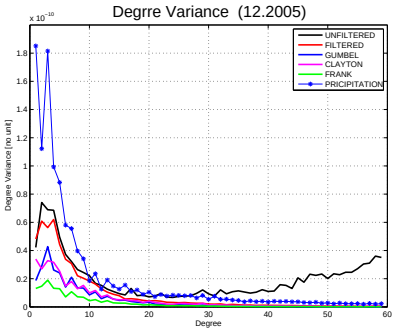

(l) December 2005

Figure G.1: *Degree variance of precipitation and* GRACE*, and Copula-based data in 2005.*

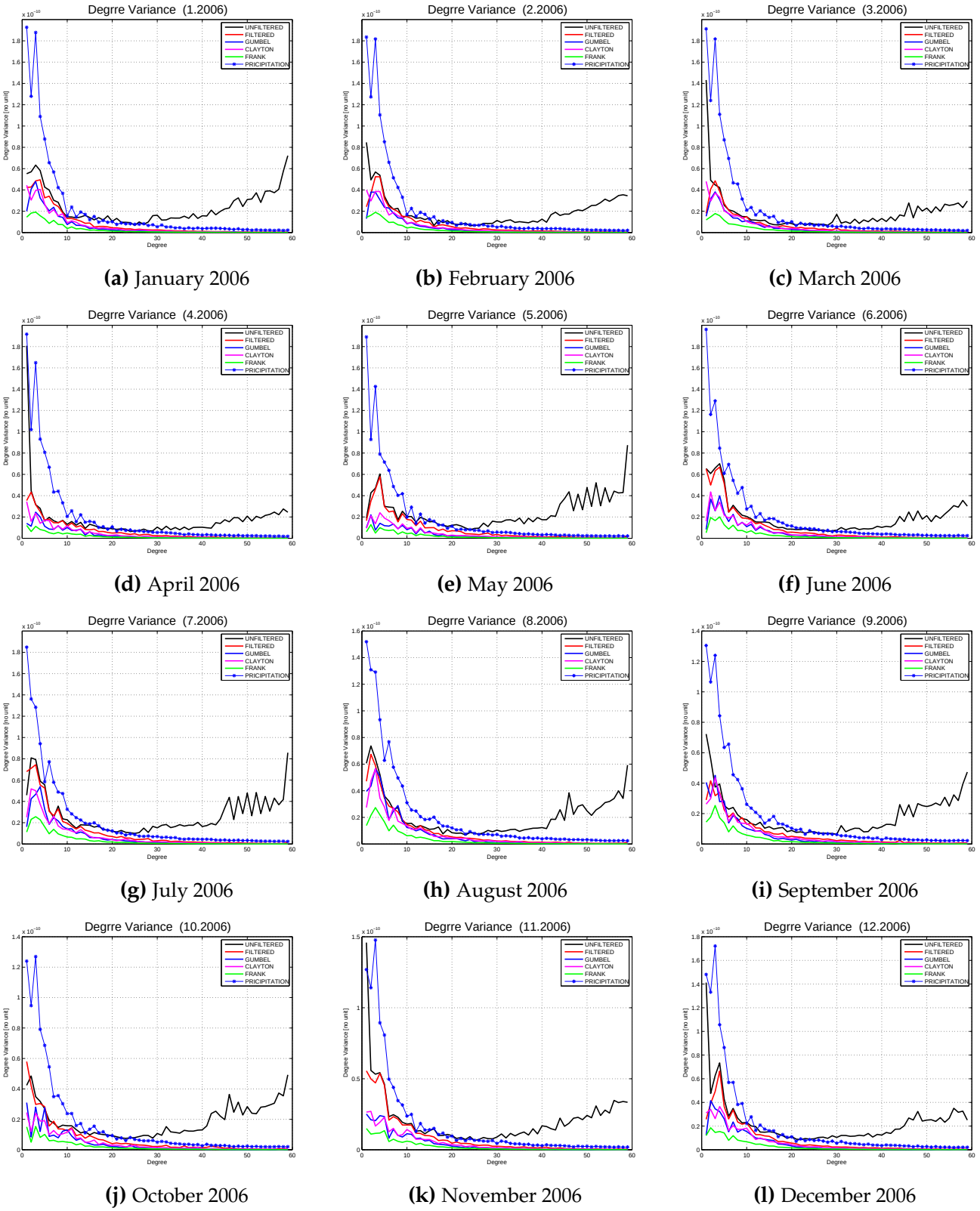

(a) January 2006 **(b)** February 2006 **(c)** March 2006

(d) April 2006 **(e)** May 2006 **(f)** June 2006

(g) July 2006 **(h)** August 2006 **(i)** September 2006

(j) October 2006 **(k)** November 2006 **(l)** December 2006

Figure G.2: *Degree variance of precipitation and* GRACE*, and Copula-based data in 2006.*

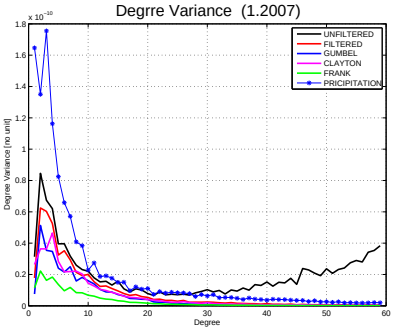

(a) January 2007

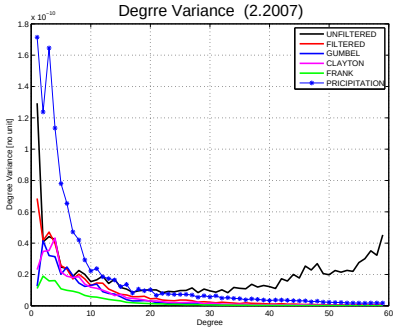

(b) February 2007

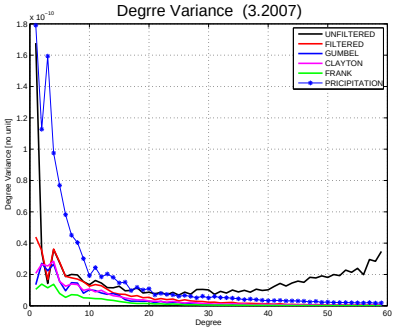

(c) March 2007

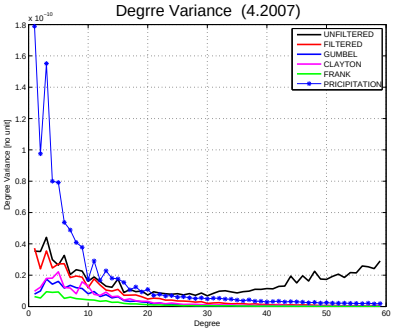

(d) April 2007

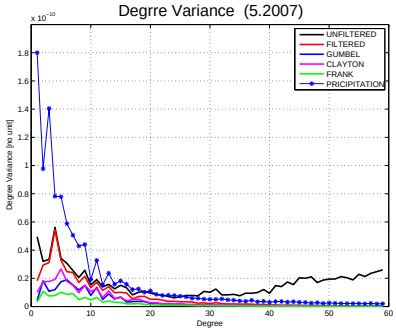

(e) May 2007

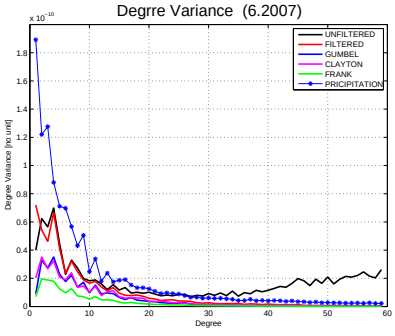

(f) June 2007

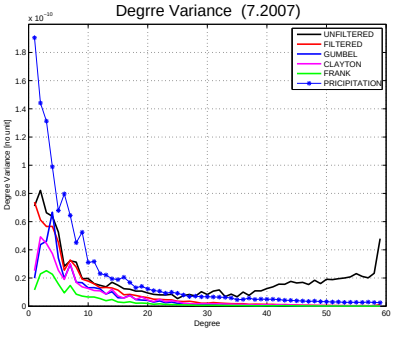

(g) July 2007

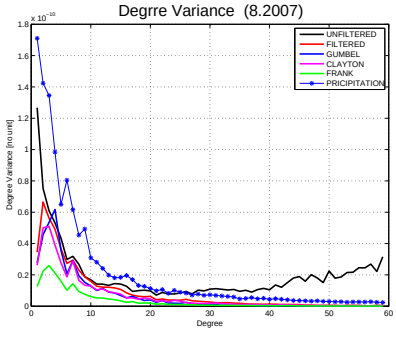

(h) August 2007

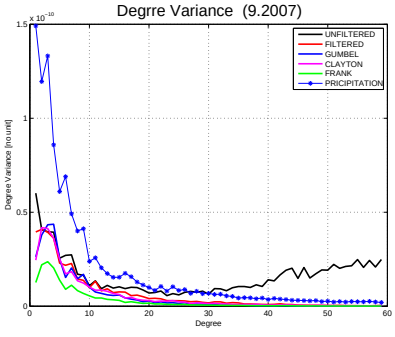

(i) September 2007

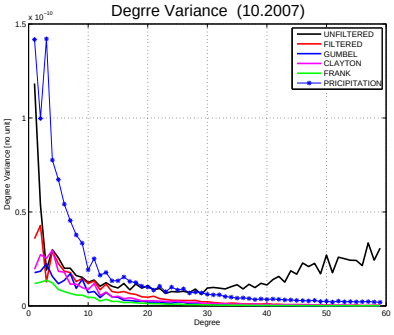

(j) October 2007

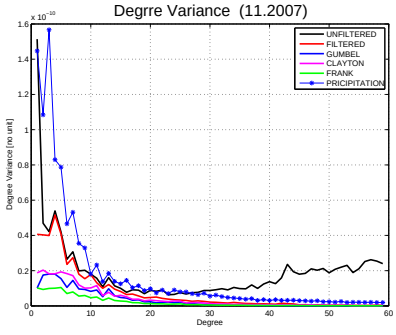

(k) November 2007

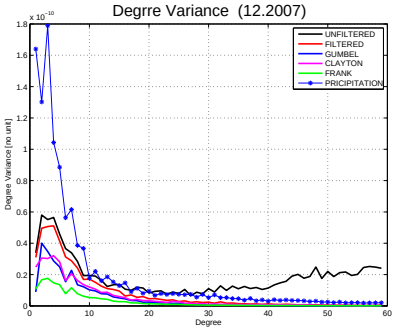

(l) December 2007

Figure G.3: *Degree variance of precipitation and* GRACE*, and Copula-based data in 2007.*

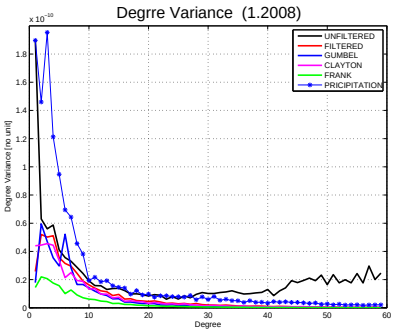

(a) January 2008

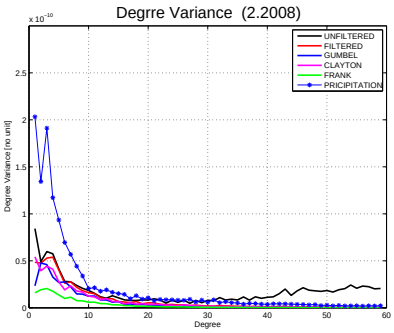

(b) February 2008

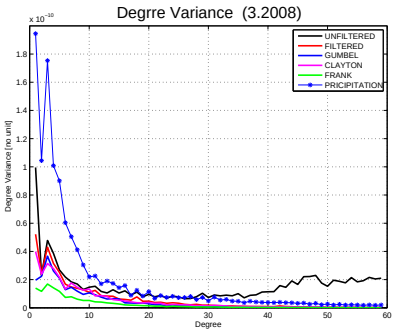

(c) March 2008

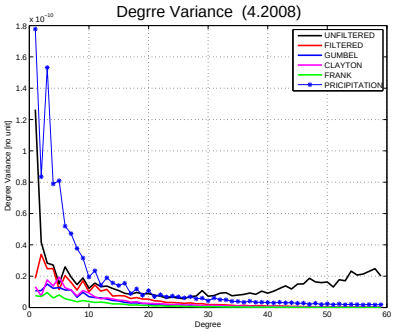

(d) April 2008

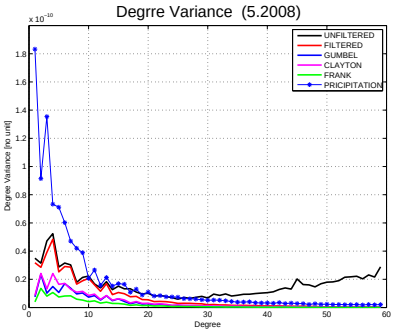

(e) May 2008

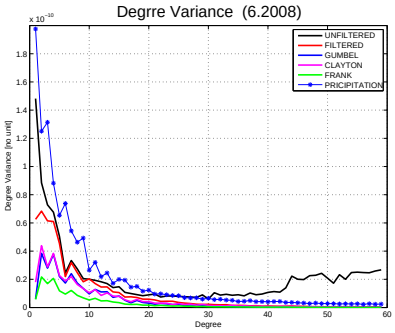

(f) June 2008

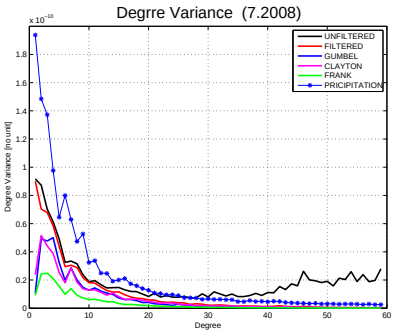

(g) July 2008

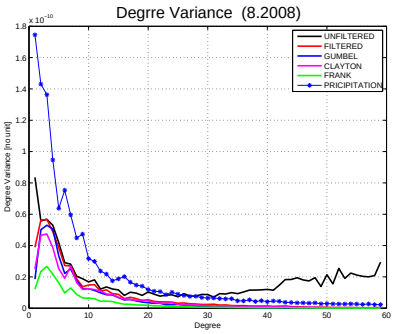

(h) August 2008

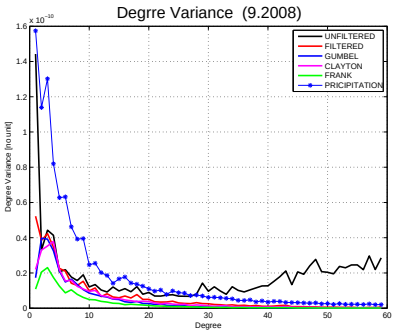

(i) September 2008

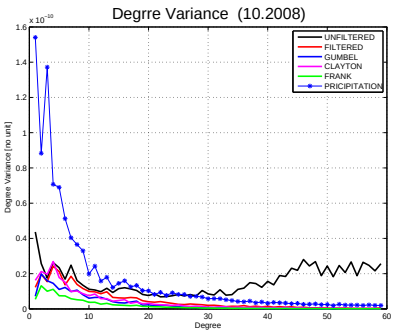

(j) October 2008

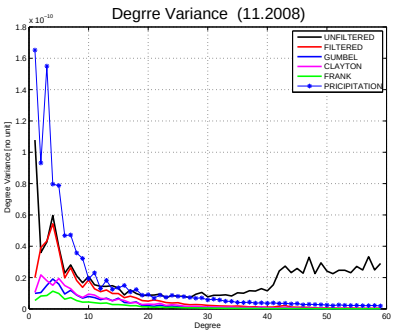

(k) November 2008

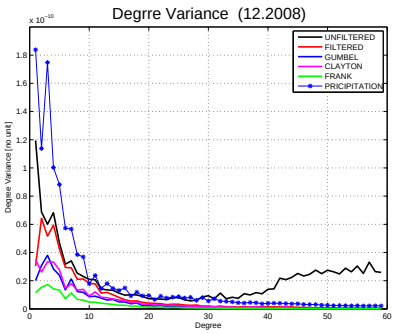

(l) December 2008

Figure G.4: *Degree variance of precipitation and* GRACE*, and Copula-based data in 2008.*

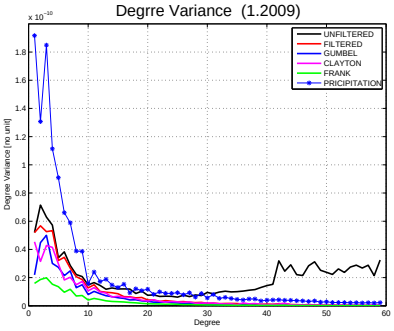

(a) January 2009

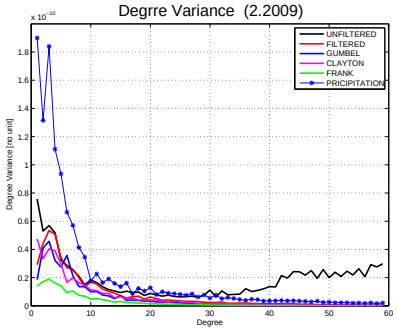

(b) February 2009

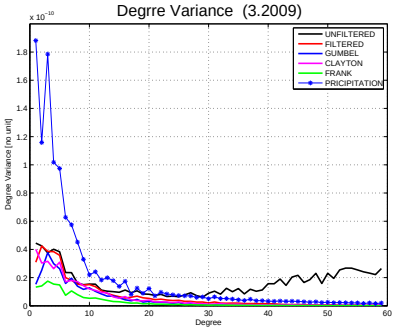

(c) March 2009

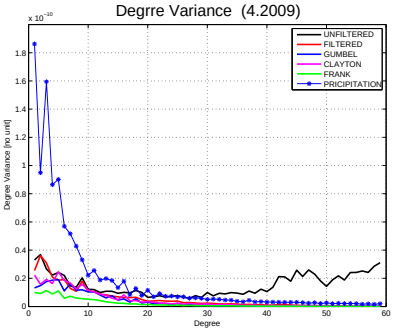

(d) April 2009

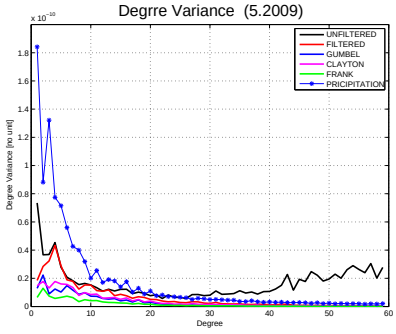

(e) May 2009

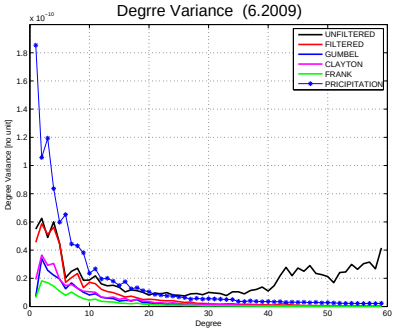

(f) June 2009

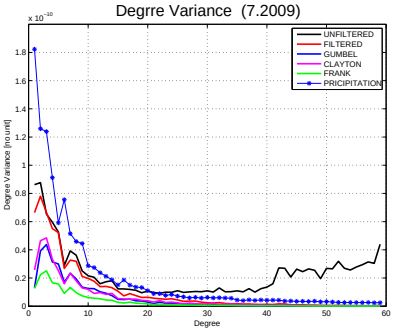

(g) July 2009

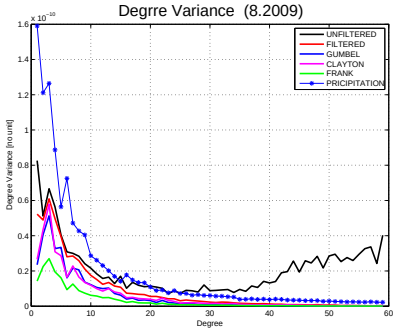

(h) August 2009

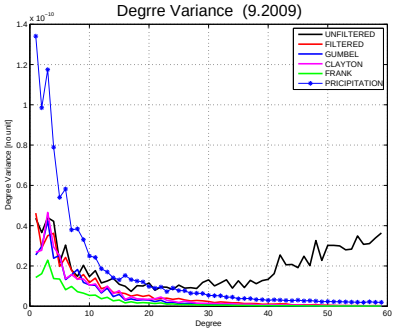

(i) September 2009

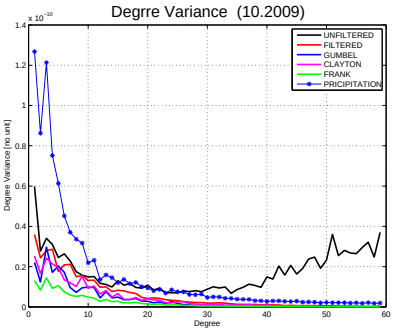

(j) October 2009

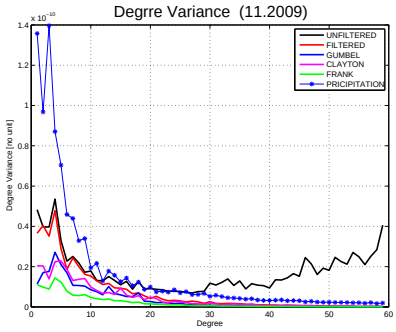

(k) November 2009

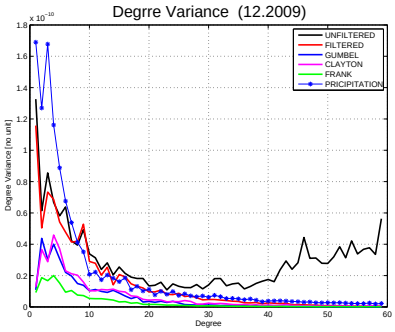

(l) December 2009

Figure G.5: *Degree variance of precipitation and* GRACE*, and Copula-based data in 2009.*